Advanced Hydraulic Studies on Enhancing Particle Removal

He, Cheng

Publication date:
2008

Document Version
Publisher's PDF, also known as Version of record

Advanced Hydraulic Studies on Enhancing Particle Removal

PhD Thesis
Defended in public at Aalborg University
(23.01.2008)

Cheng He

ISSN 1901-7294
DCE Thesis No. 11

AALBORG UNIVERSITY
Department of Civil Engineering

Aalborg University
Department of Civil Engineering

DCE Thesis No. 11

Advanced Hydraulic Studies on Enhancing Particle Removal

PhD Thesis defended in public at Aalborg University (23.01.2008)

by

Cheng He

January 2008

Scientific Publications at the Department of Civil Engineering

Technical Reports are published for timely dissemination of research results and scientific work carried out at the Department of Civil Engineering (DCE) at Aalborg University. This medium allows publication of more detailed explanations and results than typically allowed in scientific journals.

Technical Memoranda are produced to enable the preliminary dissemination of scientific work by the personnel of the DCE where such release is deemed to be appropriate. Documents of this kind may be incomplete or temporary versions of papers—or part of continuing work. This should be kept in mind when references are given to publications of this kind.

Contract Reports are produced to report scientific work carried out under contract. Publications of this kind contain confidential matter and are reserved for the sponsors and the DCE. Therefore, Contract Reports are generally not available for public circulation.

Lecture Notes contain material produced by the lecturers at the DCE for educational purposes. This may be scientific notes, lecture books, example problems or manuals for laboratory work, or computer programs developed at the DCE.

Theses are monograms or collections of papers published to report the scientific work carried out at the DCE to obtain a degree as either PhD or Doctor of Technology. The thesis is publicly available after the defence of the degree.

Latest News is published to enable rapid communication of information about scientific work carried out at the DCE. This includes the status of research projects, developments in the laboratories, information about collaborative work and recent research results.

Published 2008 by
Aalborg University
Department of Civil Engineering
Sohngaardsholmsvej 57,
DK-9000 Aalborg, Denmark

Printed in Aalborg at Aalborg University

ISSN 1901-7294
DCE Thesis No. 11

ABSTRACT

The removal of suspended solids and attached pollutants is one of the main treatment processes in wastewater treatment. This thesis presents studies on the hydraulic conditions of various particle removal facilities for possible ways to increase their treatment capacity and performance by utilizing and improving hydraulic conditions. Unlike most traditional theses which usually focus only on one particular subject of study, this thesis contains four relatively independent studies which cover the following topics: a newly proposed particle settling enhancement plate, the redesign of the inlet zone of a high-flow rate clarifier, identify the hydraulic problems of an old partially functioned CSO facility and investigate possible ways to entirely eliminate untreated CSO by improving its hydraulic capacity and performance. In order to be easily understood, each part includes its own abstract, introduction and conclusions as well as the study results. All studies were carried out with a combination of numerical model and measurements.

In the first part of the thesis a new concept of using a vortex to increase particle removal from liquid was proposed and the new particle settling enhancement plates, Vortex Plate, were tested under various flows and settling conditions. Structure of the Vortex Plate consists of multiple long narrow parallel slots which are built on a flat plate. Vortices are generated by cross-flow passing the long narrow parallel slots. The Vortex Plate can be used in the same way as the widely used lamellar plates with cross flow configuration. However, the Vortex Plate takes advantage of high flows, which generate stronger vortices and entrainment of solids in the downward direction inside the slots, the sliding particles are protected from the strong incoming main flow field. The study results show

that under the tested flow conditions and particles the new Vortex Plate outperforms the conventional lamellar plate, especially for higher inflow rates and smaller particle size.

Part two presents a numerical approach to redesign of the inlet structure of a high-rate stormwater clarifier. The inlet zone of an existing rectangular stormwater clarifier was redesigned to improve the fluid flow conditions and reduce the hydraulic head loss in order to remove the lamellar plates and adapt the clarifier to the needs of high-rate clarification of stormwater with flocculant addition. Conventional design methods based on surface loading rate, mean residence time and other parameters do not provide enough detailed hydraulic information to guide the improvement of the performance of the clarifier. This inconsistency in the traditional approach is discussed in the thesis. The redesign procedure was directed according to 3-dimensional flow and particle behavior as simulated with hydrodynamic and particle transport models under various configurations of the hydraulic structure.

In part 3, the performance of a combined sewer overflow (CSO) storage/treatment facility in North Toronto (NT), Ontario, Canada was investigated by conjunctive numerical and physical (hydraulic) modeling. The main objectives of the study were to assess the feasibility of increasing the hydraulic loading of the CSO facility without bypassing and major structural modification. Numerical simulations identified excessive local head losses and helped to select structural changes to reduce such losses. The analysis of the facility showed that with respect to hydraulic operation, the facility is a complex, highly non-linear hydraulic system. Within the existing constraints, a few structural changes examined by numerical simulation could increase the maximum treatment flow rate in the CSO storage/treatment facility by up to 31%.

In the last part, the same CSO facility as studied in part 3 was re-investigated with both the numerical and physical models. In order to keep the self contained format and to be easily understood, some background introductions about the NT CSO facility may overlap with the content of part 3. The main goal of this study is to upgrade the hydraulic capacity of the facility to totally eliminate the untreated CSO overflow (not only the bypass as the study goal in the part 3). A new and more powerful CFD model was used in this project. The study started with verifying the new model against measured data from a physical model. Two possible scenarios of structural changes were proposed and examined in detail by both physical and numerical models. Even though the study was focused on a particular CSO facility, the hydraulic conditions in the facility should represent general flow conditions in a typical water treatment facility. The numerical modeling method used in the study could be applied to solve a wide range of hydraulic problems faced in environmental and hydraulic engineering. Obviously, traditional design methods based on many simplified assumptions would not predict the actual operational performance as well as the new method outlined in the thesis.

ACKNOWLEDGEMENTS

The author wishes to thank the National Water Research Institute and Environment Canada for affording him the opportunity of continuing to upgrading his professional knowledge. Particularly, the support of division director, Dr. John Lawrence, on my pursuing higher education is greatly appreciated.

I would like to sincerely thank project chief, Dr. Jiri Marsalek, for his many thoughtful advises and suggestions throughout various study projects. His constant supports, encouragements and involvements greatly contributed much to the successful completion of the thesis.

Thanks also go to Bill Warrender, Doug Doede, Quintin Rochfort, Jim Wood, John Cooper and many other staffs around here for their kindly supports on data collection and experiment settings. Without their helps the studies would not be fully carried out.

The financial support from Government of Canada's Great Lakes 2020 Sustainability Fund, the City of Toronto, Ministry of Environment and National Water Research Institute are gratefully acknowledged.

Finally, I deeply appreciated the patience and supports of my wife Cong Wang and daughter Amy He during the period to fulfill my dream.

Table of Contents

Part 1: A Vortex Plate for Enhancing Particle Settling

1.1 Abstract:

The conventional inclined lamellar plate has been proven to be an efficient mean of increased particle removal and it has been used in a wide range of water clarification applications for many years. The functions of the inclined plate are to reduce particle traveling distance before reaching the boundary and thereby increasing the frequency of particle collisions to prompt particle flocculation. However, one of the problems with conventional inclined lamellar plate is that particles landing on the plate surface are directly exposed to incoming flows, especially for lighter particle under high flow load. A new proposed particle settling enhancing plate called the "Vortex Plate" is presented and discussed in this paper. In addition to functionalities of the conventional lamellar plate, the new plate also utilizes vertical vortices, generated by horizontal cross inflow, to entrain and transfer the particles from the outer fast flow to the relative quiescent corner of a long slot in which the particle slides down along the plate surface. Long parallel narrow slots are used to generate vortices and provide a quiescent flow regime protecting particles from disturbances during the period of particles downward movement. This flow regime enhances the removal of small and lighter particles, especially, for high-rate treatment. Numerical CFD models were used in this study to investigate flow conditions around the Vortex Plate. Measurements were also conducted in a rectangular tank to compare the effectiveness of particle removal with the newly proposed Vortex Plate, traditional lamellar plate and an empty tank. In general, the Vortex Plate performed better

than the conventional inclined lamellar plate, or the conventional settler, especially under high inflows.

1.2 Introduction

A gravity clarifier is the most economical and environmentally friendly method of removing suspended solids from flow because it uses gravity as a free source of energy, and it does not produce any side impacts. The efficiency of a discrete particle settling depends on the clarifier surface area and hydraulic loading. Hence, for a given discharge, the efficiency can be improved by increasing the clarifier area. A common method widely adopted in practice to achieve this is to use closely spaced inclined plate. This idea was suggested originally by Hazen (1904) over century ago and was further explored by Camp (1946) and many others (Culp G. et al. 1968, Yao 1973). During the last few decades there were hardly any new activities on developing new inclined plates.

The inclined plate settling system can be constructed in one of three ways with respect to the direction of the liquid flow relative to the direction of particle settlement: counter-current, co-current, and cross-flow. With the counter-current flow, wastewater suspension in the basin passes upward through the plate module and exits from the clarifier above the plate modules. The solids that settle out within the plate space move by gravity against the current downward, which reduces the solids settling velocity since they have to move against the upward current. In a co-current design, the solids and current are introduced above the inclined surface and flow down through the plates. This cause a potentially more serious problem of resuspending collected solids in the exit stream. In a cross-flow settling design, the flow is horizontal and does not interact with the vertical settling

velocity. However, since the solids are directly exposed to the current, they are still vulnerable to be swept away by a strong incoming flow, especial in the case of less dense solids.

Therefore, in a clarifier flow conditions have to be well controlled in order to achieve settling efficient close to theoretical limits. Attention must be given to providing equal flow distribution to each settler, producing good flow distribution within each settler, and collecting settled solids while preventing re-suspension. Comprehensive theoretical analyses of the various flow geometries have been made by Yao (1970). Yao's analysis is based on flow conditions in the channels between the inclined surfaces being laminar which requires the Reynolds number less than 800. However, even with all precautions taken in designing an inclined plate clarifier, the removal of small and lighter solids under high flow loads is always challenging. Consequently, in practice, most high-rate clarifications applications have to employ both physical and chemical treatment processes. In the physical settling process the turbulence is often considered as a negative factor disturbing particle settling and causing sediment re-suspension, which is particularly true in the settling region far from the boundaries or near a sediment bare bed. However, in the boundary layer it may not always be the case. For instance, in flume experiments conducted by Cuthbertson et al (1998) to study settling characteristics of non-cohesive fine grained sediment (150-500 microns) in a turbulent open channel flow over a rough porous bed, measured particle settling velocities near the channel bed, water turbulent flow conditions, were generally up to 2.5 times greater than the measured settling velocities in still water conditions. The reason was that vortices generated by the rough

bottom enhanced the transfer of particles from the high speed outer flow to the near-bed low-speed flow.

Research on particle behaviours in the wall region of turbulent boundary layers with the coherent structure (Marchioli and Soldati, 2002) revealed that coherent sweeps and ejections, generated by quasi-streamwise vortices, were efficient transfer mechanisms for particles. For instance, it is widely accepted that heavy particles have a tendency to migrate toward the wall (Caporaloni et al. 1975; Reeks 1983; McLaughlin 1989; Brooke et al. 1992) and that, when in the wall layer, they segregate preferentially in regions characterized by streamwise velocity lower than the mean velocity (Pedinotti et al. 1992; Eaton & Fessler 1994; Pan & Banerjee 1996). Particle behaviour in turbulent boundary layers can be explained by the relationship between the turbulence structure and particle dynamics. Once a particle is entrained in a sweep, i.e. there is a fluid downwash toward the wall, it is expected to continue within the sweep and to approach the wall. In the near wall region, the rear end of a quasi-streamwise vortex that is very close to the wall in preventing particles in the proximity of the wall from being re-entrained by the pumping action of the large forward end of a following quasi-streamwise vortex. The local flow structure produced by this couple prevents a number of the particles that have entered the wall layer from being entrained toward the outer flow. In particular, even though the strongly coherent sweep events required to drive particles to the wall are associated with strongly coherent ejections capable of driving the particles toward the outer flow, the offspring vortex acts as to reduce the width of the 'ejection channel'. In practice, only particles which enter the wall layer with a specific trajectory curvature may be able to be entrained back into the outer flow.

The hypothesis that pits function as preferred-particle collection devices for benthic organisms were investigated by Yager et al. (1993) under different flow conditions and pit geometries. Particle deposition experiments using pits and low-excess-density particles in a small annular flume indicated a significantly enhanced deposition rate compared to smooth, flat patches of the same diameter because pits altered the local fluid and depositional environment. Experiments also showed that with the same surface velocity, adding gravel to the bed dramatically increased particle flux to the pit. With a hydraulically smooth bed, deposition rates were low since few beads had any significant component of motion toward (rather than parallel to) the bed. A change in bed roughness increased the number of particles deposited to the bed over time since particle motion near the bed had an increased vertical component and also since the beads could come to rest in the quiet spaces (or mini-pits) between gravel particles. Under some conditions, pits, like ripple troughs, tend to fill in with finer-than background sediments (Risk and Craig, 1976; Nelson et al., 1987).

All the above research results have shown that near the boundary vertical vortices would increase suspended particle flux toward to the boundary, the critical question is how to keep the approaching particles staying on the boundary (bottom bed) without being re-suspended. To explore the answer, in this thesis a new boundary structure the so called Vortex Plate, designed to generate vertical vortices with boundary mean flow energy and to convey the trapped particles to proper location, is presented. The goals of this study are to investigate with numerical model and experiments: (1) flow conditions generated by the proposed Vortex Plate, (2) the particle removal efficiency of the proposed Vortex

Plate and comparing it with the efficiency of the well-known lamellar plate under various flow conditions.

1.3 Vortex Phenomenon

The vortex is a phenomenon that can be plagued with confusion and misunderstanding. The intensity of a vortex can be characterized by Vorticity which could be described with a 3D vector. Each of the three components represents the vorticity associated with flow in a 2-d plane normal to the respective component. The x-component of the vorticity (ξ) is perpendicular to the y-z plane, the y-component of the vorticity (η) is perpendicular to the x-z plane, and the z-component of the vorticity (ζ) is perpendicular to the x-y plane. Positive values of the vorticity components follow the right-hand rule. Meteorologists, in general, are most accustomed to dealing the vertical component of vorticity (ζ). The strong ζ is not necessary associated with strong vertical velocity and induced velocity does not have to be in the same direction as ζ .The vortex can be generated by either curved flow or sheared flow and its hydrodynamic condition can be very complex.

The phenomena associated with the vortex are everywhere around us. For example, water draining from the bath tub flows through the plug hole in the spiraling vortex fashion. Water will always try to follow the path of the least resistance. This is what the vortex enables to do. It reduces resistance by curving more and more inwards, thereby avoiding the confrontational resistance of straight motion and it also makes the flow change direction much easier. This is the fundamental reason for the plug hole vortex phenomenon.

For a circular vortex, except in the center core where the velocity is zero at the center and increases with the radius R, the tangential velocity V_t of a rotation flow at the radius can be simply expressed as

$$V_t = \frac{1}{2R} a^2 \omega \qquad (1),$$

where a^2 is a constant and ω is the flow rotation angular speed. From this equation, it appears that in general the flow tangential velocity in a vortex is proportional to the inverse of the radial distance R. The pressure, P, due to circular vortex can also be given as

$$P = \Pi - \frac{\omega^2 a^4 \rho}{8R^2} \qquad (2),$$

where Π is the pressure at infinity, and ρ is the water density.

A characteristic feature of a vortex (except in the center core) can be deduced from equations (1) and (2) that the outside of the vortex moves slowly and the centre moves fast, resulting in a reduced pressure gradient from outside to inside of a vortex. As water is imploded in a vortex, suspended particles, which are denser than water are sucked into the centre of flow, frictional resistance is reduced and the speed of the flow increased. However, it has to be pointed out and easily derived from equation (2) that under a slow rotation angular speed ω, the center suction effect is very limited. Therefore, the proposed Vortex Plate in this study is not mainly based on this principle to enhance the particle settling.

Since in natural phenomena, such as hurricanes and tornados, the vortex is often associated with strong vertical forces, usually generated by a sharp gradient of a physical parameter such as temperature, sometimes, it might give a wrong impression that

horizontal swirl motions always induce strong vertical velocities and forces. This incomplete image of the vortex is often reproduced in many products, for instance, a solid-liquid separator or a clarifier built with a bottom closed cylindrical container and having swirled flow passing through it can not actually generate a major vertical flow movement and strong central suction effect. The flow behaviours in such cylindrical container are very much similar to that in a stirred tea-cup. The sediment would be pushed toward the center of the cup bottom due to friction of the container bottom. However, this flow pattern is not necessary to enhance solids settling.

In general, a small-scale eddy or swirl in flow is considered as an unwanted turbulence phenomenon in most solid separation because of random characteristics of turbulent flows. However, if utilizing a spatially fixed vortex properly, it could have a positive effect on particle settling by changing particle travel trajectory toward a more favourable direction within the vortex.

1.4 Particle Movement in a Vortex

The mechanisms of particle suspension and transport in turbulence are quite complex, involving interaction of particles with a complex and incompletely understood turbulent flow. In view of the complexity of the particle suspension process, substantial simplifications are often used by only including the major forces acting on particles to describe the motion of suspended particles. In most situations involving solid particles in general flow conditions, the particle motion will be determined by the effects of inertia, viscous drag, and gravity (Lazaro and Lasheras, 1989), with all the other forces being at least one order of magnitude smaller. For a particle moving in the vortex field, the drag

force created by the radial inward fluid motion due to pressure gradient would tend to balance the centrifugal force, thereby preventing the particle from being ejected. A similar argument concerning a balance between the centrifugal and drag force was put forward by Maxworthy (1968).

In actual vortex cells there is always some degree of turbulence present, so that there will always be some turbulent exchange across trajectories of particles. In such a case, the region of particle retention must gradually lose some of its particles by turbulent exchange with the outside region, the rate of loss depending upon the degree of turbulence.

1.5 Proposed Vortex Plate Structure

The structure and layout of the tested Vortex Plate is shown in Fig. 1.1. It has many uniformly spaced slots along the face of a 100 cm (long) x 50 cm (wide) smooth flat plate, the slots were about 2 cm wide and 2 cm deep, running along the full length of the Vortex Plate. In the actual operation, the inclined Vortex Plates are placed in the settling tank at 60 degrees about the horizontal, with flow velocities parallel to the plate. The ambient flow passing the top opening of the slots generates vortices in the narrow parallel long slots, which entrains particles and make them slide downward along slots. Because the vortex is generated by cross flow, the faster the cross flow is, the stronger the vortex is produced. Thus, the Vortex Plate is potentially more effective in removal of suspended solid under high flows than the traditional smooth lamellar plates. Also, because the slots protect the particles inside the slot against flow disturbances, even lighter particles

probably have an improved chance to move downward, compared to the smooth plate design.

1.6 Numerical Study of the Vortex Plate

As mentioned before the vortex is a complex physical phenomenon, which is difficult to study experimentally, especially, small-scale weak vortices, because of the possible interference with the measurement device. In order to examine the effectiveness of vortex generation by the newly proposed Vortex Plate and to better utilize the vortex for enhancing particle settling as proposed, it is important to understand hydraulic conditions in the vicinity of the Vortex Plate. Toward this end, a commercially available CFD software was used in this study as a primary investigation tool to evaluate the performance of the proposed Vortex Plate. Since low particle concentrations were used in particle transport simulations, the influence of suspended particle on its carrier can be neglected, which allows simulation being carried out in two steps: first, the flow field was calculated with the 3D hydrodynamic single phase model and the k-ε turbulent model, and then, the Lagrangian particle tracking model was used on the basis of obtained flow information to simulate particle settling rates under different inclined plates. The dispersion of particles in the fluid phase due to turbulence can be predicted using a stochastic tracking model. The stochastic tracking (random walk) model includes the effect of instantaneous turbulent velocity fluctuations on particle trajectories. At the same time, particles do not directly impact the generation or dissipation of turbulence in the continuous phase. When particles reach the boundary it is assumed, in particle tracking simulations, that 50% of the momentum carried by particles will be lost. Details of the

model can be found in He et al. (2004). It was realized that some physical phenomena of particle transport could not be realistically simulated by numerical modelling, such as particle behaviours after they reach the boundary and the particle re-suspension at the bottom for a strong bottom flow. Therefore, in the numerical study the particle transport simulation mainly focused on investigating flow condition effects on the particle settling under different particle settling enhancement plate designs instead of looking for the absolute particle removal. The experiments were also carried out to compare the performance of the proposed Vortex Plate with that of the conventional lamellar plate, and such results are presented later.

The numerical simulations were done for particles traveling in a closed top 100 cm (L) x 26 cm (W) x 40 cm (D) rectangular tank fitted with either two Vortex Plates or two lamellar plates, positioned in the settling chamber at a 60 degree angle from the horizontal and the structural arrangements shown in Fig. 1.2. The inlet and outlet are located at top of the tank upstream and downstream ends, and the size of the particle settling enhancing plate is 60 cm (L) x 50 cm (W). The main flow patterns for the two different plate designs are represented as streamlines in Figs. 1.2A and 1.2B. It is not surprising that the main flow patterns are similar for the two different situations. With an inflow velocity of 0.5 m/s used in the simulation, around 60% of flow passing through the top part of the tank directly. However, some flow, as indicated in both Fig. 1.2A and Fig. 1.2B, could reach all the way down to the tank bottom before bending upward to exit from the outlet. These curved flows could affect the direction of the induced vertical flow along the slots of the Vortex Plate, which will be discussed below in detail.

Fig. 1.3 shows the simulated velocity in the individual slot of the Vortex Plate. For the sake of clarity, only a few slots are shown in Fig. 1.3, the velocity patterns in all slots are quite similar and negative vortices induced by horizontal flow can be seen clearly in all the slots, which confirms the design concept. Also, from the vector lengths in Fig. 1.3 it seems, at first glance, that the velocity at the vortex center is the smallest and will increase with radius until reaching the wall, which seams difference from the assumed the velocity distribution in a circular vortex described in the section of vortex phenomena. However, by closely examining the velocity amplitude distribution at the same cross-section as shown in Fig. 1.3 with a colour contour map (not shown here because it is not very useful when displayed as a black-white map), it was found that the simulated tangential velocities increased from the center to about the midpoint between the center and wall, and then started decreasing toward the slot wall, which matches a general velocity pattern in a circular vortex. At the two bottom corners of slot, as expected the velocity was almost zero, which provides a potential quiescent channel allowing particles to slide down easily along the slot.

The vortex distribution along the whole Vortex Plate can be better displayed with contour lines as shown in Fig. 1.4. Density of the contour lines indicates the intensity of vortex. The vortices generated in the top part of the plate were stronger than those near the bottom, because of a faster horizontal flow in the upper part. Based on simulated flow patterns it was expected that once nearly horizontally moving suspended solids enter swirl flow, their trajectory would be changed. As mentioned before the movement of particles along either vortex direction (a nearly vertical direction) should be easier due to less hydraulic resistance. The vertical velocity contours in three horizontal cross-sections

are displayed in Fig. 1.5. The arrows are used to show the vertical velocity direction in different regions. It can be seen that there are quite strong nearly vertical flows in the parallel slots, the negative vertical velocity (downwards) is generated in the upstream part of the tank and a positive vertical velocity (upwards) occurs in the downstream half of the tank. The size of arrows indicate that vertical velocity at the two ends of the Vortex Plate was strongest and it would be gradually reduced towards the middle of the Vortex Plate, the similar vertical flow distribution in the settling tank could also be seen from main flow velocity distribution in Fig.1.2. Therefore, the strong vertical flow was mainly generated by vertical component of mean stream flow instead of by the vortex itself. Obviously, the downwards vertical velocity would increase particle settling speed. In the region with upwards velocity in the sliding slots, particle settling process should also be enhanced based on the principle of lamellar plate settling with the counter current setting to enhance the settling, however, it has much weaker flow to against because main flow maintains in the horizontal direction. To investigate the particle transport behaviour under hydraulic conditions generated by the Vortex Plate, the Lagrangian particle tracking model was used to evaluate the performance of particle removal under both lamellar and the Vortex plates.

With the consideration of computer running time, the particle tracking model was run to simulate 60 seconds real-time event. The time step was 0.01 and a total of 75000 particles were tracked in the tank during the simulation period, which should be large enough to represent particle movement under the given conditions. With the 0.5 m/s inflow velocity, for a particle moving straight forward with the carrier speed would take only 2 seconds to reach the exit. So, a simulated 60 seconds real-time event would be long enough to test

particle behaviour under the influence of the settling enhancing plates in a 100 cm rectangular tank. The simulated particle capture rates for different settling enhancing plates are shown in Fig. 1.6. It shows that if only the flow condition influence on suspended solid movement (the model could not realistically simulate the boundary effects) is considered, the simulated particle capture rate of the Vortex Plate is about 8% higher than that of the lamellar plate, which was most likely attributed to the vortices generated in the slots of the Vortex Plate. With such promising simulation results, further studies were pursued with experiments to confirm what has been found in the numerical study and experiment results are be presented in next section.

1.7 Experiments

Two sets of experiments were carried out to investigate the particle removal efficiency of the proposed Vortex Plate. The first group of tests focused on comparing the performance of different individual particle settling enhancement plates, only one plate was placed in the testing tank at a time under the various flow rates tested. However, because the structure of the new proposed Vortex Plate was built on the top of a flat plate, it occupies extra space compared to the lamellar plate, which would reduce the effective width of flow path in the testing tank if the multiple Vortex Plates are used together as an array, which results in increased flow speed and reduced particle residence time. Therefore, even if measurement results have shown that the individual Vortex Plate performs better than others, it is still necessary to find out how effective it is when used in a multi plate system, which was investigated in the second group of the tests.

1.8 Testing a Single Plate

The experiments were conducted in a 1500 cm (L) x 30 cm (W) x 60 cm (D) open-top tank. The surface sizes of both the Vortex Plate and the lamellar plate were the 100 cm (L) x 50 cm (W) built with epoxy-coated marine plywood. On the back of both plates there were two re-enforcing metal bar to keep the plate straight. The structure and layout of the tested Vortex Plate is shown in Fig. 1.1. As tested, the slots were about 2 cm wide and 2 cm deep, running along the full length of the Vortex Plate. In the actual operation, the 60 degree inclined Vortex Plates were placed in the settling tank, with flow parallel to the plate. The plates were firmly retained in the position with screws to prevent vibration caused by the strong incoming flows. During the testing, the water surface under maximum inflow rate reached about the same height as the top edge of the plates.

The inlet structure of the testing tank was constructed with a U shape channel, the width of the channel was 10 cm and on the wall of the outside channel between the inlet and the settling tank there were three narrow openings with a horizontal baffle on the top of each opening, which forced flow entering to the settling tank to be more evenly distributed in both vertical and horizontal directions (He and et al., 2005). The lengths of the settling chamber and outlet section were 1200 cm and 10 cm, respectively. A 50 cm high wall separated the settling chamber and the outlet channel, and as shown in Fig. 1.7. During the experiment particles were released from top of the upstream end of the inlet channel, just in front of the inflow entering the inlet. In such a way, the particles would be very well mixed with incoming fast, strong turbulent flow. The flow carrying particles passes the particle enhancing plate in the settling chamber and eventually exits from the bottom opening of the outlet channel. Before flowing into the large particle capture tank,

effluent has to pass a screen preventing particles from escaping. Water was pumped back through a 2 inch pipe from the capture tank to the inlet. Between the pump and the inlet, there is a flow meter and a control valve to regulate inflow rates.

Recognizing that large light particles are more sensitive to flow conditions than small heavier particle, crushed walnut shell particles (density = 1.35 g/cm^3 and average size = 350 μm) were chosen for most of the experimental studies. Also, larger particles are much easier to handle with respect to preventing their re-entry into the circulation system in the experiments. Other advantage of using the crushed walnut shells is that because of their brownish color, their movement in the flow is easy to be observed, which helps to understand and improve the flow conditions in the settling tank. The duration of all conducted experiments was 11 minutes, and 300 g of crushed walnut shells were used in each experiment, they were divided into 10 even amounts and released by hand in 1 minute time interval. After all particles have been released at the end of 10 minutes, the pump was kept running for one more minute before it was turned off. So, even the last entered particles had chance to pass through the particle settling enhancing plate in the settling chamber. After the experiment was finished, the flow was drained off through the bottom holes in both the settling chamber and the inlet channel. The particles were captured by a 62 μm screen before they could escape into the capture tank from draining hole. The collected particles were put in an oven with temperature around 40^{o}C for over night drying. All the experiments were carefully operated, there were no signs that any particles had re-entered the circulation system.

The main purpose of the experiment was to compare the particle removal efficiency under three different particle settling settings: 1) a tank with a Vortex Plate, 2) a tank

with a lamellar plate, and 3) a tank with no plates. Five flow rates, 4, 5, 6, 7 and 8 L/s, were used in the experiments, respectively. The corresponding surface loadings are around 40 m/h – 80 m/h, which represents very high values in stormwater treatment applications. The experimental results in Fig. 1.8 indicated that the Vortex Plate performed better than the lamellar plate for all inflow rates. The dash and solid lines in Fig. 1.8 were measured results for the case of the lamellar plate and the Vortex Plate tilted in the same direction and flows passing on the left side of the particle settling enhancing plate face when looking down from upstream (negative vortices are generated in the slots, thus the Vortex Plate in this position is called the negative Vortex Plate in the following text). The average particle capture rate has been improved by 4% between the solid curve and the dash curve, which may not appear very significant, but considering that only one plate was used in this test, at least half of the tested particles were not affected by the plate at all. Improvements in the solids removal would be larger if more Vortex Plates are used. Depending on the tilt direction, the same Vortex Plate can generate positive or negative vortices in the slots. The solid line with point symbols in Fig.1.8 represents the particle capture rate of the same Vortex Plate with the same experiment setting, except that the Vortex Plate was tilted in the other direction, generating positive vortices in the plate slots (thus called a positive vortex plate). In principle, in a uniform flow field, the positive or the negative vortices would have similar effects on particle vertical movement because the particle rotation direction should not affect the particles movement in vertical direction. However, the measured results in Fig. 1.8 showed that the particle capture rate of the positive Vortex Plate was notable higher

than that of the negative vortex plate, for all flow rates, which has to be investigated further.

To find possible answers, the two vertical profiles of flow velocity without any settling enhancement plate presenting in the settling chamber were measured. The measurement locations were from 5 cm above the bottom to the top of the tank, with 10 cm increments, at the middle section of the settling chamber and 5 cm from each side wall. The measurements were done with an ADV (Acoustical Doppler Velocity) probe measuring all the three velocity components. The measured velocity component profiles are shown in Fig. 1.9 for a 6 L/s inflow rate; the left side (front of the tank) and the right side (back of the tank) follow the convention of looking down stream. The measurements showed that the x-component (along the tank) of the velocity profiles at two side-walls were very similar. However, for the other two velocity components, the differences were unexpectedly large. A possible explanation for the large velocity deviation in the rectangular tank was, after carefully examining the tank physical structure, the lack of accuracy in the construction of the inlet compartment. The three narrow rectangular openings on the wall between the inlet and the settling tank were spaced unevenly. The opening height at the two ends was not the same, which made the flow rate and flow direction slightly varies along the opening, and might also induce a flow rotation motion, when passing through the tank. Fig. 1.10 shows the velocity profiles measured at the same measurement locations after the opening structure has been corrected. The velocity differences at the two locations for both y and z components were smaller than those shown in Fig. 1.9, even though there were still some room for further improvement. It may also have to be recognized that with such a short settling chamber and strong

turbulent flow, it is almost impossible to achieve ideal laminar flow in the settling chamber. The additional measurements of particle removal for both the negative and positive Vortex Plates were done after the structure has been fixed and the results (not given here) showed that the removal rates were similar and have been improved slightly in the negative setting case. The above exercise has demonstrated that the performance of the Vortex Plate is quite sensitive to flow conditions.

It has been observed during the experiments that large amounts of particles, after sliding off the plate were carried away by a strong current along the bottom. To reduce this phenomenon, four lateral baffles extending to the full tank width were placed evenly in the settling chamber to reduce the bottom flow circulation.

It can be seen in Fig. 1.11 that after changing flow conditions in the settling tank by adjusting the inlet structure and inserting the bottom lateral baffles, particle capture rates for both the lamellar plate and the Vortex Plate have notably increased. It can be concluded that the performance of solids removal of the Vortex Plate is quite sensitive to flow condition, which could be a complex issue and can also be exploited in practice, if done properly. In order to fully understand the performance of the Vortex Plate under various flow conditions, further more comprehensive tests would be needed, which is beyond the scope of this study.

So far, all experimental results indicated that the proposed Vortex Plate used in a single plate configuration would contribute to settling more particles than the lamellar plate, under the same test conditions. The simple explanation should be that sediment particles interact with the vortex structure, which lead to a stronger settling motion of particles on the downside of vortices, transferring the particles from the high-speed outer flow to the

near slot bed low speed flow. Then, particles slide down along the quiescent upstream corner of parallel slots, which was observed from all experiments with the Vortex Plate.

The Vortex Plates with different slot structure patterns were also tested in this study to explore the effects of slot geometry. There could be many different slot designs to generate the vertical vortex and various hydraulic conditions. Based on the same vortex principle, two slightly modified Vortex Plates shown in Fig. 1.12 and Fig. 1.13 have been tested. The design shown in Fig. 1.12 has angled slots paralleled to each other with a tilt angle of 70 degree. The purpose of this kind of structure arrangement is to generate small downward flow along the slot as illustrated in Fig. 1.14. In practice the Vortex Plate is placed in such a way that the one component of horizontal incoming flow would have the same direction as the slot, which would push particles downward. Another potential benefit with this kind of design is that the majority of sliding particle would be concentrated at the bottom inside corner (downstream bottom corner of a vortex), which would increase the chance of particle collision and also make the particle collection easier to preventing particles being washed away by strong current along the bottom. Testing results showed that for single plate this Vortex Plate performed a little better than the original one, possibly due to extra downward flow effect. However, if it is used in an array, much too strong downward flows could be generated and would increase the risk of particle resuspension on the bottom or being washed away before they reach the bottom. Extra efforts have to be made to solve the return flow without disturbing too much particles.

The second modified plate tested is shown in Fig. 1.13. The idea of this structural configuration is to generate smaller sized vortices in the slot as illustrated in Fig. 1.15, so

the lower edge of the vortex does not reach all the way to the bottom of slot. Therefore, particles sliding down along the bottom of slots may be less likely to be disturbed by the above vortex. However, the testing results showed that the plate with this type of slot arrangement performed much worse than the original one. One possible explanation is that the vortex generated with this Vortex Plate was not strong or stable enough to effectively entrain particles from outer fast flow in the tank.

1.9 Testing plate array

As mentioned before the protruding structure of the proposed Vortex Plate is about 2cm above the flat smooth surface. In practice, in order to maximize the particle separation, multi-plates are often used together as an array in a limited size tank. In this arrangement, the cross-section of the flow path would be reduced, resulting in an increased flow speed and reduced residence time, which may diminish the effectiveness of the Vortex Plate. Therefore, arrays of the Vortex Plate and smooth flat plate were built and tested in the same experimental setting as mentioned above.

The experimental setting is shown in Fig. 1.16 and the schematization of cross-section of plate array in the testing tank, viewed from downstream, is displayed in Fig. 1.17. The dash lines in Fig. 1.17 represent the slot height of the Vortex Plate and the units of measurement are centimetres. Both sets of tested plate arrays consisted of 5 parallel plates with the same horizontal surface sizes which were 2 x 14 cm x 80 cm, 2 x 28 cm x 80 cm and 1 x 50 cm x 80 cm. The plates being placed around 63 degrees from the horizontal were mounted on a support with two 10 cm high walls above the tank bottom blocking the whole the cross section to reduce the bottom current. In order to prevent

particles being washed away by strong current, a small isolated settling chamber was built between the front wall of the tank and a transparent plastic sheet with three horizontal openings as shown in Fig. 16. Lower ends of the three top particle enhancing plates were inserted into a separate chamber, so particles sliding down from the plates were minimally disturbed by strong inflow. In order to minimize the possible flow circulation induced by downward flow from the parallel slots in the isolated settling chamber, seven vertical walls were used to divide the isolated settling chamber into eight smaller sections.

The extra space occupied by the Vortex Plate due to slid slots could be estimated with a simple geometry calculation as about 360 cm^2. Due to the reduced cross-sectional area by the Vortex Plates, the water level in the testing tank was also increased by about 1.5 cm. Therefore, the total tank effective cross-section has been reduced, in term of percentage, by about 35%, which could, in principle, increase the flow velocity by 35%. To quickly assess the influence of the Vortex Plate array on velocity changes, a Pitot tube was used to measure flow velocity between two parallel plates under the two different plate arrays. The velocity measurement setup can be seen in Figs. 1.16 and 1.17. Results showed that the flow velocities at the measurement location indicated by a circle with a cross inside in Fig. 1.17 were 16 cm/s and 21 cm/s, respectively, for the lamellar plate array and the Vortex Plate array. In the latter array, the flow velocity increased by about 37.5 %, which is consistent with the above estimate. With such a large flow velocity increase, it was natural to raise the question, whether the Vortex Plate could still outperform the lamellar plate, when used in an array.

To answer this question, a series of tests were conducted with both the Vortex Plate and lamellar plate arrays under various flow rates and particles, the results were listed in Table 1. Initially, crushed walnut shells were used again as testing particles. The results showed (rows 1 to 4 in Table 1) that the particle removal rates of the Vortex plate and lamellar plate array under both tested inflow rates were about the same, which indicated that the particle removal efficiency of the Vortex Plate used in an array has been reduced due to the blocking effect of the Vortex Plate structure, thus, the attractiveness of the proposed Vortex Plate for use in practice removal seemed to be much reduced.

Further investigations were carried out with glass beads of two average sizes, 66 μm and 150 μm. Because the density of glass beads (2.5 gm / cm^3) is much higher than that of walnut shells, small size glass beads had to be used in order to bring down the particle settling velocity. The main purpose of using glass beads as sample was to evaluate the performance of the Vortex Plate with small and slow settling particles. In order to prevent small particle from escaping from the test system, a 32 μm screen mesh was used to capture the particles in the effluent. The testing results (rows 5 to 8 in Table 1) showed that with 66 μm glass beads, and for both tested flow rates, the Vortex Plate array performed better than the lamellar plate array. However, for larger size glass beads (150 μm), the results were not quite the same as above, even though for a higher flow rate of 8 l/s (rows 10 and 12 in Table 1) the Vortex Plate still outperformed the lamellar plate. But at a lower flow rate (5 l/s), the test results (rows 11 and 13) indicated that the lamellar plate array and the Vortex Plate array captured about the same amount of particles, which was a finding very similar to that in tests with crushed walnut shells. By closely examining the particle settling velocities of the crushed walnut shell and 150 μm glass

bead, it appears that they are about the same, which might explain why their behaviour is similar under the same hydraulic conditions. The possible physical explanation for two different plate arrays performing similarly under lower inflow rates with larger particles could be that in such a situation the likelihood of the particle landing on the lamellar plate and being flushed away by the incoming flow were much smaller than in the case of small particle settling in a larger inflow, resulting in the Vortex Plate losing the advantage of the "shade" effect. Also large particles are much more likely to land on the lamellar plate surface, with the entrainment effect of the Vortex Plate becoming the less important. For the smaller particles or under higher flow rate, both "shade" and "entrainment" functions of the Vortex Plate became more effective, and therefore, it was not surprising to see that the Vortex Plate performed better. This experiment verified the design hypothesis that the Vortex Plate should work better for smaller particle or under higher flow rates than the lamellar plate. Actually, in the testing of the single plate this tendency has been shown, as indicated in Fig. 1.11. For higher flow rates the Vortex Plate performance compared to lamellar plate was notably better than for lower flow rates. Also, it is worth while to mention here that when the surface load was less than 50 m/h, the two tested plates have very similar particle removal rates, which was implied by the similar values of both performance curves for low flow rate in Fig. 1.11. This result was consistent with that measured in the plate array (listed in rows 1 to 4 in Table 1).

1.10 Conclusions

A numerical study and experiments were carried out under various inflow rates and different particles to investigate the particle removal by the proposed Vortex Plate, in

comparison to that of the well known and widely used lamellar plates. In general, large and light particles settling would be more affected by the flow conditions than small and high density particles. Therefore, crushed walnut shells were chosen as test particle in experiments as well as glass beads. The concepts of the newly proposed particle settling plate were based on:

(1) Use of the flow energy to generate a steady vortex at a desired location to change the particle movement direction and to make the particle slide downward easily with less disturbance by fast horizontal flow.

(2) Reduced particle traveling distance by increasing the contact surface area, which would enhance the particle settling. The surface area of a Vortex Plate has been doubled compared to the traditional lamellar plate.

(3) Increase the particle collision frequency within the swirling flow to prompt particle flocculation.

Numerical modeling and experimental observations verified that strong vortices were generated in the parallel slots of the Vortex Plate, as expected. The generated vortices captured the passing by particle and retained some of them in slots, by providing a quiescent settling zone. Both the simulation and measured results showed that the new particle settling enhancing plate outperformed the traditional lamellar plate under the same test conditions, especially for lighter particles with large inflow rates. Most particles were sliding down the Vortex Plate along the upstream slot bottom corner, because of less flow activities in this region, which would also increase particle collisions. The vertical slot flow mainly generated by the main flow can help push particle to slide down to the settling tank bottom along the parallel slots, however, it may also induce a stronger

bottom current sweeping particle away before they have a chance to settle on the sediment bed. Thus, extra care should be taken to reduce the bottom flow circulation.

Main purpose of this study intended to propose a new concept with additional mechanism (i.e., vortex force) for particle settling. The numerical modeling and experiments provided the general assessments about performances of the Vortex Plate, instead of trying to give the optimum design of the plate layout. Further studies of the various flow hydraulic conditions and their effects on the particle movement along the particle settling enhancing plate could help better understand and improve the performance of the Vortex Plate.

1.11 Acknowledgements:

The authors wish to thank Doug Doede for his assistances in data collection and to NWRI Research Support Branch staff Bill Warrender for his thoughtful construction of the experimental facilities.

1.12 Notation

The following symbols are used in study 1:

a = a constant;

P = pressures;

R = radii;

V_t = tangential velocity;

ω = angular speed;

ρ = water density;

Π = flow pressure at infinite.

1.13 References:

Ashurst, W.T. (1991). “Is turbulence a collection of Burgers Vortices?”

Brooke, J.W., Kontomaris, K., Hanratty, T.J. & McLaughlin, J.B. (1992). “Turbulent deposition and trapping of aerosols at a wall. Phys. Fluids A 4,825-834

Camp, T. R. (1946). “ Sedimentation and the design of settling tanks” Trans. ASCE, 111, 895-936.

Caporaloni, M., Tampieri, F., Trombetti, F. & Vittori, O. (1975). “Transfer of particles in nonisotropic air burbulence. J. Atmos. Sci. 32 565-568

Cuthbertson, A.J.S., Ervine, D.A., Hoey, T.B., Heinrich, O. (1998). “Settling Characteristics of Fine Grained Sediments in Turbulent Open Channel Flow” Proc. 3rd Int. Conf. Hyd. Eng., Cottbus/Berlin.

Eaton, J.K. & Fessler, J.R. (1994). “Preferential concentration of particles by turbulence. Intl. J. Multiphase Flow, 20 169-209.

Culp G., Hansen, S., and Richardson, G. (1968). “High Rate Sedimentation in Water Treatment Works.” J. Amer. Water Works Assn., 60, 681.

Hazen, A. (1904). “On Sedimentation.” Trans., ASCE 53, 45-71.

He, C., Marsalek J. and Rochort Q. (2004).“Numerical Modelling of Enhancing Suspended Solid Removal in a CSO Facility.” Water Qual. Res. J. Canada, 39(4) 457-465.

He, C., Wood, J., and Marsalek, J. (2005). “Evolutional Design of the Inlet Structure of a High-Rate Stormwater Clarifier” Submitted to J. of Env. Eng.

Lazaro, B.J. and Lasheras J.C. (1998), “Particle dispersion in a turbulent, plane, free shear layer,” Phys. Fluids A 1, 1035

Marchioli, C. and Soldati, A. (2002). “Mechanisms for particle transfer and segregation in a turbulent boundary layer.” J. Fluid Mech. 468 283-315.

Maxworthy, T. “ Storm in a Tea Cup.” J. Appl. Mesh. 35, 453

McLaughlin, J.B. (1998). “Aerosol particle deposition in numerically simulated channel flow.” Phys. Fluids 1, 1211-1224

Nelson, C.H., Johnson, K.R. and Barber, J.H. (1987). “Gray whale and Walrus feeding excavation on the Bering shelf, Alaska.” J. Sed. Petr., 57, 419-430.

Pan, Y. & Banerjee, S. (1996). “Numerical simulation of particle interactions with wall turbulence.” Phys. Fluids 8 2733-2755.

Pedinotti, S., Mariotti, G. & Banerjee, S. (1992). “Direct numerical simulation of particle behavior in the wall region of turbulent flow in horizontal channels.” Intl. J. Multiphase Flow, 18, 927-941.

Reeks, M.W. (1983). “The transport of discrete particles in inhomogeneous turbulence.” J. Aerosol Sci. 14, 729-739

Risk, M.J. and Craig H.D. (1976). “Flatfish feeding traces in Minas Basin.” J. Sed. Petr., 467, 411-413.

Yager, P.L., Nowell, A.R.M. and Jumars, P.A. (1993). “Enhanced deposition to pits: A local food source for benthos.” J. Mar. Res., 51, 209-236

Yao, K. M. (1970). “Theoretical study of high-rate sedimentation.” Journal Water Pollution Control Federation, 42, 218-228

Yao, K. M. (1973). “Design of high-rate settlers” proc. ASCE, 99(EE5), 621-637

1.14 Tables:

Table 1: Testing results of Vortex and smooth plate array under various inflow rates and particles.

Plate Type	Inflow (l/s)	Sample Type	Settling Vel. (m/s)	Input(gm)	Recovered(gm)
Vortex	5	WT(350 μm)	0.0167	500	330.6
Vortex	8	WT(350 μm)	0.0167	500	233.3
Smooth	5	WT(350 μm)	0.0167	500	334.5
Smooth	8	WT(350 μm)	0.0167	500	234.9
Vortex	5	GB(66 μm)	0.0025	600	243.1
Vortex	8	GB(66 μm)	0.0025	600	152.5
Smooth	5	GB(66 μm)	0.0025	600	229.1
Smooth	8	GB(66 μm)	0.0025	600	120.9
Vortex	5	GB(150 μm)	0.0133	600	491.3
Vortex	8	GB(150 μm)	0.0133	600	386.4
Smooth	5	GB(150 μm)	0.0133	600	500.8
Smooth	8	GB(150 μm)	0.0133	600	353.8

Note: WT= Crushed Walnut Shell, GB=Glass Beads.

1.15 Figures

Fig. 1.1: Picture of the tested Vortex Plate in a 1500cm (L) x 50cm (W) x 60cm (D) rectangular tank with transparent glass in front and partial experiment setting.

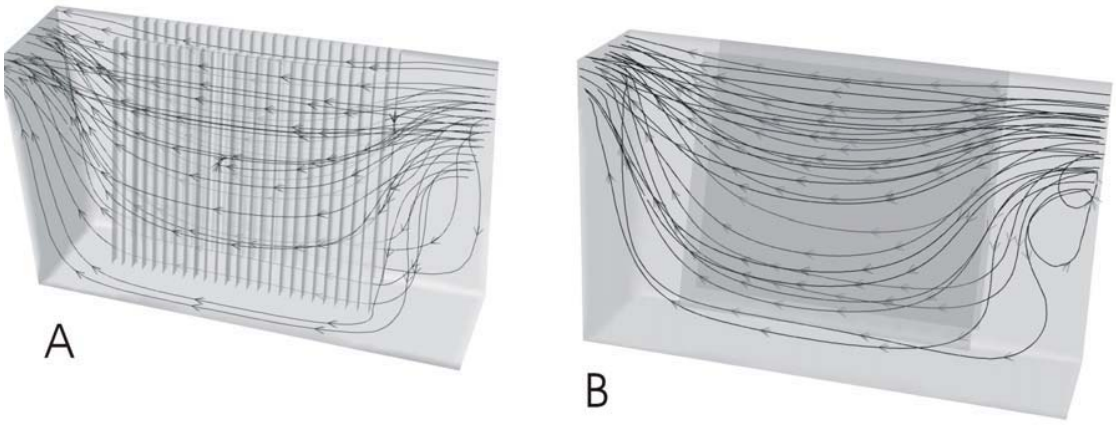

Fig. 1.2: Streamlines represent numerical simulated flow field with two particle settling enhancing plates in a top closed rectangular tank, (A) with proposed Vortex plates in the settling chamber, and (B) with two lamellar in the settling chamber.

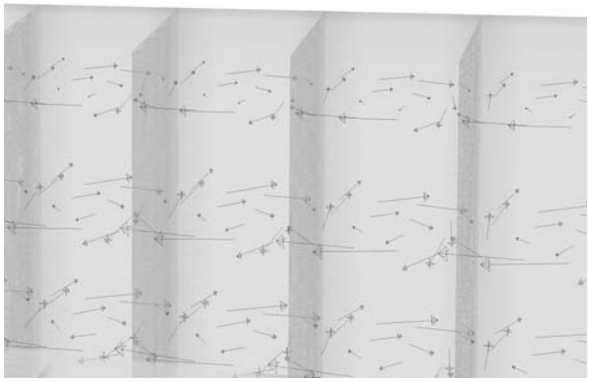

Fig. 1.3: Typical computed flow pattern in the individual long narrow slot on the surface of the proposed Vortex Plate. The strong swirl flow is generated by horizontal flow.

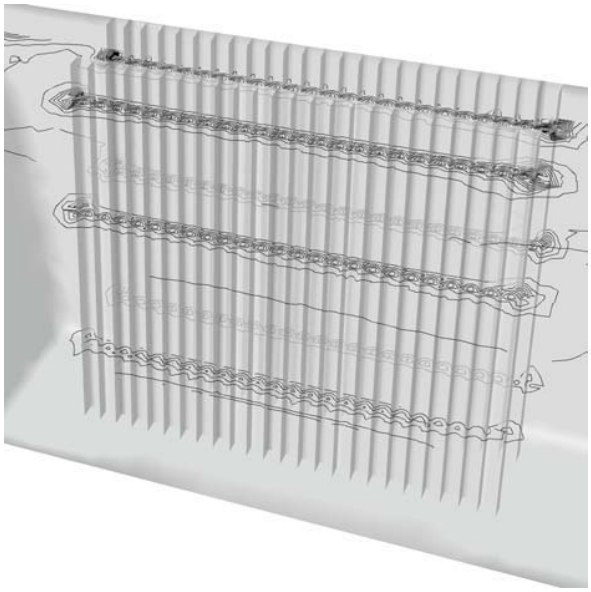

Fig. 1. 4: The vortex distribution in the vicinity of the Vortex Plate displayed with the contour lines. Density of the contour line tells the intensity of vortex.

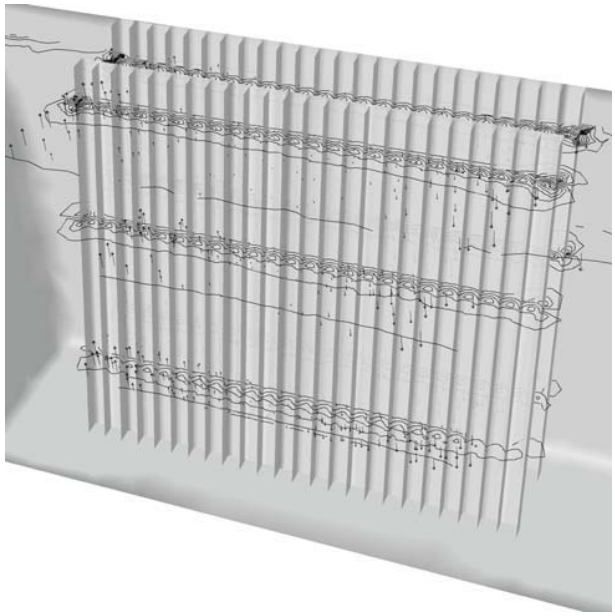

Fig. 1.5: Simulated contours of vertical velocity magnitude on vertical cross cut plan at depth 11cm, 30 cm and 45 cm from the tank bottom.

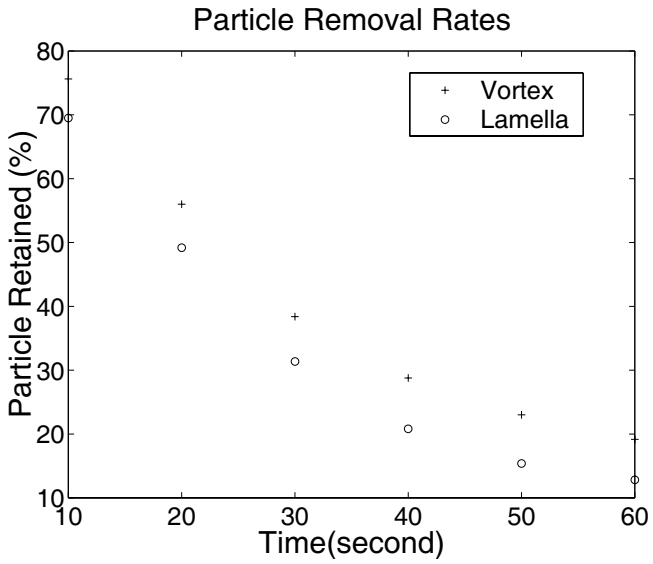

Fig. 1.6: Simulated particle removal rates of the proposed Vortex Plate and the flat smooth plate using Lagrangian particle tracking model.

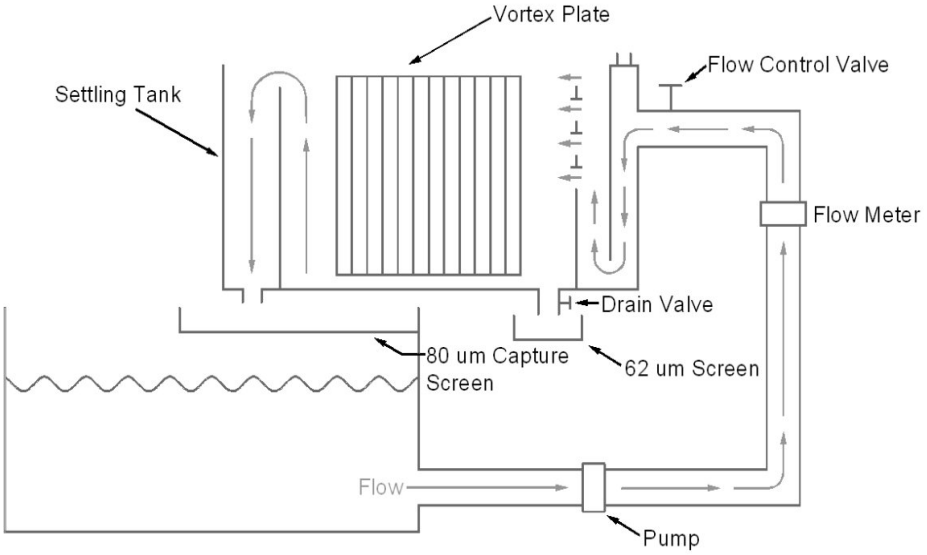

Fig. 1.7: Schematic of experiment arrangement for testing particle removal of different particle settling enhancing plates.

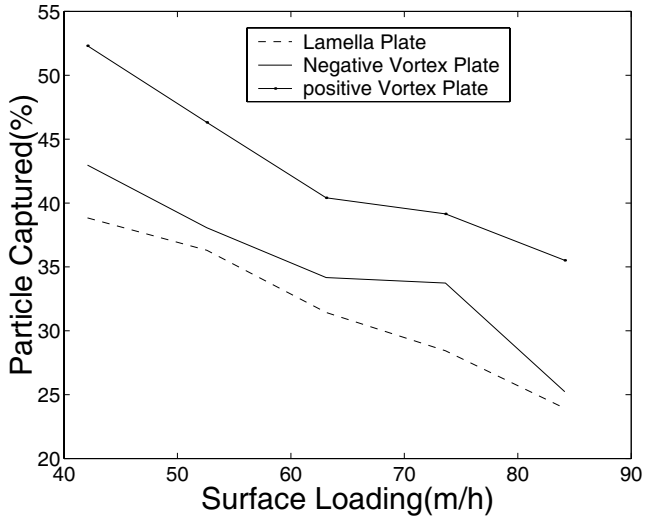

Fig. 1.8: Measured particle removal rates of the Vortex and lamellar plates under various inflow rates.

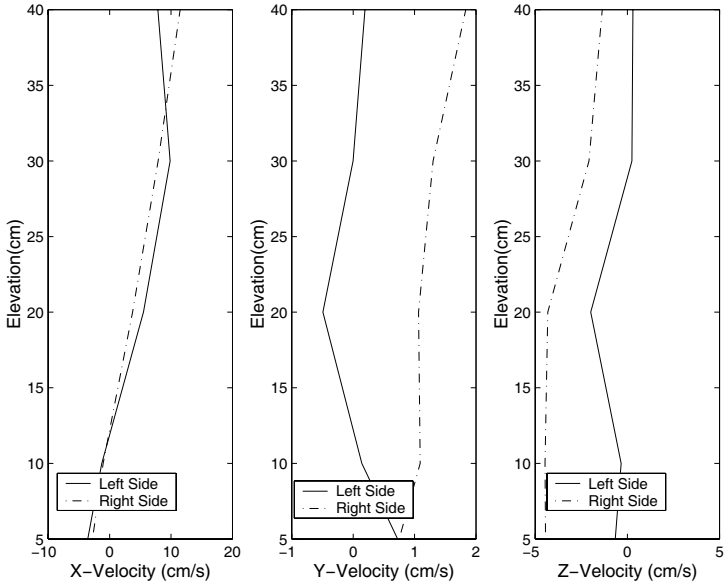

Fig. 1.9: Vertical profiles of three flow velocity components measured from 5 cm above the bottom to the top with 10cm increment at the middle section of the empty settling chamber and 5 cm away from each side wall were collected. The flow was measured before the inlet structure being fixed.

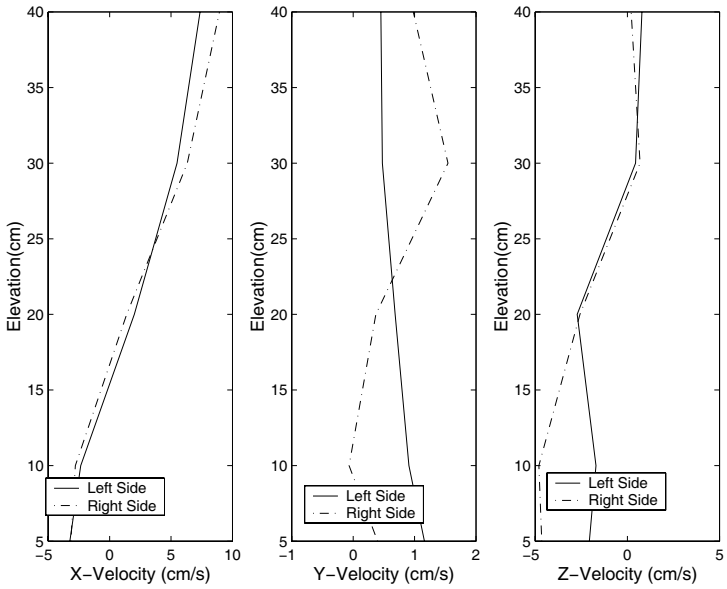

Fig. 1.10: The same flow measurement as in Fig. 1.9 except for that the flow was measured after the inlet structure being fixed.

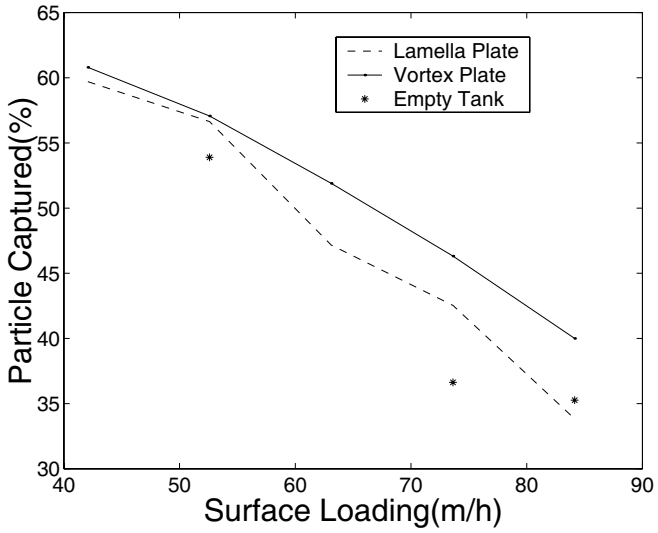

Fig. 1.11: Remeasured particle removal rates of the Vortex plate, lamellar plate and empty settling chamber under various inflow rates after the inlet structure was fixed.

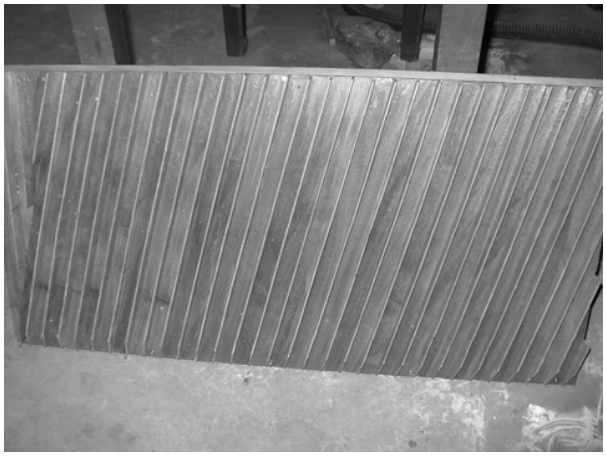

Fig. 1.12: The Vortex Plate with angled parallel slots on the flat surface. Intention of this design is to generate the downward pushing flow from horizontal incoming flow.

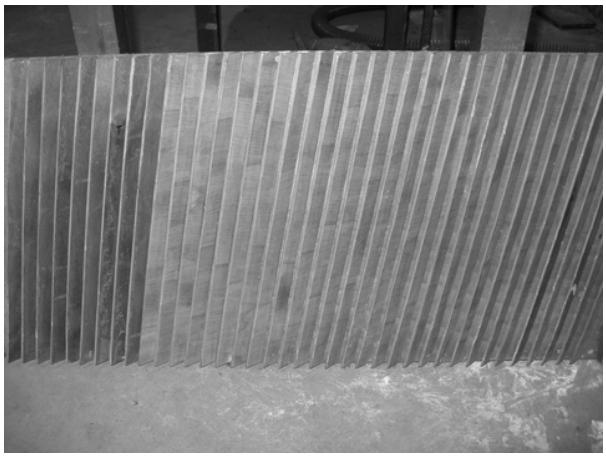

Fig. 1.13: The Vortex Plate with straight parallel slot and tilted slot wall on the flat surface. The induced vortex would be concentrated on up part of slot, and it may have less disturbance on bottom sliding particles.

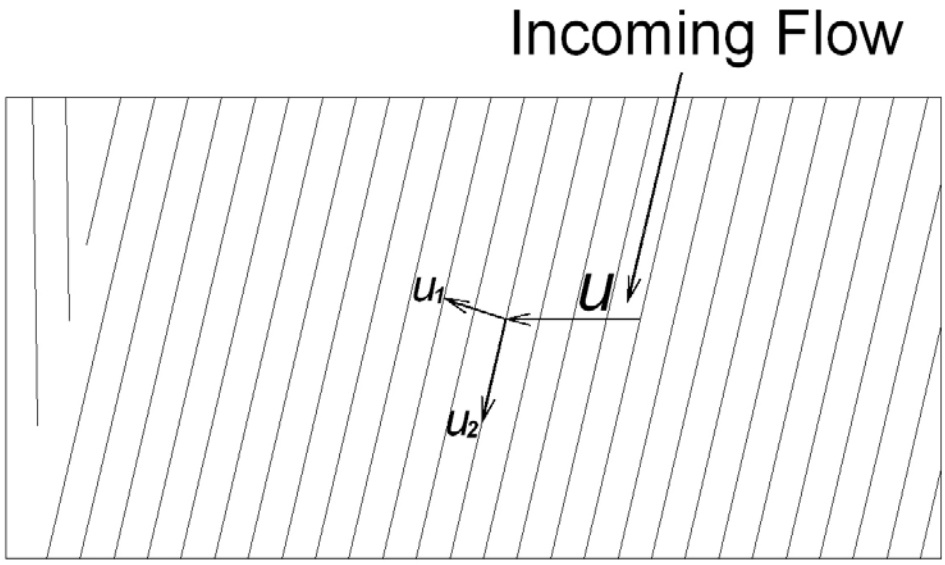

Fig. 1.14: Illustrate that an along slot downward velocity component can be generated from incoming horizontal flow when it passes through the angled parallel slot.

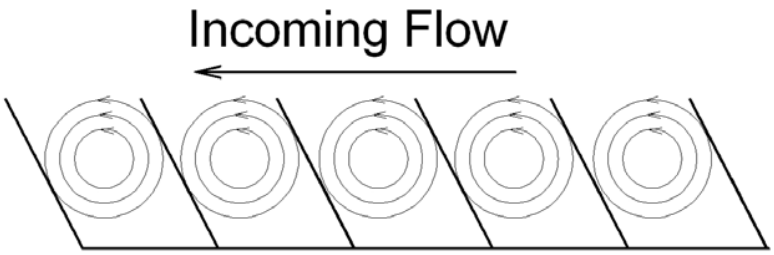

Fig. 1.15: Showing that the smaller size vortex could be generated in the slot with tilted wall, so the low edge of the vortex does not reach all the way to the bottom of slot, resulting in less chance to disturb sliding particles by above the vortex.

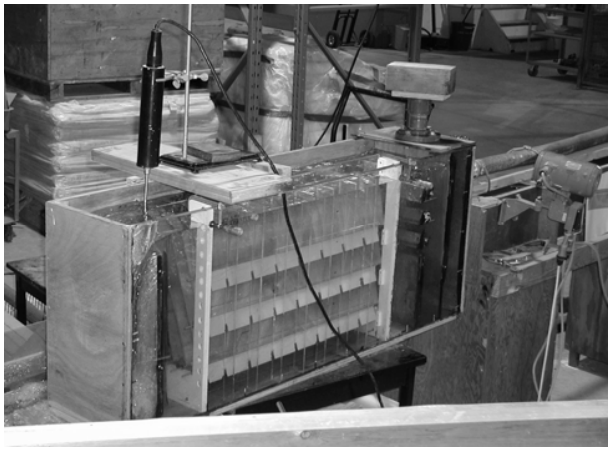

Fig. 1.16: Picture of experiment setting for testing plate array and measuring velocity in a 1500cm (L) x 50cm (W) x 60cm (D) rectangular tank with an isolated chamber.

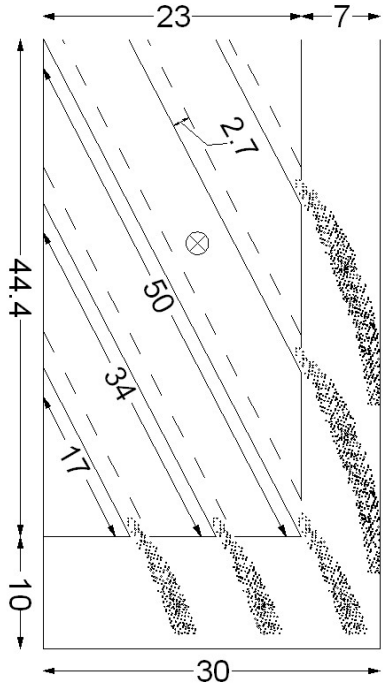

Fig. 1.17: The schematization of cross-section of plate array in the testing tank viewed from down stream. The label of the cross in a circle indicates the location of flow measurement.

Part 2: Evolutionary Design of the Inlet Structure of a High-Rate Stormwater Clarifier

2.1 Abstract:

A computational fluid dynamics (CFD) model was used for redesigning a lamellar clarifier for high-rate stormwater treatment. Flow patterns in the clarifier were simulated using a volume of fluid (VOF) model and the simulated flow fields were analysed for various layouts of the inlet structure. The results showed that the hydraulic conditions in the clarifier could be improved by spreading the flow uniformly in both the horizontal and vertical directions, and reducing vertical circulation in the clarifier by attaching horizontal trailing baffles to the top edges of the inlet opening slots. Hydraulic improvements then resulted in better solids removal efficiency. Computer simulations and field data showed that compared to the original clarifier, the new inlet design produced two benefits: (a) improved flow conditions in the settling zone and (b) greatly reduced energy head losses (increase the treatment capacity). In chemically aided clarification, the conventional clarifier with the new inlet design produced better suspended solids (SS) removal than the original conventional clarifier, even at a three times higher surface load rate. The field data also indicated that the SS removal efficiencies of the original clarifier with lamellar plates and the modified clarifier, without lamellas but with the new inlet design, were comparable. Thus, the main goal of this study, reducing maintenance (cleaning) costs of chemically aided high-rate clarification of stormwater by removing the lamellar plates, without a significant loss of settling performance, was achieved. Finally, it was noted that the numerical CFD model, compared with conventional methods of hydraulic clarifier design, was a flexible,

powerful tool providing distinct advantages with respect to the speed, efficiency and reduced analysis costs, and a better understanding of the clarifier operation.

2.2 Introduction

Settling is one of the most common unit processes applied in wastewater, combined sewer overflow (CSO) and stormwater treatment. In this process, separation of suspended solids (SS) is achieved in settling tanks (clarifiers), and this has been extensively studied for wastewater treatment applications (Krebs, 1991). There is a great wealth of information on the optimal design of wastewater clarifiers, addressing such issues as surface loading rates (SLRs) typically ranging from 1.4 to 2.5 m/h (Metcalf and Eddy, 2003), geometry of circular and rectangular clarifiers (Deininger et al., 1998; Zhou and McCorquodale, 1992), special clarifier structures including inlets, feedwells and baffles (Krebs et al., 1995; Ueberl and Hager, 1997), modes of operation with or without sludge return (Kinnear, 2000), and high-rate operation involving chemical additions and ballasted flocculation (Metcalf and Eddy, 2003).

The settling of stormwater differs from typical wastewater settling with respect to the lower concentrations of suspended solids (typically 100 mg/L – USEPA, 1983), high and variable SLRs of settling facilities (50 m/h or more), and the expected levels of suspended solids removal ranging from 60 to 80% (MOE, 2003). Consequently, only some of the information produced primarily for wastewater clarifiers can be applied in stormwater settling and further research is needed. In view of the low TSS concentrations, stormwater clarifiers behave similarly to primary clarifiers and the density effects typical for final clarifiers can be neglected (Krebs et al., 1998). The

intermittent use of stormwater settling facilities imposes cost constraints on such facilities, which may be achievable with high-rate clarification techniques employing lamella plates or tube settlers and chemical addition.

Stormwater settling in various facilities was described extensively in the literature, as reviewed e.g., by Wood et al. (2005). However, the literature data are of limited help, because the clarifier performance for low SS concentrations without density effects are based on such factors as tank geometry; surface-loading rate; inlet, outlet and settling zone configurations; sludge collection; and incoming solids density and settling regime (Kinnear, 2000). These are typically not reported in the literature, because for most of these factors there is no simple way to describe them. Most of these factors were kept constant in the earlier phases of the study described here, and the TSS removals were reported as 5, 26 and 84%, for a conventional clarifier (SLR=15 m/h), a lamella clarifier (SLR=15 m/h), and a lamella clarifier with polymer addition at 4 mg/L (SLRs ranging from 10 to 36 m/h) (Wood et al. 2005).

While lamellar settling with polymer additions exceeded the target TSS removal (60-80%), there were concerns about laborious cleaning of lamellar plates after every storm event. To eliminate this expense, the lamella plates had to be removed while improving the clarifier hydraulics, in order to maintain the target TSS removal. Towards this end, clarifier modifications, which focused on the redesign of the inlet zone, were carried out in this study using a numerical model. The modified clarifier performance in SS removal was verified in two ways: (a) by computational fluid dynamics (CFD) simulations of velocity fields and particle transport for various clarifier configurations, and (b) by comparing the actual field performance of the modified and original clarifiers in SS

removal. Such analyses served to verify the performance of a new inlet design and to demonstrate the usefulness of CFD modelling in (high-rate primary) clarifier design.

2.3 Clarifier Studies

The study partners, the City of Toronto, the National Water Research Institute (NWRI, Environment Canada) and the Ministry of the Environment (MOE) have been operating a pilot-scale demonstration project on high-rate stormwater clarification with a polymeric flocculant addition, which holds a promise of cost-effective mitigation of stormwater pollution (Wood et al., 2005). The main objective of this project was to evaluate an innovative compact treatment of stormwater flows and thereby support the implementation of the City of Toronto's Wet-Weather Flow Management Master Plan.

The focus of the stormwater treatment study was to evaluate the removal of suspended solids and associated pollutants by flocculant-aided clarification, under controlled experimental conditions. Constant flow rate experiments were conducted in a pilot-scale clarifier vessel with and without lamellar plates, and with and without varying dosages of a cationic polymer flocculant. At high surface loads, the cross-flow lamellar plates represented an essential component of the process apparatus. The total suspended solids (TSS) removal performance of the clarifier during the 2001 to 2003 operating seasons was encouraging (Wood et al., 2005), but with more than 50 stormwater events treated annually the cost and difficulty of cleaning the upper and lower surfaces of the lamellar plates was of concern. Therefore, the study team examined the feasibility of removing the lamellas, modifying the clarifier inlet structure, and evaluating the resulting flow patterns in the clarifier by numerical modeling.

The dimensions of the commercially supplied clarifier vessel are 3 x 1.4 x 2 m (length x width x depth) and its configuration is shown in Fig. 2.1. The clarifier vessel consists of three comparably sized zones. The original inlet zone was fitted with a series of horizontal louvers and vertical baffles designed to promote a uniform, low-turbulence flow field across the separation zone, which contained a removable lamellar plate pack. The outlet (withdrawal) zone, which was not changed in the new design, contains a skimmer plate for the retention of floating material. The relatively fast inflow enters the clarifier through two 100 mm diameter pipes and impacts the horizontal inlet deflector louvers. The function of these louvers is to reduce the inflow speed and disperse the flow by angled baffles (louvers) with small openings that can be seen in Fig. 2.1. The potential problem associated with this configuration is that flow direction distribution at the deflector exit is highly non-uniform and generates strong turbulence. However, at the same time this arrangement increases the energy head loss.

After flow passes through the inlet louvers, it enters the inflow energy dissipater, which is shown in enlarged detail in the upper left corner of Fig. 2.1. The dissipater consists of two rows of vertical baffles placed in two parallel vertical planes, 50 mm apart. The two rows of baffles are offset so that the downstream baffles block the flow passing through the slots between the upstream baffles. However, the flow exiting from the downstream baffles contains lateral velocity components disrupting flow conditions in the settling zone. The dissipater also causes a large head loss, which limits the hydraulic capacity of the clarifier. The maximum SLR in the original clarifier before reducing the height of the inlet energy dissipater was about 30 m/h, well below the proposed maximum experimental rate of 50 m/h. Unsatisfactory hydraulic conditions in the clarifier with

respect to limited flow capacity, high turbulence and high velocity fluctuations were reported by Marsalek and Doede (1997), who measured 3D velocity distributions in the clarifier. These unfavourable hydraulic conditions were improved by using a removable lamellar plate pack, which is shown in Fig. 2.2.

The principle of suspended solids removal in lamellar plate clarifiers is well described in the literature (Metcalf and Eddy, 2003) and was further tested in the original clarifier, where the lamellar plates were found very effective in improving suspended solids removal (Wood et al., 2005). However, the original lamellar plate pack was not designed for easy cleaning of the lamellas when polymer flocculants are used. Polymer addition makes the produced sludge sticky and the cleaning of plate undersides is very labourious. Furthermore, the higher surface loading rates attainable with flocculants generate several times more sludge than unaided tests.

2.4 Hydraulic design considerations

High-rate clarifier design and particle separation considerations are a challenge because of high flow volumes and complex flow conditions, large hydraulic head loss, and fast flows with associated high turbulent energy in the particle separation zone. The inlet structure of a high-rate clarifier needs to dissipate the turbulent energy within a small space without sacrificing too much head loss and plays a very important role in determining the flow characteristics in the downstream particle separation zone.

In the conventional method (Metcalf and Eddy 2003) of settling tank design, the smallest settleable particle size under the expected flow rate is selected first, and then the

corresponding settling (terminal) velocity v_c is calculated according to the particle physical properties from the Stokes law as

$$v_c = \frac{g(sg_p - 1)d_p^2}{18\upsilon} \qquad (1)$$

Where g, sg_p and d_p are the gravity acceleration constant, particle specific gravity, and diameter of the smallest settleable particle, respectively, and υ is the kinematic viscosity. The particle settling may occur in different flow regimes, laminar, transitional or turbulent, and adjustments of velocities calculated from equation (1), valid for laminar flow, may be required (Metcalf and Eddy, 2003).

Finally, based on the terminal velocity, the size of the settling tank can be estimated so that all particles with settling velocities equal to or greater than terminal velocity v_c will settle, and particles with settling velocities smaller than v_c either pass through the tank or will be partly removed. The terminal velocity, residence time (RT), and settling tank depth (D) are related as follows:

$$v_c = \frac{D}{RT} \qquad (2)$$

and RT can be estimated by the formula:

$$\mathrm{RT} = \frac{V}{Q} \qquad (3)$$

Where Q and V are the inflow rate and the tank volume, respectively. Equation (2) can be expressed in terms of the surface loading rate (SLR) by substituting Equation (3) for RT and assuming a rectangular tank, for which $V = D \bullet A$, where A is the surface area of the tank:

$$v_c = \frac{D}{\frac{V}{Q}} = \frac{Q}{A} = SLR \qquad (4)$$

Therefore, the surface area, A, can be easily obtained from above relationship after terminal velocity v_c and treated flow rate have been determined. However, equation (4) also implies that the settling tank depth is unimportant in settling tank design, which is obviously not true in practice. The problem appears to be that in the estimation of the SLR, it is assumed that the entire flow passes through the settling tank along the tank surface. However, in the residence time calculation, it assumes that the active flow would occupy the whole tank volume. Obviously, neither assumption reflects reality and is questionable (Zhou and McCorquodale, 1992; Bretscher et al., 1992). Thus traditional design methods, which treat the various physical variables as simple averaged parameters without considering the hydrodynamic behaviour of the fluid particle carrier are inadequate for producing an optimal clarifier design, especially, for particle removal at high flow rates with high turbulence.

2.5 Numerical Modeling Strategies

Models based on a mass-balance analysis are widely used to investigate bulk hydraulic flow characteristics and performance of primary and secondary clarifiers (Ott 1995; Dochain and Vanrolleghem 2001) since the flow speed and turbulence are usually small in those facilities. However, they are inadequate to diagnose detailed hydraulic conditions, turbulent intensity and other critical information needed to optimize the performance of different zones of a clarifier. Fluid-dynamic models (Kluck 1996; Krebs 1995; Pollert and Stransky 2003) have also been used to study various simple low SLR stormwater

settling facilities. Most of them only focused on improving hydraulic conditions without further analyzing particle transport modeling.

In this study, commercially available CFD software was used to evaluate alternative clarifier designs by simulating flow conditions and particle transport in different structural configurations of the clarifier. The main objective of numerical simulations was to correct the observed problems in the original clarifier, rather than comparing the original and new designs. Therefore, simulation of hydraulic conditions in the original clarifier was not addressed in this study.

In order to calculate a 3-dimensional flow field, resolve the air and water interface, account for the hydraulic pressure effect on flow behaviour and simulate mass particle transport in a structure with complex geometry within a reasonable time frame, a two-stage approach was adopted by ignoring the interaction between the particles and their carrier. Thus, flow patterns were simulated first by means of a volume of fluid (VOF) model and subsequently formed a basis for simulating particle transport by the discrete phase (DP) model. This approach was found feasible by Adamson et al. (2003) for flows with low SS concentrations (< 1000 mg/L), which would be met in most practical situations.

After obtaining the flow field from the VOF model, the particle transport model was run on the basis of flow simulation data. The Lagrangian particle tracking method was used to track individual particle movement by calculating the balance of forces on the particle, which is written in a Lagrangian reference frame. Since this procedure includes more forces in the calculation of particle movement, it usually gives a better prediction of particle movement than the models using particle concentration changes to simulate the

particle transport, but with higher computing times. The Lagrangian particle tracking approach assumes that the suspended particles are spherical and do not interact with each other. Even though the actual stormwater solids might not be discrete, or spherical, it was felt that this approach would still give good insight into the hydrodynamics of suspended solids inside the clarifier. Furthermore, since the focus of this study is to examine the particle removal rate for different inlet structures, it is not necessary to know the absolute particle removal rates for specific structural configurations. Therefore, the verification of simulated absolute particle removal rates using the particle tracking model was omitted. Also, in order to simulate flow behaviour and particle transport in realistic time, 30 minute simulations for real events were carried out for both flow hydrodynamic and particle tracking simulations. Such durations of simulations were sufficient to show the removal rate variations for different designs.

2.6 New Clarifier Inlet Zone Designs

In the original rectangular horizontal-flow clarifier (Fig. 2.1), the suspension enters at the upstream end and the treated water exits at the downstream end. The inlet flow structure must quickly generate a flow distribution that maximizes the opportunity for particles to settle. Therefore, the redesigning process started with modifying the internal inlet zone structure of the original clarifier. As stated earlier, the lamellar pack, one of which functions is to condition clarifier flow, was to be excluded in the new design. Therefore, it was essential that the new inlet zone structure provided maximum dissipation of kinetic energy and equalized the flow distribution over a minimum distance.

After many numerical simulations, three inlet designs with similar "U-shaped" structures (Figs. 2.3-2.5) were selected for more detailed studies. For all three proposed inlets, fast inflows exiting from three 0.075 m diameter pipes strike an impact baffle, which is 0.20 m downstream of the inlet pipe ports. The flow is forced downward through the entrance section of the duct, for about 0.9 m, and then it turns upward into the exit section of the duct through a bottom opening slot which is 0.25 m high. In the exit section, flow moves upward and this process should convert some turbulent kinetic energy into gravity potential energy. The exit duct has the same width as the entrance duct, 0.2 m (i.e., measured in the longitudinal direction), but the size of the bottom opening slot connecting the two duct sections is slightly larger than the width of the two side ducts to account for additional hydraulic resistance in the right-angle corner. In such an arrangement, the flow would travel at the same speed along the direction of the inlet structure with minimum lateral movement, which reduces the risk of generating turbulence. The structural differences among the three inlet designs were: (a) presence or absence of openings in the wall separating the inlet duct and the settling zone, and (b) configurations of the openings, which strongly influence flow conditions in the particle settling zone as described below.

In Design 1, there are no slot openings in the wall between the inlet duct and the settling zone (Fig. 2.3A), which is a common design feature of inlet structures used for releasing flow into the settling tank. One of the possible hydraulic advantages to this configuration is that there is little disturbance of the bottom sediment under low flow rates because the main flow stream is far from the vessel bottom. However, for high flows this reasoning may not be so plausible and has to be verified by numerical simulations. It can be seen

from the simulated velocity pattern in Fig. 2.3B that without any openings in the separation wall, most of the flow passes directly through the clarifier in a very narrow surface layer. There are large recirculation zones in the clarifier, with poor hydraulic utilization of the clarifier volume, and this contributes to high flow velocities in the fast-flow surface layer. Therefore, for most of the flow, the hydraulic residence time is short, which explains the low simulated particle capture rates indicated by cross symbols in Fig. 2.6.

Design 2 (Fig. 2.4A) features three horizontal slot openings spanning the full width of the clarifier. These slots were proposed on the basis of many numerical simulations discussed later. The height of each of the three slot openings is 0.10 m, the space between two adjacent slots is formed by solid vertical walls, 0.10 m high. The openings are used to distribute the inflow uniformly in the vertical direction, instead of allowing the entire flow to enter the particle settling zone at the top of the wall, which would utilize only a small cross-sectional area of the clarifier and result in high velocity flows and shorter residence times. The size of the slot openings has a large influence on flow distribution along the vertical axis and it is difficult to choose the "best" size, because of the sensitivity to the inflow rate. The 0.10 m opening was chosen as the final size on the basis of numerical simulations with SLRs of 50 m/h. The simulated velocity pattern showed that the region of the "active" flow in Design 2 becomes much larger than in Design 1, and this feature should reduce the flow speed and increase the particle settling rate. The simulated results on particle removal rates are shown in Fig. 2.6 as circle symbols, and indicate some improvement when compared to Design 1. However, a closer examination of the velocity pattern in Fig. 2.4B shows that the flows exiting from

the three slot openings move upward, rather than longitudinally. This upward flow is undesirable, because (a) it reduces the thickness of the active flow layer, with most flow passing through the clarifier in the surface layer, and (b) it induces a strong, tank-scale vertical circulation due to the negative pressure generated from upwards moving flow in the vicinity of the inlet, which may disturb bottom sludge. In order to improve this flow pattern, a third set of simulations with modified opening slot configurations were carried out.

Design 3 (Fig. 2.5A) is similar to Design 2, but with horizontal trailing baffles added at the top of each slot opening to force the flow exiting the slots to travel in the horizontal direction. The length of these baffles in the horizontal direction, as used in simulations, was about 0.15 m (see Fig. 2.5A). When comparing the flow pattern in Fig. 2.4B (Design 2) to that in Fig. 2.5A (Design 3), a more uniform flow distribution becomes apparent in the latter case. The size and strength of the vertical eddy was reduced, which resulted in better particle removals presented as a solid line in Fig. 2.6.

To further improve flow conditions by directing flow in the longitudinal direction and suppressing lateral flow components, three vertical baffles were placed in the downward and upward inlet ducts, dividing them into four sub-channels. In such a configuration common to Designs 1-3, the turbulence associated with horizontal flow movement would be minimized.

In spite of the hydraulic improvements described above, even in Design 3, the flow distribution along the vertical axis is highly non-uniform, with only 50% of the total flow passing through the three slot openings and the remaining 50% over the top, for the simulated case with an inflow corresponding to SLR of 26 m/h, and even less (26%) for a

larger SLR of 50 m/h. Forcing more flow through the horizontal slot openings should further reduce the longitudinal velocities in the clarifier and possibly improve the opportunity for particle settling. This could be achieved by extending the horizontal baffles (Design 3) upstream inside the duct. The length of such extensions would vary and increase from bottom to top. The optimal flow distribution among the three openings and the top for maximum particle removal is a complex issue and highly depends on the inflow rates and other factors, which will be instigated in future.

To further understand the particle removal performance for the three proposed inlet configurations, the flow residence time was calculated and used as a performance indicator. Obviously, the conventional calculation of clarifier residence time (volume/flow rate) yields the same residence time for all flow conditions and does not provide any meaningful information for further analysis. Since the particle settling zone was sub-divided into three similar narrower chambers, the hydraulic conditions among them would not be expected to vary much, and flow conditions in the middle chamber should be representative of those in the adjacent chambers. The velocity distributions along the clarifier longitudinal axis are shown in Figs. 2.7-2.9, indicating the vertical profiles in the settling zone near the inlet, in the centre and near the outlet, respectively. Fig. 2.7 displays the flow velocity profile near the inlet and shows that Design 1 produces the largest surface velocity (concentrated in the top 0.2 m surface layer) as indicated by cross symbols. As expected, in Design 3 (i.e., an inlet with three openings with horizontal trailing baffles), the active flow occupies a much larger portion of the flow depth with lower velocities represented by asterisk symbols in Fig 2.7. Design 2, designated by circular symbols in Figs. 2.7-2.9, shows an interesting feature occurring in

front of the solid walls between the adjacent slot openings (their locations can be identified by zero velocities corresponding to the Design 3 curve) - the velocity is larger than that in front of the slot openings, which indicates a strong upwelling flow from an opening without a horizontal trailing baffle.

When flows reach the mid point of the clarifier length (after travelling about 1. m), the velocity profiles shown in Fig. 2.8 are similar to that near the inlet in the top half of the settling zone. A steep velocity gradient is observed for both Design 1 and Design 2, with maximum velocities much larger than in the case of Design 3. Strong opposite flows generated in Designs 1 and 2 indicate the presence of a strong vertical circulation. The maximum negative velocity near the bottom indicates that the vertical eddy extends all way to the sediment bed, which may potentially resuspend some of the settled particles. However, with the addition of trailing horizontal baffles (Design 3) the flow conditions were significantly improved, which can be documented by small variation in the velocity distribution curve with a much smaller range of velocities (Fig. 2.8) for all depths, and the absence of a large vertical eddy. When the flow reached the outlet after travelling another 1 m the velocity profiles maintained the same magnitude as that found at the mid point of the tank, except that the maximum velocities were reduced due to flow momentum dissipation, as seen in Fig. 2.9. Because of the scum baffle (or outlet tank wall), all velocity distribution curves indicate a flow direction reversal near the surface. The comparison of locations of the maximum negative velocities (along the vertical) for Designs 1 and 2 in Fig. 2.8 to those in Fig. 2.9, indicates that the maximum velocities in the latter case are found at higher depths, and this shows that the flow is at the edge of a large vertical eddy.

Fig. 2.10 shows the lateral distribution of longitudinal velocities at the mid-point of the tank. It is obvious that surface velocities in Design 3 are much smaller than those in the other two designs, because of the horizontal baffles on top of the openings forcing the flow to spread across a larger vertical space. Design 2 shows only a marginal surface flow velocity reduction compared to Design 1. Small lateral variations in flow velocities indicate that flows in the longitudinal plane of the each settling zone are relatively similar and uniform, which is favourable for particle settling.

Using the information in Figs. 2.7-2.9, the flow detention time can be estimated for the three different inlet structures. As a result of the complex flow patterns in the settling chamber, some simplifications have to be made before the detention time can be estimated. From Figs. 2.7-2.9 it can be seen that the vertical circulation exists in all the three designs. After this motion is established it may be reasonable to assume that the new inflow only provides the momentum to keep the circulation continuing without participating recirculation in the settling zone and negative velocity could be ignored in flow detention calculation. It can be approximated in Figs. 2.7-2.9 that the positive velocities occupy a space from the depth of 0.8m to water surface (1.6m) in all three locations for all three designs. The zero velocity point is about 0.8 m below the water surface, which is about the same depth as that of the lowest opening slot. Since the sections of all positive velocities are relatively linear, the detention time can be easily calculated by dividing the tank length by the averaged positive velocity. The calculated detention time is 23, 23 and 55 seconds for Designs 1, 2 and 3, respectively. It is not surprising to see that Design 1 and Design 2 have the same flow detention time since they share similar velocity profiles in the settling zone. With a minor modification of the inlet

structure, consisting in adding the horizontal baffle on top of each opening slot, the flow detention time can be doubled. Such a modification is more efficient than doubling the tank length, because it also minimizes the vertical circulation generated by fast surface flow.

Having addressed the hydraulic flow conditions in the clarifier settling zone for each inlet structure design, the remaining concern for the U-shaped inlet was the conveyance of large particles which may accumulate in the inlet channel during clarifier operation. These materials would reduce the effective channel cross-section, and thereby increase hydraulic resistance and ultimately cause a partial blockage of the inlet channel. This problem had to be addressed before the proposed clarifier inlet design could be implemented in the pilot installation.

The pilot clarifier was fed directly with stormwater by a pump, without grit removal. In field operation, gravel, brick and concrete chips were transported into the clarifier. During field tests with inlet Design 3, debris particles accumulated on the bottom horizontal surface (see Fig. 2.5) because of dead flow zones in the compartment corners. The initial inlet design included a few circular holes in the bottom of the U shaped inlet channel for grit removal, which were blocked quickly and made cleaning the vessel at the end of a test difficult.

After many additional numerical simulations, the most promising and practical design for continuously transporting large particles (grit and gravel) out of the inlet channel was to use part of the available fluid flow energy for this purpose. The revised design featured a V-shaped floor, with a 35 mm slot opening in the centre, extending across the full vessel width (Fig. 2.11). In order to reduce simulation times, only the inlet section and a small

portion of the settling zone were included in numerical simulations. Large grit particles were directed into the sludge zone via the bottom grit outlet of the inlet structure, and continued towards an inlet bottom wall, which prevented excessive flow from directly entering the settling zone and potentially stirring up settled sludge. Furthermore, an existing vertical baffle could be employed to prevent flow passing through the grit opening moving longitudinally into the vessel. This original vertical baffle was not extended to the tank bottom because the captured material was removed via a sludge wasting outlet situated at the upstream end of the clarifier. The size of the opening between the vertical baffle and floor of the clarifier is about 0.3 m which could be retrofitted with a sliding gate and closed if there is too much flow passing through during storm events. However, in field trials it was found that the bottom opening of this lateral tank wall became blocked by the accumulated sediment soon after the event started. The flow pattern in the inlet and part of the settling zone with the modified inlet structure is also shown in Fig 2.11 with 3-dimensional velocity vectors. Simulations at a flow rate of 60 L/s show that about 16% of total inflow passes through the inlet structure grit discharge slot.

2.7 Clarifier Performance in Stormwater Treatment

In a pilot-scale demonstration project of high-rate treatment of stormwater by clarification with a polymeric flocculant aid, the modified clarifier with the newly developed inlet structure (Design 3) was built and operated on line. In this project, suspended solids removals were measured under various inflow rates, polymer dosages and clarifier structure configurations during a four 4 year period study (Wood et al.,

2005). The clarifier performance data discussed here focus just on the performance of the clarifier with the lamella pack and the modified clarifier with a redesigned inlet. Details of the pilot installation, stormwater characteristics and treatment results can be found elsewhere (Wood et al., 2005).

A comparison of chemically aided lamellar plate clarification, at a total vessel SLR of 35 m/h, and conventional clarification (without the lamellar plate pack) at a total vessel SLR of 43 m/h in the modified clarifier with the new inlet baffle system (Design 3) is presented in Fig. 2.12. Total suspended solids (TSS) concentrations are indicated for samples of the influent (raw stormwater) and polymer treated effluents of the lamellar and conventional clarification processes. Each curve represents cumulative frequency of non-exceedance for "n" grab samples (n is listed in the legend) collected during storm events at 10 minute intervals and analysed for TSS. All tests were conducted at a constant rate of inflow, in a steady state mode. Both the lamellar plate clarifier and conventional clarifier tests employed a polymer dosage of 4 mg/L. The lamellar plate clarification test series shown in Fig. 2.12 totalled 56 hours of operation during 11 stormwater events, while the conventional clarifier test series was operated for 49 hours during 13 stormwater events. Stormwater concentrations of TSS for the lamellar plate and conventional clarification tests were comparable during the test periods. The overall mean effluent TSS concentration of the lamellar test series was 57 mg/L while that of the conventional clarification effluent was 49 mg/L.

In the earlier conventional clarification tests (prior to the installation of the new clarifier inlet baffle system), seven tests conducted with the conventional clarifier at 4 mg/L polymer dosage and a total vessel surface load of 15 m/h, produced an average of 67%

TSS removal (Wood et al., 2005). Thirteen tests completed in 2004 with the new clarifier inlet baffle system at a 4 mg/L polymer dosage were conducted at a total vessel surface load of 43 m/h and the average TSS removal efficiency was 77%. Thus the new design offers a 10 % improvement in TSS removal compared with the conventional clarifier even with a surface loading rate which was almost three times higher.

2.8 Conclusions

A CFD model was found to be an effective tool for the examination of alternative inlet structures for a high-rate clarifier. A VOF model was used to simulate flow patterns in the clarifier and the flow fields simulated for various inlet structures were analysed. To select the most favourable flow conditions for suspended particle removal among the various inlet configurations, a particle tracking model was applied to determine particle removal rates. The results showed that the hydraulic conditions in the original clarifier could be improved by spreading the flow in both the horizontal and vertical directions uniformly and reducing vertical circulation flow with the addition of horizontal trailing baffles on top of each flow opening slot. This resulted in better particle removal efficiency. Computer simulations and field data showed that, compared to the original clarifier (with or without lamellar plates), the new inlet design has two advantages: (a) improved flow conditions in the settling zone inducing more effective settling, and (b) greatly reduced energy head losses. In chemically aided clarification, the conventional clarifier with the new inlet design produced better suspended solids (SS) removal than the original conventional clarifier, even at three times the surface loading rate. The field data also indicated that the TSS removal efficiencies of the original clarifier with lamellar

plates and the clarifier without lamellas but with the new inlet design were comparable. Thus, the main goal of this study, reducing maintenance costs by removing lamellas, but without sacrificing settling efficiency, has been achieved. Finally, the numerical CFD model, compared with conventional hydraulic design methods, was found to be a powerful tool providing distinct advantages with respect to the speed, efficiency and lower costs of analysis, and a better understanding of the clarifier operation.

2.9 Acknowledgements:

The support received from Environment Canada's Great Lakes Sustainability Fund (GLSF), Sandra Kok (GLSF, Environment Canada), Mingdi Yang and Patrick Chessie (The City of Toronto), and Bill Warrender and Brian Taylor of the NWRI Research Support Branch is greatly appreciated.

2.10 Notation

The following symbols are used in study 2:

Q = inflow rate;

A = tank surface area;

V = tank volume;

D = tank depth;

g = gravity acceleration constant;

sg_p = particle specific gravity;

d_p = smallest particle diameter;

υ = kinematic viscosity

v_c = terminal velocity.

2.11 References

Adamson A, Stovin V, Bergdahl L. (2003). Bed shear stress boundary condition for storage tank sedimentation. J. Environ. Eng. 129(7):651-658.

Bretscher, U., Krebs, P. and Hager, W.H. (1992). Improvement of flow in final settling tanks. J. Environ. Engng, 118(3): 307-321.

Deininger, A., Holthausen, E. and Wilderer, A. (1998). Velocity and solids distribution in circular secondary clarifiers: full scale measurement and numerical modeling. Water Res. 32: 2951-2958.

Dochain, D. and Vanrolleghem, 2001. "Dynamical Modeling and Estimation in Wastewater Treatment Processes." Published by IWA Publishing, Alliance HOUSE, 12 Caxton Street, London, UK.

Kinnear, D.J. (2000). Evaluating secondary clarifier capacity and performance. Proc. 2000 Florida Water Resources Conference, Tampa, Fl.

Kluck, J. (1996). "Design of Storm Water Settling Tanks for CSOs" 7th International Conference on Urban Storm Drainage Hannover, Germany.

Krebs, P. The hydraulics of final settling tanks. (1991). Wat. Sci. Tech., 23: 1037-1046.

Krebs, P. Success and shortcomings of clarifier modeling. (1995). Wat. Sci. Tech., 31(2): 181-191.

Krebs, P., Vischer, D. and Gujer W. (1995). "Inlet-Structure Design for Clarifiers." J. Envir. Engrg. 121(8) 558-564.

Krebs, P., Armbruster, M. and Rodi, W. (1998). Laboratory experiments of buoyancy-influenced flow in clarifiers. J. Hydraulic Res., 36(5): 831-851.

Marsalek, J. and Doede, D. (1997). Hydraulic assessment of the plate clarifier: flow capacity and outflow zone velocity field. NWRI technical Note AEPB-TN-97-002, National Water Research Institute, Burlington, Ontario.

Metcalf & Eddy, Inc., (2003). "Wastewater Engineering Treatment and Reuse", 4th ed., McGraw-Hill, New York, NY.

Ministry of the Environment (MOE) (2003). Stormwater management planning and design manual. MOE, Toronto, Ontario.

Ott, C. R., (1995). "Numerical Approach to Clarifier Operation According to Flux Theory." J. Envir. Engrg. 121(7) 544-545

Pollert, J. and Stransky, D. (2003). "Combination of computational techniques – evaluation of CSO efficiency for suspended solids separation." Water Sci. Technol., 47(4): 157-166.

Ueberl, J. and Hager, W. H., 1997. "Improved Design of Final Settling Tanks." J. Envir. Engrg. 123(3) 259-268

U.S. Environmental Protection Agency (EPA) (1983). Final report of the nation-wide urban runoff program, Vol. I. U.S. EPA, Washington, D.C., available from NTIS as PB84-185552.

Wood, J., He, C., Rochfort, Q. Marsalek, J., Seto, P., Yang, M., Chessie, P. and Kok, S. (2005), " High-rate Stormwater clarification with polymeric flocculant addition." Water Sci. Tech., 51(2): 79-88.

Zhou, S. and McCorquodale, J.A. (1992). Modeling of rectangular settling tanks. J. of Hydraulic Engng, 118(10): 1391-1405.

2.12 Figures

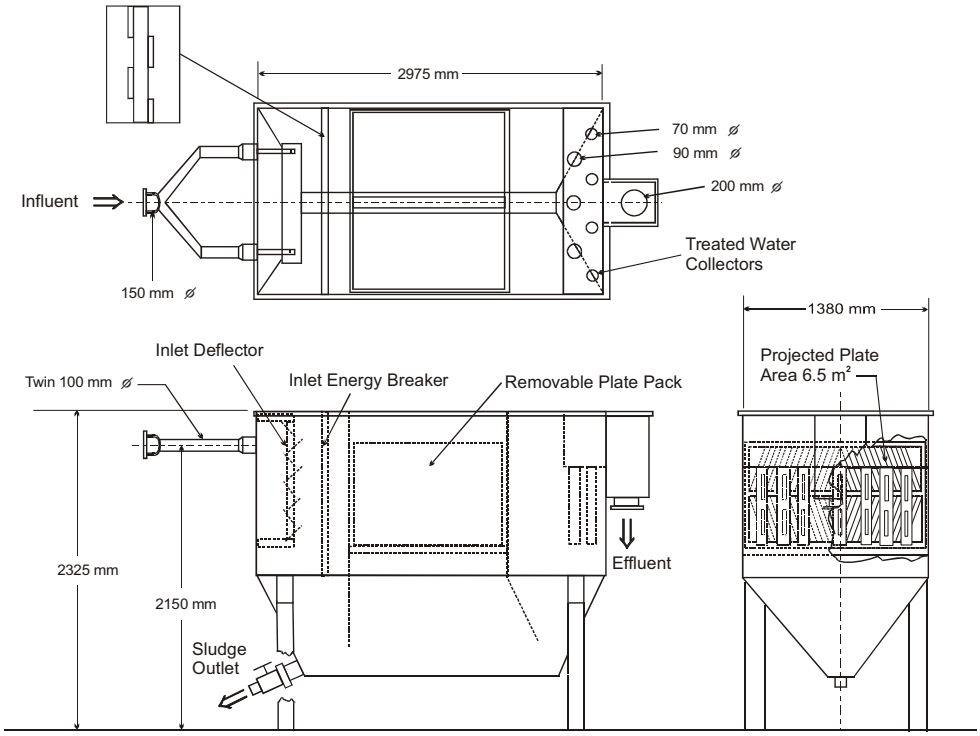

Fig. 2.1: Original design of pilot-scale cross-flow plate clarifier.

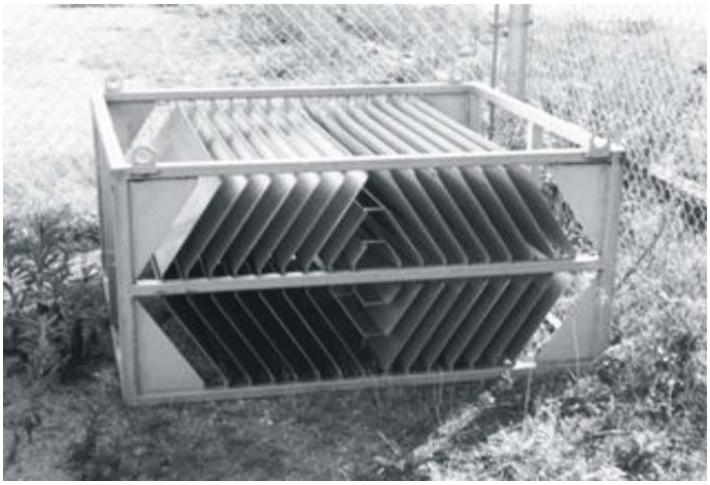

Fig. 2.2: Structure of the removable lamellar plate pack used in the original clarifier.

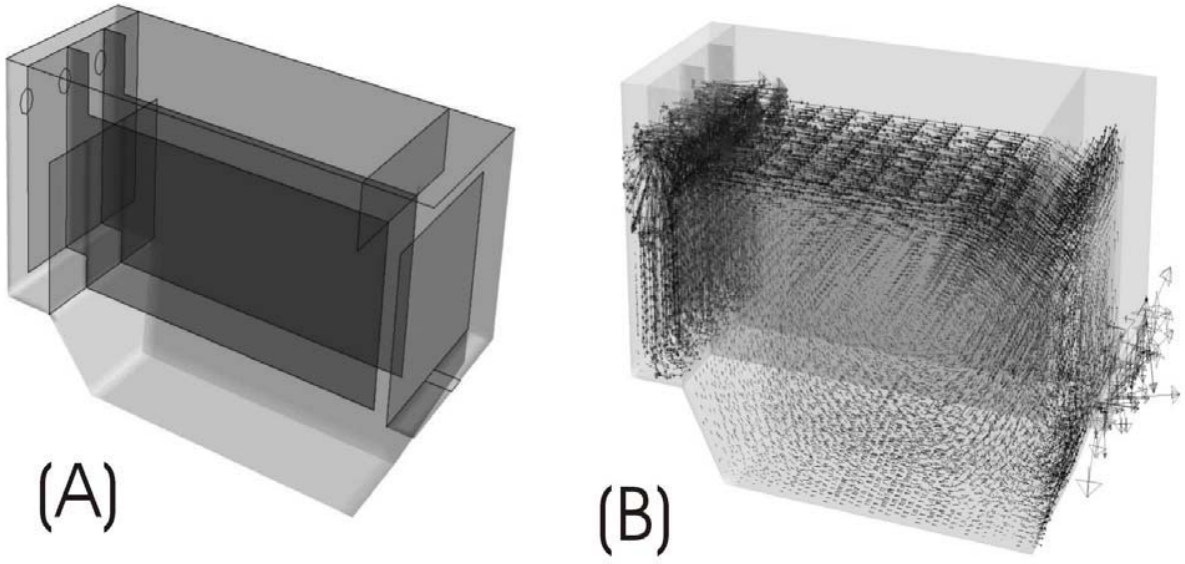

Fig. 2.3: (a) Inlet Design 1 with one vertical baffle between the inlet and particle settling zones, (b) Simulated clarifier flow patterns depicting strong surface flow.

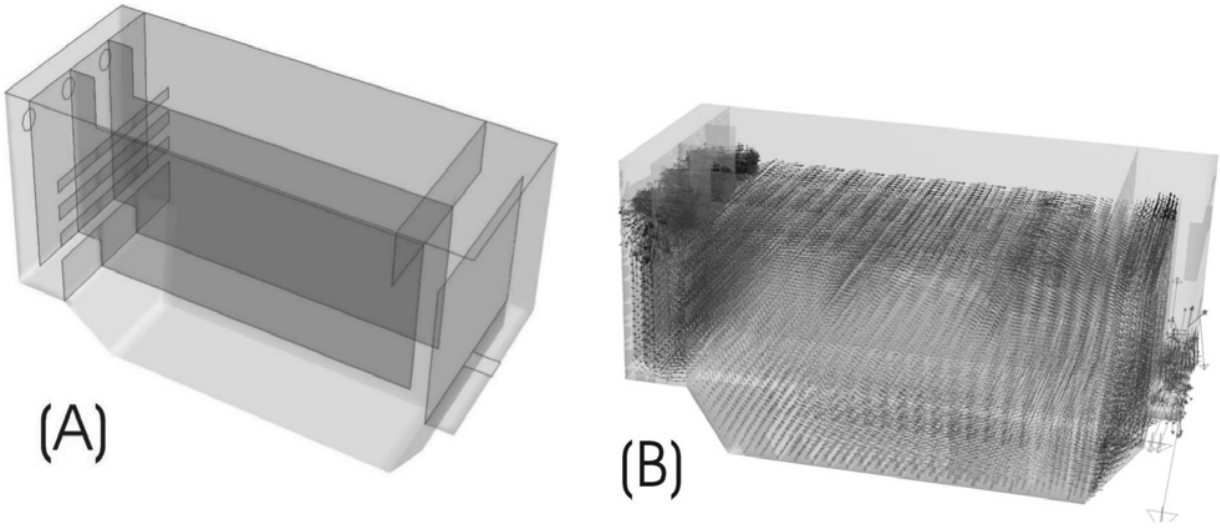

Fig. 2.4: (a) Inlet Design 2 with three openings (slots) in the baffle between the inlet and particle settling zones, (b) Simulated clarifier flow patterns indicating large vertical circulation extending to the bottom of the clarifier.

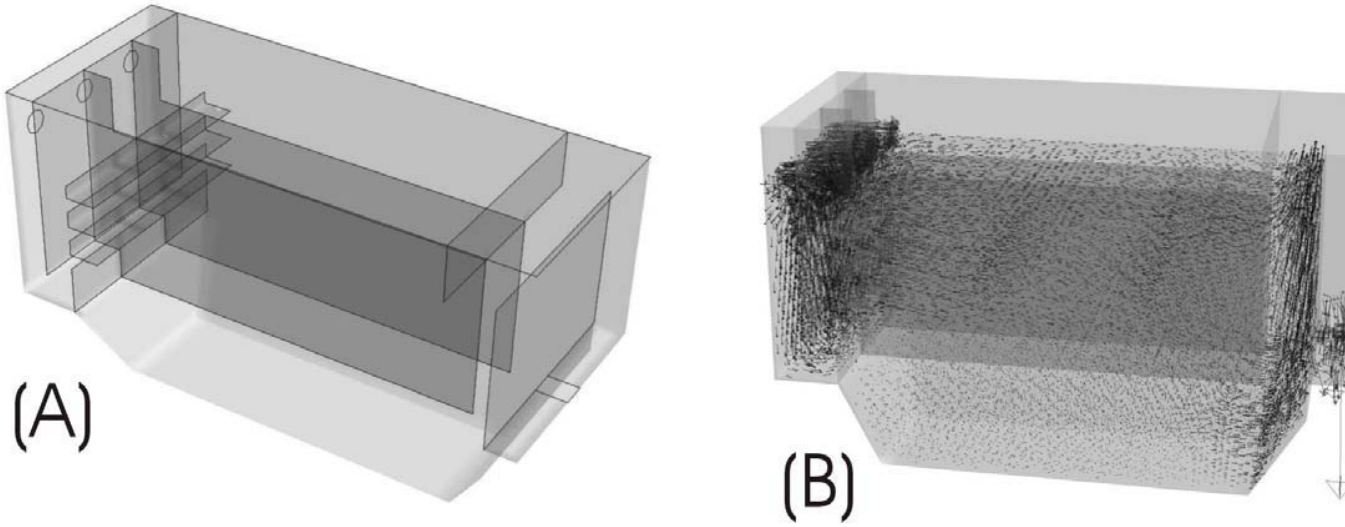

Fig. 2.5: (a) Inlet Design 3 with three open slots in the baffle between the inlet and particle settling zones and horizontal trailing baffles at the top of slots, (b) Simulated clarifier flow patterns showing improved longitudinal flow conditions in the particle settling zone.

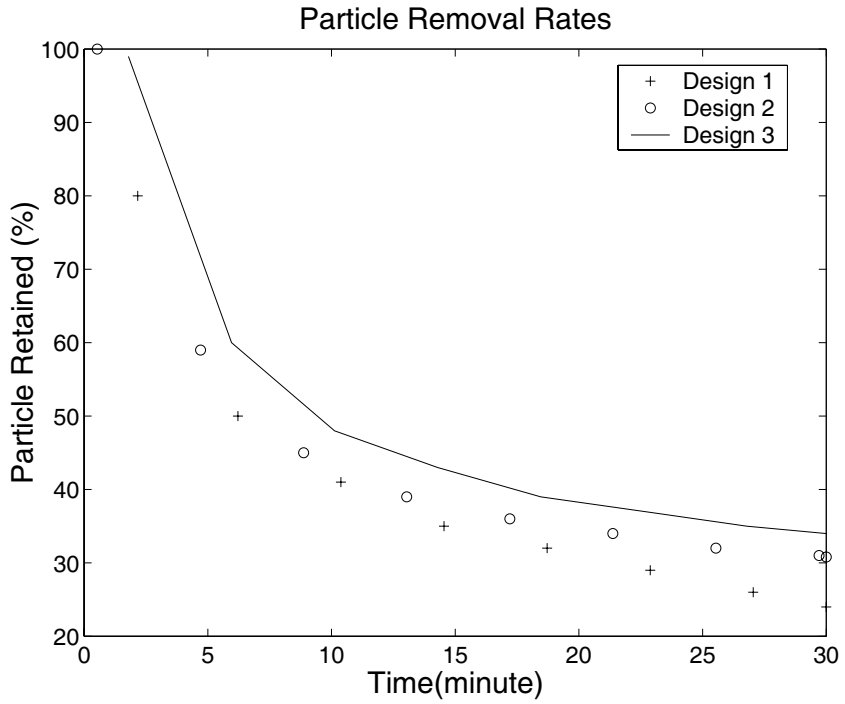

Fig. 2.6: Discrete particle removal rates for the three numerically modelled inlet structures.

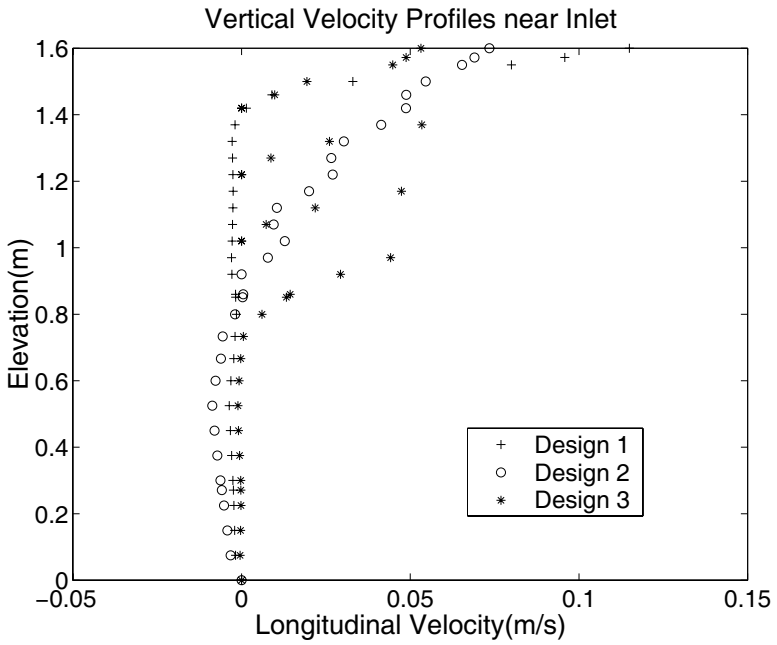

Fig. 2.7: Comparison of vertical profiles of horizontal velocities at 0.2 m downstream of the inlet structure for the three inlet designs studied.

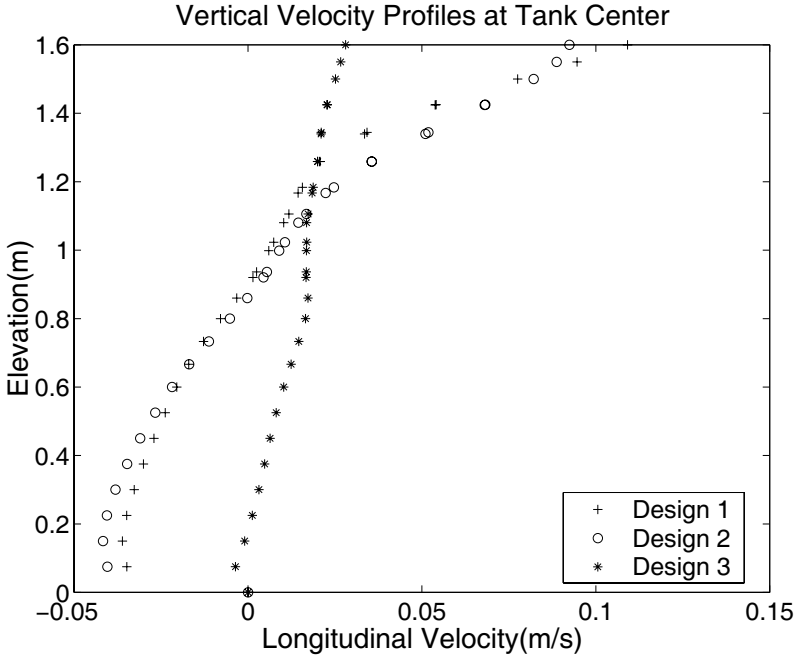

Fig.2.8: Comparison of vertical profiles of horizontal velocities at the mid point of the particle settling zone for the three inlet designs studied.

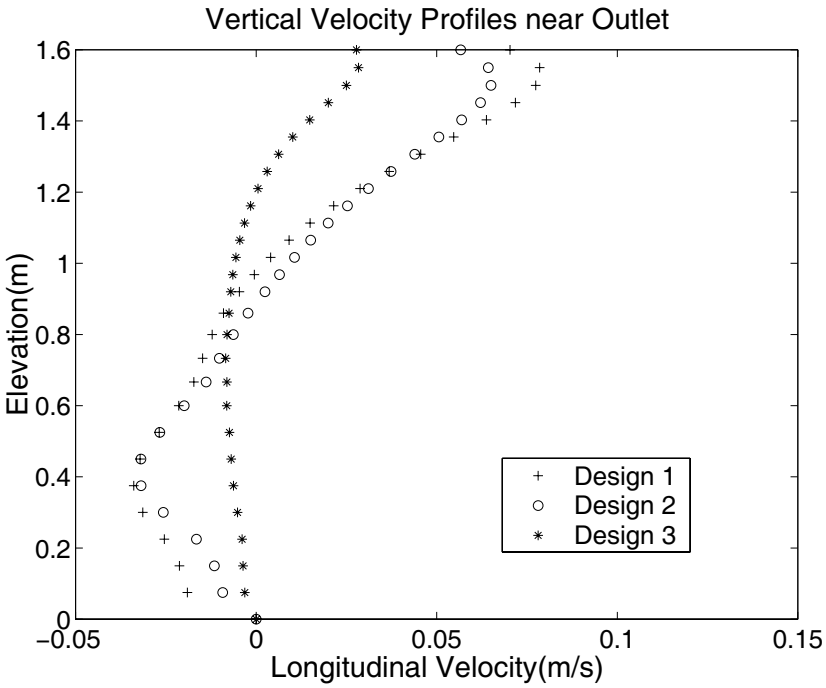

Fig. 2.9: Comparison of vertical profiles of horizontal velocities near the clarifier outlet for the three inlet designs studied.

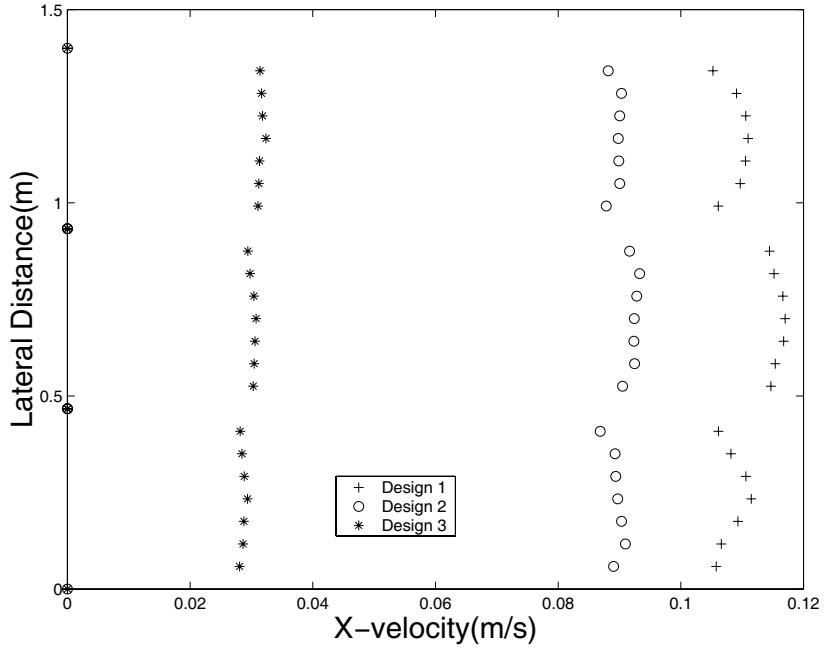

Fig. 2.10: Surface horizontal velocities across the clarifier in the middle of the particle settling zone for the three inlet designs studied.

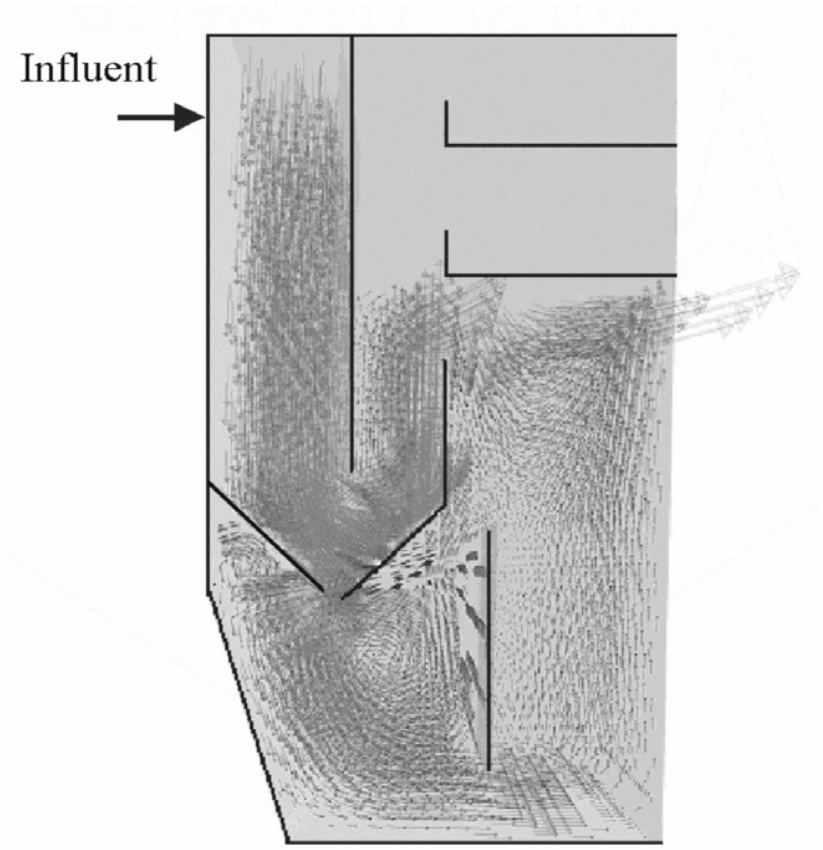

Fig. 2.11: Proposed configuration of the redesigned inlet with an added gravel outlet and the simulated flow patterns.

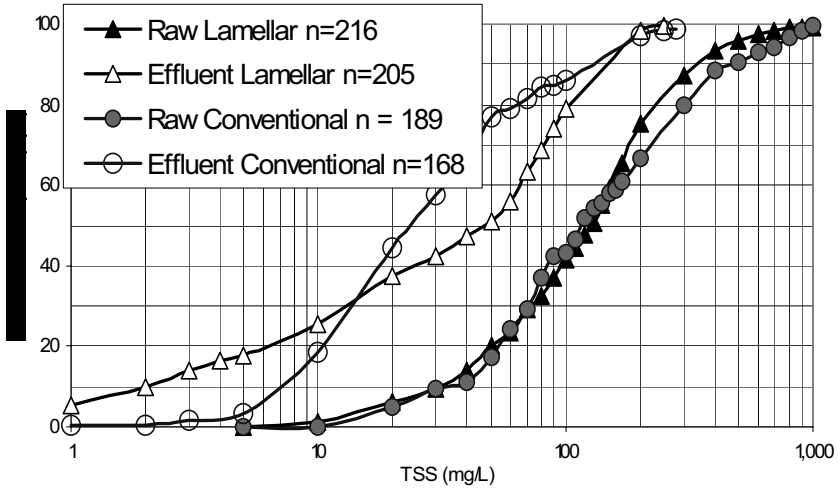

Fig. 2.12: Lamellar and conventional clarifier performance, both with chemical additions (2003-2004 seasons).

Part 3: Case Study: Refinement of Hydraulic Operation of a Complex CSO Storage/Treatment Facility by Numerical and Physical Modeling

3.1 Abstract:

The performance of a combined sewer overflow (CSO) storage/treatment facility in North Toronto (NT), Ontario, Canada was investigated by conjunctive numerical and physical (hydraulic) modeling. The main objectives of the study were to (a) assess the feasibility of increasing the hydraulic loading of the CSO facility without bypassing, and (b) establish a verified numerical model of the facility for future work. The numerical model (a commercial CFD, PHOENICS) was validated and verified using results from a hydraulic scale model (1:11.6). The results obtained show that the CFD model can simulate hydraulic conditions in the facility well, as demonstrated by accurate reproduction of the filling rate, water levels at various locations, flow velocities in feed pipes, and overflows from the inflow channel. Numerical simulations identified excessive local head losses and helped select structural changes to reduce such losses. The analysis of the facility showed that with respect to hydraulic operation, the facility is a complex, highly non-linear hydraulic system. Within the existing constraints, a few structural changes examined by numerical simulation could increase the maximum treatment flow rate in the CSO storage/treatment facility by up to 31%.

3.2 Introduction

Older parts of many Canadian and U.S. cities are serviced by combined sewer systems, which convey both municipal sewage and surface runoff. In wet weather, such systems

are overloaded by high inflows of runoff and, to prevent flooding of downstream sewer reaches and the sewage treatment plant, combined sewer systems are equipped with flow regulators, which are set to divert excess flows into nearby receiving waters in the form of combined sewer overflows (CSOs). CSOs represent a highly polluted mixture of raw sewage, urban stormwater and resuspended sewer sediment, and their uncontrolled discharges into receiving waters represent a major environmental problem (US EPA 2004). Consequently, municipalities with CSO problems have developed or are developing CSO control and treatment programs, following guidance documents produced by government agencies (MOE undated; US EPA 1995).

Over the years, many measures for the abatement of CSO pollution have been proposed and some tested in municipal practice. One of the early abatement measures was storage of CSOs, with subsequent return of stored flows to the central STP for treatment, after flows in the system subsided and the plant developed a spare capacity to accept additional inflow (US EPA 1995). Such a storage facility has been operated by the City of Toronto at a North Toronto site for more than 12 years (Marsalek et al., 2004). In recent years, it was however noted that the facility does not meet the current expectations on CSO control, because too many events (30-40 per year) exceed the facility capacity and overflow without appropriate treatment (Averill et al. 2001). In view of these shortcomings, the City is examining the ways of increasing the facility's effectiveness in CSO control by optimizing the hydraulics of the flow through CSO treatment tanks, and thereby reducing the requirements on storage volume. Such measures would serve to optimize the utilization of the existing facility and are recommended as one of the first

steps in improving the combined sewer system effectiveness in pollution abatement (O'Connor and Field 2002; Marsalek et al. 2004).

Initially, analysis of the hydraulics of the NT CSO facility was based on physical scale modeling of the facility. After the study started, an opportunity presented itself to extend this approach by applying computational fluid dynamics (CFD) modeling as well, and taking advantage of benefits from both approaches. Recent publications indicate the continuing reliance on physical modeling when dealing with complex flow problems, such as e.g., forces on blocks in stilling basins (Nakato 2000), or flushing of sediments from CSO tanks (Guo et al. 2004). In other studies, both physical and numerical models were used, e.g., for wastewater sludge flow (Bechtel 2003), and ogee-crested spillway (Savage and Johnson 2001).

Many examples of CFD modeling of CSO structures were reviewed in the literature (Kluck 1996; Faram and Harwood 2002, Harwood 2002; Saul 2002) focusing on flow pattern simulation, particle tracking and multiphase flows. Compared to the more traditional physical modeling, all authors credit CFD modeling with the following main advantages: (a) speed and efficiency, (b) cost savings (in the development of new products or modification of the existing structures), (c) producing a better understanding of flow conditions, and (d) amenability to trouble shooting (e.g., the poor performance can be corrected using CFD results). However, most of the 3D numerical CFD modeling studies of the hydrodynamic behavior of CSO facilities were limited to simulating a single part of the entire facility due to its complexity. In this study, the entire facility had to be simulated because the flow behavior was influenced by all parts of the facility. On the other hand, it is important to note that numerical modeling results always contain

uncertainties arising from both approximations of actual processes and numerical schemes, and consequently, some verification of modeling results is desirable.

The main objectives of the case study of the NT CSO facility were to examine the feasibility of increasing the facility's hydraulic capacity without major reconstruction or large reduction in storage volume of the downstream tank, and to verify the effectiveness of CFD modeling against the results obtained in a physical model.

3.3 The NT CSO Facility

Upgrading of the NT CSO facility requires a good understanding of the relatively complex hydraulics of the existing facility. In wet weather, CSOs escaping from an adjacent combined sewer enter the inlet channel of the facility (see Fig. 3.1), and continue through four connecting pipes into a distribution channel, and over inlet weirs into three parallel storage tanks. The inlet weir elevations are such that the storage tanks are filled sequentially. Overflow from the CSO tanks is conveyed by the effluent channel into a stormwater tank where it mixes with the stormwater discharge from a separate storm sewer. When the stormwater tank is filled, a CSO and stormwater mixture overflows the final effluent weir to be blended with the secondary effluent from the North Toronto Water Pollution Control Plant (WPCP) before being discharged to the nearby Don River. After storms, the wastewater retained in the NT CSO Facility (approximately 6,000 m^3) is pumped to the WPCP for treatment.

For larger volume events ($V > 6{,}000\ m^3$), the facility overflows. Ideally, all inflows should undergo settling in the CSO storage tanks. However, because of the limited transport capacity of the pipes connecting the inlet and the distribution channels, when

the inflow rate exceeds about 4 m^3/s the excess flows are diverted from the inflow channel via a bypass weir directly into the stormwater tank without undergoing any settling (see Fig. 3.1).

Reducing overflows via the bypass weir of the inflow CSO channel has been a long time goal of the City of Toronto. Unfortunately, there is no easy solution to this problem due to the complexity of the hydrodynamic characteristics of the NT CSO treatment facility. The distribution of flows between the three CSO tanks and the overflow from the inflow channel bypass weir is controlled by the elevations of several weirs, including the three tank outflow weirs, the inlet channel bypass weir, and the final effluent weir. For example, the elevation difference between the inlet channel bypass weir and the CSO tank outflow weirs controls how much flow passes through the three CSO tanks without overflows from the inlet channel. Also, the final effluent weir elevation controls (but not exclusively, as discussed later) the backwater pressure in the effluent channel, which, in turn, affects the maximum flow that can be treated in the CSO tanks.

A proposal has been put forward to increase the flow through CSO tanks (to reduce inlet channel overflows) by reducing the elevation (overall height) of the final effluent weir. Before implementing such changes, several questions had to be answered: (a) How much should the final effluent weir height be reduced? (b) What are the effects of such a weir height reduction with respect to flow increase? (c) Is it sufficient just to reduce the weir height without taking other measures? Such questions were answered by modeling.

3.4 Numerical Model

Since most of the flows in the CSO storage/treatment facility are open channel flows and their hydraulics are controlled by water head (hydrostatic pressure), it is essential to employ a model which can accurately predict the water surface profile throughout the facility and its changes with time, for varying inflows. Obviously, the single phase model could not be used to resolve the air-water interface. The Commercial CFD, PHOENICS (Rosten and Spalding 1984), contains several multi-phase models developed for this purpose. Based on its applicability, reasonable computational time, stability, and suitability to simulate particle transport (to be addressed in the future), the "Algebraic-slip" method referred to in the PHOENICS documentation was selected.

The choice of turbulence models tested in this study was limited to two options, which best described the case studied; (a) the well-known standard two equation k-ε turbulence model described, e.g., in Launder and Spalding (1974), and (b) the zero equation LVEL turbulence model that is better suited for low turbulence flows in open channels and pipes (Rosten and Spalding 1984). Due to the complex nature of the CSO facility studied, neither of these two turbulence models can fully represent the wide spectrum of turbulence in the facility, but both should perform adequately. Testing results showed that the k-ε model results agreed with measurements slightly better than those from the LVEL turbulence model, and consequently, the k-ε turbulence model was adopted in this study, in spite of longer computer running times.

The numerical accuracy of flow simulations increases with the number of cells in the grid, but so does the computation time. For structures with complex geometry, a very large number of cells may be needed, and the correspondingly large computer running time may become unacceptable. Thus, some balance has to be struck between computing time

and the accuracy of the simulation by examining simulation results with different mesh sizes.

Also, the choice of the modeling grid is very important for numerical modeling. It not only directly affects computer running time and the accuracy of final results, but it also greatly affects model stability. Adjustments have to be made in various regions of the schematization to avoid sudden changes in cell sizes, by creating more cells in regions with important hydraulic features. Although the depth of the CSO facility is much smaller than its whole surface area, in order to predict the air-water interface more accurately (which directly affects overall simulations) and also to be able to better represent the sloped tank bottom with the structured mesh, in this study, 55 x 45 x 25 uneven fixed nodes were used in the X, Y, and Z directions, respectively. The time step was 0.182 seconds, with 15 iteration sweeps and the typical simulation running time of 24 hours was acceptable. A similar, but higher resolution grid with 65 x 55 x 30 nodes was also tested, but the results were practically the same as those simulated with 55 x 45 x 25 nodes. Therefore, the simulation results can be regarded as independent of the grid choice and are true results of the mathematical model simulations.

3.5 Model Verification

Although most of the models in commercial CFD software have been validated to a certain degree, it is a good practice to check model results against observations because the applications and parameter settings can be quite different in each case. Especially, when using a relatively complex multiphase model, particular care has to be taken on the

boundaries to prevent mass leakage, which can happen due to model settings and other factors, rather than the finite volume method itself.

In order to check flow leakage from the structure boundary in the numerical model, water mass conservation was tested. In this test a constant 5 m^3/s inflow rate was used in numerical simulations for 25 minutes to reach steady state, and it produced a simulated outflow at the end of the effluent channel of 4.97 m^3/s, or 99.4% of the inflow. Various inflow rates and running times were also tested and produced similar results, with outflows agreeing with inflows within 1%, which should be expected from a finite volume based model using proper parameter settings.

Filling rates and water levels simulated at various locations were compared to the available physical model measurements. These tests were particularly important in this study, in which the numerical model was used to predict water levels throughout the entire system to find out how structural changes would increase the system capacity. Fig. 2 shows a comparison of simulated and measured (in the physical model) water levels at various locations in the facility and water level changes with time. The locations are indicated in Fig. 3.1 as black round dots labeled 1 to 5. The flow rate applied in this test was 5 m^3/s and the water depths plotted in Fig. 3.2 were measured from the tank bottom at each reference point. Because of tank depth variations, all water surface levels were not identical, even after reaching steady state flow conditions.

At all locations shown in Fig. 3.2, simulated and observed (in the physical model) time-varying water surface profiles agreed quite well with the rms errors from 0.11 to 0.23. Thus, the numerical model was capable of accurately predicting the filling time and water levels for both transient and steady-state flows in the whole system. It took about 18

minutes for the entire system to fill up (i.e., for an inflow of 5 m^3/s), as shown by all profiles reaching a constant elevation at that time. When water starts flowing into the CSO tanks, the water level at upstream locations reaches a plateau, until each tank has been filled up, so both the measured and modeled profiles display a step-wise shape. Thus, the curves in Fig. 3.2 can be characterized by four steps; the first three correspond to filling the CSO tanks 1, 2 and 3, in sequence, and the last step represents the attainment of the steady-state flow.

The flow velocities at the center of each of the four distribution channel feed pipes were measured with a Pitot tube in the scale model and compared to modeled values. The results are shown in Table 1. In this table, the measured velocities represent point velocities along the longitudinal axis of pipes, but because of limited spatial resolution of the numerical model, the modeled velocities represent average velocities for the entire pipe cross section. This explains why the modeled velocities are slightly smaller than the measured ones. Another numerical model approximation used in the adopted Cartesian coordinate system is that the round feed pipes were represented in the numerical model as square conduits, which have a slightly larger cross section. This approximation was accounted for in the modeled velocities listed in Table 1. The total discharge through feed pipes was about 4.96 m^3/s, or 99.1% of the inflow rate.

In an overall evaluation, the numerical model was found capable of simulating flow physical characteristics quite well, compared to the observations, especially for situations controlled by the hydrostatic pressure. Comparisons of numerical results with observations in the scale model were helpful in explaining numerical results and were

conducted throughout the study. Thus, the PHOENICS model was found to be suitable for evaluation of the performance of the CSO storage and treatment facility.

3.6 Numerical Modeling of Flow Rates

In the initial series of PHOENICS runs, the final effluent weir height was set equal to zero (i.e., the weir was removed). Under such circumstances, the CSO tank outflow weir crest should be always above the water level in the effluent channel, and there should not be any backwater influencing water levels in the CSO tanks. The numerical model was run with different inflow rates, until the water level in the inlet channel reached the crest of the bypass weir and the system reached steady state, as shown in Fig. 3.2F. In this figure, the straight horizontal line indicates the elevation of the bypass weir, and the curve represents simulated water levels just upstream of the bypass weir. The results show that the maximum inflow rate to this treatment facility is about 5.46 m^3/s, which agrees with measurements in the physical model, within the range of measurement errors. However, in the actual facility, there is a noticeable effect of the final effluent weir, which produces a backwater and raises the water level in the CSO tanks. Increased water levels in these tanks then cause overflow over the bypass weir, well before the maximum flow can be attained. With the existing final effluent weir position, numerical simulations indicate a maximum (no bypass) flow rate of about 3.9 m^3/s. Thus, because of the facility configuration and the final effluent weir, the maximum treatment capacity of the existing facility is reduced by 29% from the free-flow state.

Reducing the height of the final effluent weir seems to be an obvious choice for increasing the treatment capacity of the system. However, if the final effluent weir is too

low, the storage/treatment function of the stormwater tank would be diminished, and any flow overflowing the inlet bypass weir would not be treated at the NT CSO facility. To balance both requirements (increasing the treatment rate and preserving the storm tank volume), three different height reductions (20, 40 and 60 cm) of the final effluent weir, were considered and the results of such simulations are shown in Fig. 3.3. The reduction of 60 cm is the maximum that would be allowed by the regulatory agency.

The horizontal straight line in Fig. 3.3 denotes the elevation of the inlet tank bypass weir and the curves displayed represent water levels simulated in the inlet tank next to the bypass weir, for different final weir heights. In all simulations, the inflow rate was set at 5.46 m^3/s. It can be seen that all water surface profiles overtop the bypass weir after 18 minutes of inflow. This means that even if the final weir height is reduced by 60 cm, bypassing from the inlet channel would still occur. It was noted that the water level variation in the inlet channel was not very sensitive to changes in the final effluent weir height. For example, a 40 cm reduction in the weir height (i.e., moving from a 20 cm height reduction to a 60 cm reduction), reduced the water level in the inlet channel by just 10 cm. Since the water level difference between the inlet channel and the effluent channel should be similar for the same inflow, this indicates that the water level in the effluent channel also changes much less than the final effluent weir height. This finding prompted further investigations of flow hydraulic characteristics in the region between the CSO tank outflow weir and the final effluent weir.

Water levels in the effluent channel and in the stormwater tank were plotted in Fig. 3.4 for different heights of the final effluent weir. Recognizing that the reduction of the final effluent weir height by 20 cm was insufficient to significantly improve the system

capacity, the discussion of numerical simulations focuses on reducing the final effluent weir by 40 and 60 cm, respectively. The plots in Fig. 3.4 represent water level profiles starting from the final effluent weir and moving upstream (see Fig. 3.1A) against the flow direction indicated by an arrow. In both panels of Fig. 3.4, curve A indicates the water level for the existing facility without any modifications, except for reducing the final effluent weir height. Water surface profiles indicate that additional hydraulic resistance generated by the 90^{o} bends causes two water level peaks in the effluent channel. In order to overcome this obstruction, the flow level upstream of the bend has to rise to increase the hydrostatic pressure differential between the entry and exit sections of the bend. By reducing the final effluent weir height, the velocity in the effluent channel will increase, as will the hydraulic head needed to pass a higher flow through the bend. Consequently, the influence of reducing the final effluent weir height on water levels in the CSO tanks becomes much smaller, because of the obstruction effect of the two 90^{o} abrupt bends. Therefore, the hydraulic resistance at the two bends needs to be reduced in order to improve flows.

The second (downstream) 90^{o} bend, which is directly connected to the stormwater tank, can be fixed more easily either by widening the exit cross-section of the channel, or by cutting the downstream (left) sidewall of the bend at an angle larger than 45^{o}. However, due to space limitations and structural considerations, the outside dimensions of the upstream 90^{0} bend cannot be enlarged. Therefore, the only acceptable modifications of this bend have to be made inside the channel, e.g., by curving the inner corner and/or adding curved flow conditioning baffles. Computer simulations were used to explore both alternatives for improving the hydraulic efficiency of this bend.

The hydraulics of the upstream 90^{o} bend was studied in two steps. The first step focused on simulation of the flow passing through the bend in a simplified setting, which included the bend itself and some upstream and downstream sections of the flow channel. In all simulations, the inflow rate was 5 m^3/s. The purpose of this step was to find the most effective modification of the bend. With fewer structural components simulated and a higher node density, the accuracy of numerical simulations was increased and the computer running time was reduced. In total, six different bend geometries (A-F) were tested (see Fig. 3.5), and the corresponding water level profiles in the effluent channel are shown in Fig. 3.6.

Case A refers to a straight channel, which simulates flow conditions without any bend influence and is used as a reference for the other test cases. It does not show any flow obstruction, as expected for a straight channel. Case B refers to a channel with a 90^{o} bend, without any modifications. The simulation results show that the water level upstream of the bend is about 13 cm higher than in case A, due to the effect of the bend. Cases C and D represent situations, in which curved baffles were inserted into the channel outer corner, with radii of 1.5 and 1.0 m, respectively. Modeling produced somewhat surprising results; curved baffles placed in the outer corner barely affected water levels in the effluent channel. In fact, curves C and D in Fig. 6 are almost identical and similar to curve B, which represents the 90^{o} bend. This lack of effectiveness can be attributed to the reduction of the flow cross-sectional area due to the placement of the curved baffle in the outer corner, even though water flow trajectories in the corner should become hydraulically more favorable. Similar tests with curved baffles (R = 0.5 m) were

done in the physical model for different flow rates and also confirmed that these outer corner baffles barely influenced water levels.

Case E represents the layout in which the geometry of the inner corner was rounded, with a radius of 0.5 m. This modification brought about a significant reduction in the water levels in the effluent channel, as shown in Fig. 3.6. It was felt that the effect of this improvement might have been slightly exaggerated in the numerical simulation. Physical model experiments confirmed that inner corner modifications were more effective in reducing local head losses than changes of the outer corner. The flow velocity fields at the corners shown in Fig. 3.7 provide an explanation. For the inner corner of the 90^{o} bend, illustrated in the upper part of Fig. 3.7, the flow will produce negative pressure downstream of the inner corner, and thereby generate an eddy, which then functions as a flow obstruction and reduces the effective flow width. After rounding the inner corner, the eddy caused by the negative pressure disappeared, as shown in the middle panel of Fig. 3.7. Consequently, it was now easier for flow to pass through the bend, and a lower hydraulic head was needed to force water through the bend, as confirmed by the smaller difference between the crest and trough of water profile curves in Fig. 3.6. At the same time, the modeling results in the middle panel of Fig. 3.7 indicate that the velocity (and the corresponding head loss) along the outer corner is much smaller than that near the inner corner. This may explain why curved outer baffles do not contribute significantly to reducing the hydraulic resistance of the bend, even if the flow pattern has been improved (see the bottom panel in Fig. 3.7).

In the second step of the analysis, the knowledge about the hydraulics of 90^{o} bends was applied to numerical simulations of the actual facility with modified bends. The resulting

water level profiles in the effluent channel are presented in Figs. 3.4A and 3.4B as curves B and C, in both panels. The water level in the effluent channel with an improved downstream bend (Curve B) was reduced significantly compared to Curve A, for both 40 and 60 cm reductions of the final effluent weir height. The water level in the region downstream of the first bend decreased more than that upstream of the bend. This can be explained by the fact that the first (upstream) bend acts as a bottleneck, which would require a greater hydraulic pressure build up to convey the increased discharge. This finding is also indicated by the increasing water level oscillations at the upstream bend in Figs. 3.4A and 3.4B.

Curve C in Figs. 3.5A and 3.5B (both panels) shows the simulated water surface profiles for the case in which the downstream bend was "opened" and the upstream bend inner corner was rounded. Water levels were reduced even further, but the upstream bend was still causing head-loss problems requiring more study.

After addressing the bend problems, further work focused on finding the relationships between the maximum attainable inflow rate (without bypassing), Q_{in}, and various heights of the final effluent weir, under three conditions: (a) no changes of the effluent channel (existing max $Q_{in} = 3.9$ m^3/s), (b) correcting the downstream bend only (max $Q_{in} = 4.15$ m^3/s), and (c) correcting both bends (max $Q_{in} = 4.25$ m^3/s). These three cases were then re-examined for reductions of the final effluent weir height by 20, 40 and 60 cm respectively, and the results were plotted in Fig. 3.8. Discrete symbols represent the maximum flow rates measured in the physical scale model and solid lines represent modeled data. It can be seen in Fig. 3.8 that the numerically modeled maximum flow

rates were slightly smaller (< 5%) than the measured ones, except for one point. However, these minor discrepancies were considered insignificant.

The numerical simulations indicate that by lowering the final effluent weir by 60 cm and modifying both 90^o bends, the maximum inflow rate could be increased from 3.9 m^3/s to 5.12 m^3/s, which corresponds to about a 31% improvement of the system treatment capacity. An important finding can be made from Fig. 3.8 - the slopes of all water profiles decline with the decreasing final effluent weir height. In other words, the rate of improving the maximum inflow rate diminishes as the height of the final effluent weir is decreased, which also reduces the storage/treatment capacity of the stormwater tank. Depending on how much significance is assigned to maintaining the storage volume in the stormwater tank, it may be preferable to improve the system capacity by reducing the final effluent weir height by some intermediate value (e.g., 40 cm) and correcting the 90^0 bend problems at the same time.

The low sensitivity of the flow increase to the final effluent weir height reduction deserves further discussion. It is well known that the higher the flow velocity through the corner, the larger energy head required, but it is not obvious that when increasing the flow through the right angle corner by a fixed increment a larger head difference is required for a higher flow than for a lower flow. Since the flow field around a corner is very nonlinear, it is almost impossible to produce an analytical solution for flow rate changes using water head difference at a corner, however, an answer can be found with a numerical model. The numerical experiment setting is the same as shown in Fig. 3.5b, and the simulation results for different flow rates are presented in Fig. 3.9 as a solid line. In the numerical simulation, flow rates were increased from 1 m^3/s to 5 m^3/s, with 1 m^3/s

increments. The almost straight line suggests that the gradient dQ/dh (flow rate change vs. water head change) is about constant and independent of the flow rate. Thus, the influence of the corner does not provide an answer for the above question.

The second feature requiring some examination is the straight effluent channel, even though it is unlikely to contribute to the problem discussed. The flow structure in a straight effluent channel with a constant width is much simpler than that in a corner bend. The relationship between the flow rate and water head can be easily derived, as shown below. If diffusion and wall friction are ignored, a steady lateral uniform flow in a channel with a constant width should satisfy the momentum equation

$$u\frac{du}{dx} = -g\frac{dh}{dx} \qquad (1)$$

where u is the flow velocity along channel x direction, g is the acceleration due to gravity, and h is the water depth. By integrating both sides of equation (1), along the flow direction from location x_1 to location x_2, the following simple relationship is obtained

$$\frac{1}{2}(u_2^2 - u_1^2) = g\Delta h \qquad (2)$$

In equation (2), Δh is the water head difference between locations x_1 and x_2. The water depths at x_1 and x_2 can be expressed as $h_2+\Delta h$ and h_2, and to preserve continuity, this relationship can be written as

$$(h_2 + \Delta h)u_1 = h_2 u_2 \qquad (3)$$

Therefore,

$$u_2^2 = (1 + \frac{\Delta h}{h_2})^2 u_1^2 \qquad (4)$$

Substituting equation (4) into equation (2) and using flow discharge Q to replace velocity, the relationship between water discharge and water head difference is

$$Q^2 = \frac{g h_2^3 (1 + \frac{\Delta h}{h_2})^2}{(1 + \frac{\Delta h}{2h_2})} \qquad (5)$$

Since $\left|\frac{\Delta h}{h_2}\right| \langle\langle 1$, and after expanding the bottom term and ignoring the terms higher than the second order, the final expression for water discharge becomes

$$Q^2 = \left\{ g h_2^3 [1 + \frac{3}{2}\frac{\Delta h}{h_2} + \frac{1}{4}(\frac{\Delta h}{h_2})^2 \cdots] \right\} \qquad (6)$$

The relationship described by equation (6) can be examined visually in Fig. 3.9, where it was plotted as a dashed line. Since the slope of the curve is almost constant, it indicates that the water head increase for increasing flow rates is independent of the flow rate itself. Therefore, the effluent channel is also unlikely to cause the phenomena mentioned above. The third possible cause to be examined is the final effluent weir. After analyzing Fig. 3.4 closely, it can be noted that, when the final weir height is decreased by 20 cm, the

water level in the storm tank is reduced by only 10 cm. To explain the behavior of the final effluent weir, its flow structure has to be examined.

Among the many weir formulas found in the literature, a widely accepted one is based on the assumption of outflow from a stilling basin, as given in Chow et al. (1988):

$$Q = \frac{2}{3} Cbh\sqrt{2gh} \qquad (7)$$

where C = the discharge coefficient, which depends on weir geometry, b = length of the weir, and h = water depth above the weir.

The above formula may be valid for a weir in a stilling basin, where gravity is the sole force driving flow over the weir and the outflow direction is perpendicular to the weir plane. In the North Toronto CSO facility, the flow from the effluent channel is forced into the stormwater tank by hydraulic pressure, which generates a strong current in the stormwater tank, and numerical simulation showed that there is a strong flow component parallel to a portion of the final effluent weir. Thus, the stormwater tank can not be considered as a stilling basin of the final effluent weir, because the flow over the weir is caused by both gravity and inertia forces. It was also noted that a side weir formula, assuming the approach flow direction parallel to the weir, did not apply to the situation studied, because of complex flow circulation in the storm tank caused by the flow jet from the effluent channel. It is clear that under such a situation, the upstream hydraulic conditions greatly influence water levels in the storm tank, instead of being exclusively determined by weir height as is the case in a stilling basin. Thus, because the water level in the effluent channel is determined by both the water level in the stormwater tank and

the discharge from the channel, the magnitude of the final effluent weir height reduction can not be fully reflected in the water level change in the effluent channel because of the limiting discharge. In turn, this will affect how closely the water level in the stormwater tank will follow the height reduction of the final effluent weir.

The discussion of the relationship between the flow rate change and the final effluent weir height indicates that, by considering the influences of the corners, the effluent channel and the final effluent weir separately, it can be stated that the final effluent weir is the main cause for diminishment of flow rate improvement with a decreasing weir height. If all of these factors are considered together, the real reasons for the observed hydraulic system behavior are the complex hydraulic interactions among these factors. In any case, an aggressive reduction in the final effluent weir height could not be recommended, because of potential impairments to the stormwater tank function and the lack of effectiveness in improving the treatment system capacity.

3.7 Conclusions

The assessment of flow behavior in the North Toronto CSO Storage/Treatment Facility by numerical and physical modeling provided a good insight into the facility operation and performance improvements by structural changes. The main objective of this study focused on increasing the maximum flow capacity. Numerical modeling was accomplished using a 3-D hydrodynamic model PHOENICS, which was run on a PC. The results demonstrated that the 3-D multiphase model in the PHOENICS package was clearly capable of simulating water level, flow velocities and other physical flow characteristics in this complex structure with many hydraulic interconnections. Most of

the numerical model results were verified by measurements in a 1:11.6 physical scale model, and the differences between the numerical model output and measured results were less than 5%, in most cases. The analysis of the facility showed that with respect to passage of flows, the facility is a complex, highly non-linear hydraulic system.

When examining the feasibility of increasing the facility flow capacity, several problems were identified. Water profiles through the facility were affected by the 90^{o} bends in the effluent channel and by flow control weirs. Modeling results showed that:

(a) reducing the height of the final effluent weir may only be a partial solution for this complex system. A more comprehensive plan may be needed and should address the effluent channel bend problems;

(b) the rates of flow change in the system also depend on the height of the final effluent weir itself. For lower weirs, increases in flow rate become smaller when reducing the final effluent weir by a constant step, because the water level in the stormwater tank is also affected by the hydraulic conditions upstream. Thus, even if further reductions of the final effluent weir height may appear feasible, considering the decreasing efficiency of this measure and the environmental consequences of sacrificing the stormwater tank storage, a more balanced approach combining effluent channel improvements and lowering the final effluent weir should be taken.

Finally, it was concluded that the numerical model, used in tandem with a physical model, was a very flexible, powerful tool that could provide a distinct advantage in future investigations of the North Toronto CSO Facility.

3.8 Acknowledgements:

The contributions made by Government of Canada's Great Lakes 2020 Sustainability Fund, the City of Toronto staff Patrick Chessie and Sandra Ormonde, and NWRI Research Support Branch staff Bill Warrender, John Cooper and Brian Taylor, are greatly appreciated.

3.9 Notation

The following symbols are used in this paper:

b = length of the weir;

C = discharge coefficient;

g = gravitational acceleration;

h = water depth;

Δh = water head difference;

Q = flow discharge;

Q_{in} = inflow rate;

x = distance in x direction;

u = velocity in x direction;

3.10 References

Averill, D., P. Chessie, D. Henry. S. Kok, J. Marsalek and P. Seto (2001). "Field experience with chemically aided settling of combined sewer overflows." Proc. NOVATECH Conf. on Innovative Technologies in Urban Drainage, June 25-27, 2001, Lyon, France, pp. 237-244.

Bechtel, T.B. (2003). "Laminar pipeline flow of wastewater sludge: computational fluid dynamics approach." J. Hydr. Engrg, 129 (2), 153-158.

Chow, V. Maidment, and Mays, L. (1988). "Applied Hydrology." McGraw-Hill.

Faram, M.G, and R. Harwood (2002). "Assessment of the effectiveness of stormwater treatment chambers using Computational Fluid Dynamics." In: E.W. Strecker and W.C. Huber (eds), CD-ROM Proc., Global Solutions for Urban Drainage, Proc. 9th Int. Conf. on Urban Drainage, Sept. 8-13, 2002, Portland, OR, available from ASCE, New York, N.Y.

Guo, Q., C.-Y. Fan, R. Raghaven and R. Field (2004). "Gate and vacuum flushing of sewer sediment: laboratory testing." J. Hydr. Engrg, 130 (5), 463-466.

Harwood, R. (2002). "CSO modeling strategies using Computational Fluid Dynamics." In: E.W. Strecker and W.C. Huber (eds), CD-ROM Proc., Global Solutions for Urban Drainage, Proc. 9th Int. Conf. on Urban Drainage, Sept. 8-13, 2002, Portland, OR, available from ASCE, New York, N.Y.

Kluck, J. (1996). "Design of storm water settling tanks for CSOs." Proc. 7th International Conference on Urban Storm Drainage, Hannover, Germany, Sept. 9-13,181-186.

Launder, B.E. and Spalding, D.B. (1974). "The numerical computation of turbulent flows." Comp. Meth. In Appl.Mech. & Eng., 3, 269.

Marsalek, J., C. He, Q. Rochfort, K. Exall, J. Wood, B.G. Krishnappan, P. Seto and P. Chessie (2004). "Upgrading the North Toronto CSO storage and treatment facility." In: J. Marsalek, D. Sztruhar, M. Giulianelli and B. Urbonas (eds), Enhancing urban environment by environmental upgrading and restoration. NATO Science Series, Earth and Environmental Sciences Vol. 43, Kluwer Academic Publishers, Dordrecht/ Boston/London, 111-121.

Ministry of the Environment (MOE) (undated). "Procedure F-5-5. determination of treatment requirements for municipal and private combined and partially separated sewer systems" <www.ene.gov.on.ca/envision/gp/F5-5.pdf>.

Nakato, T. (2000). "Model test of hydraulic performance of Pit 6 dam stilling basin." J. Hydr. Engrg, 126 (9), 638-652.

O'Connor, T.P. and R. Field (2002). "U.S. EPA Capstone report: control system optimization." In: E.W. Strecker and W.C. Huber (eds), CD-ROM Proc., Global Solutions for Urban Drainage, Proc. 9th Int. Conf. on Urban Drainage, Sept. 8-13, 2002, Portland, OR, available from ASCE, New York, N.Y.

Rosten, H.I. and Spalding, D.B. (1984). "The PHOENICS reference manual, TR/200." CHAM Ltd, Wimbledon, London.

Saul, A.J. (2002). "CSO: State of the art review." In: E.W. Strecker and W.C. Huber (eds), CD-ROM Proc., Global Solutions for Urban Drainage, Proc. 9th Int. Conf. on Urban Drainage, Sept. 8-13, 2002, Portland, OR, available from ASCE, New York, N.Y.

Savage, B.M. and M.C. Johnson (2001). Flow over ogee spillway: physical and numerical model case study. J. Hydr. Engrg, 127 (8), 640-649.

U.S. Environmental Protection Agency (USEPA) (1995). "Combined sewer overflows: guidance for long-term control plan." EPA 832-B-95-002, U.S. EPA, Edison, NJ, USA.

U.S. Environmental Protection Agency (USEPA) (2004). Report to Congress: impact and control of CSOs and SSOs. EPA 833-R-04-011, U.S. EPA, Washington, D.C., USA.

3.11 Tables:

Table 1. Numerically modeled and measured flow velocities in the connecting pipes between the inlet and distribution channels.

	Pipe1	Pipe2	Pipe3	Pipe4
Measured Vel. (m/s)	2.28	2.18	2.31	1.28
Modeled Vel. (m/s)	2.14	2.14	2.17	1.21
Difference (%)	6.14	1.83	6.06	5.47

3.12 Figures:

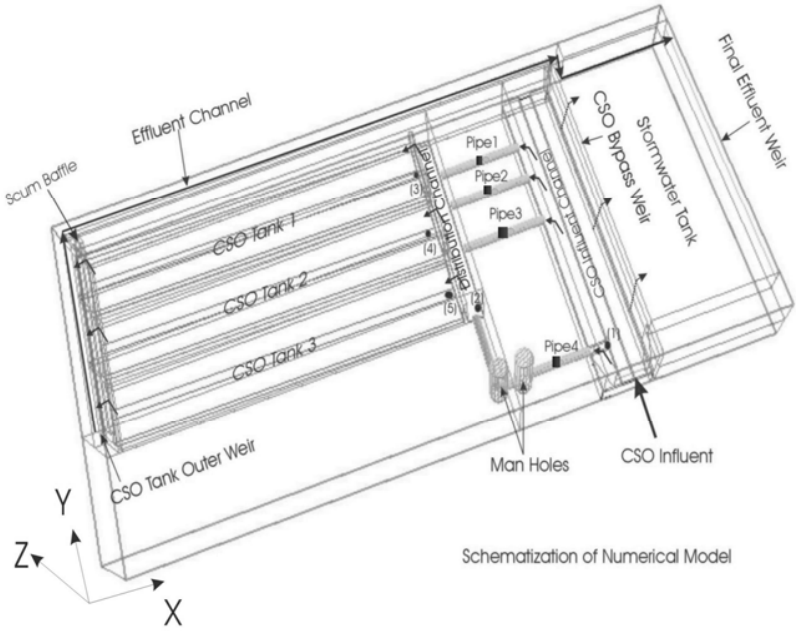

Fig. 3.1. 3-D Schematization of the North Toronto CSO Facility used in numerical modeling.

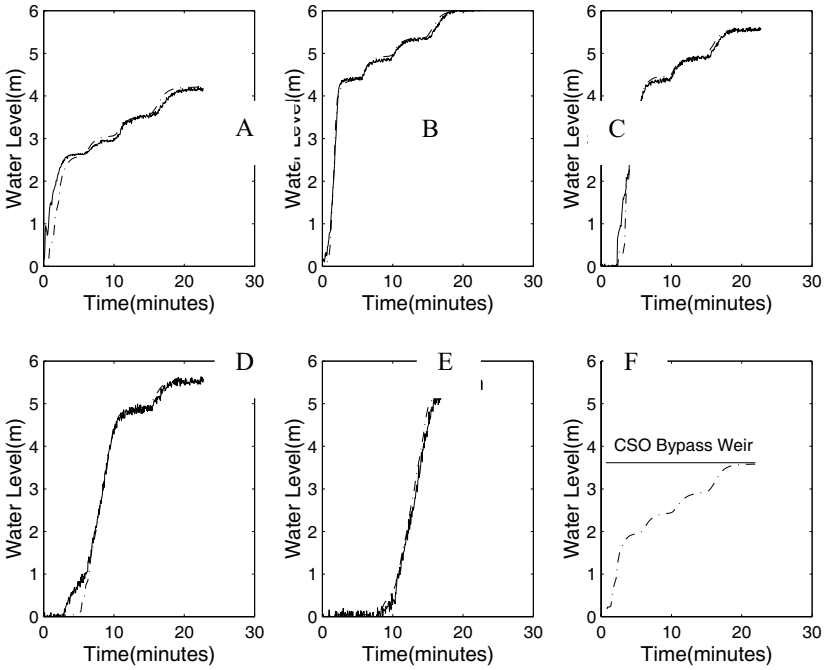

Fig. 3.2. Comparison of numerically modeled and measured water level changes in time, at various locations. Solid lines represent numerical model output, broken lines represent measured results. (2A) Inlet tank (2B) Distribution channel (2C) CSO Tank 1 (2D) CSO Tank 2 (2E) CSO Tank 3, and (2F) by the bypass weir.

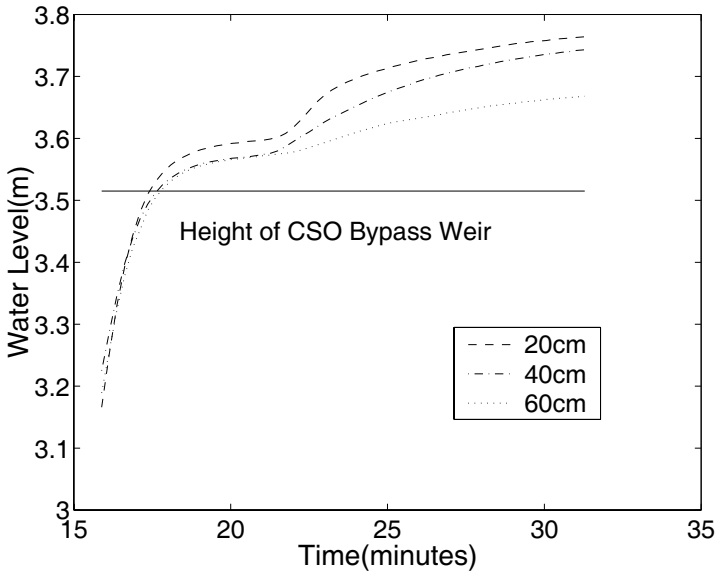

Fig. 3.3. Numerically simulated water levels in the CSO influent channel for different heights of the final effluent weir.

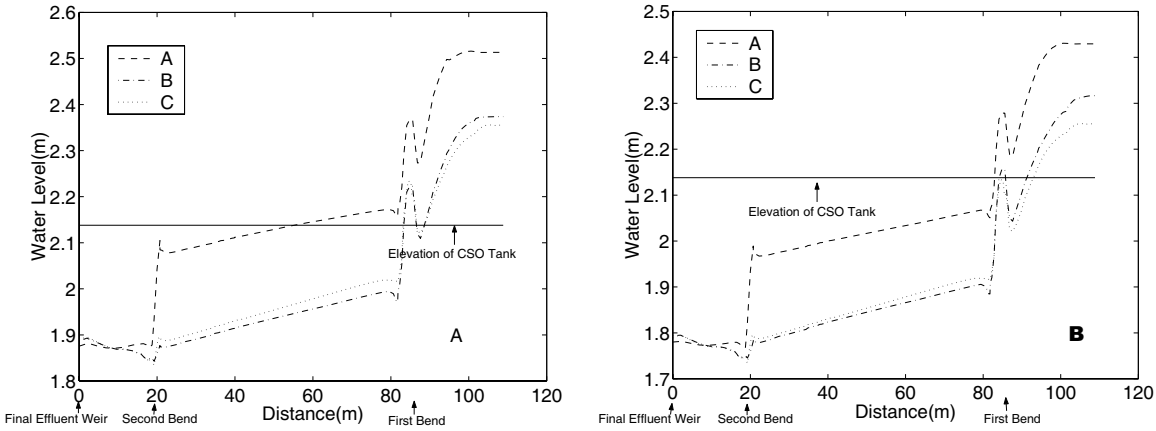

Fig. 3.4. Water levels in the effluent channel and the adjacent part of the stormwater tank for different bend conditions and final effluent weir height reductions. (4A) Weir height reduction by 40 cm, (4B) Weir height reduction by 60 cm.

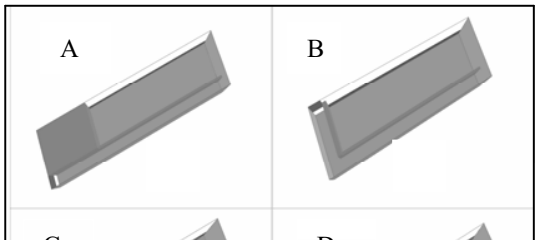

Fig.3.5. Different corner arrangements (A-F) used in numerical simulations.

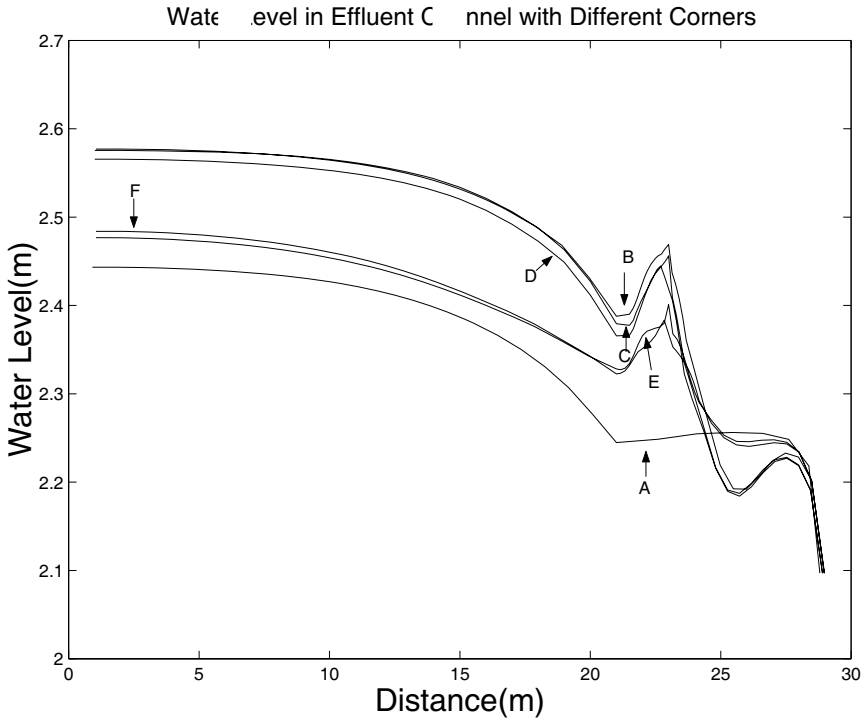

Fig. 3.6. Simulated water levels in the effluent channel and the adjacent part of the stormwater tank for different corner bend arrangements (A-F).

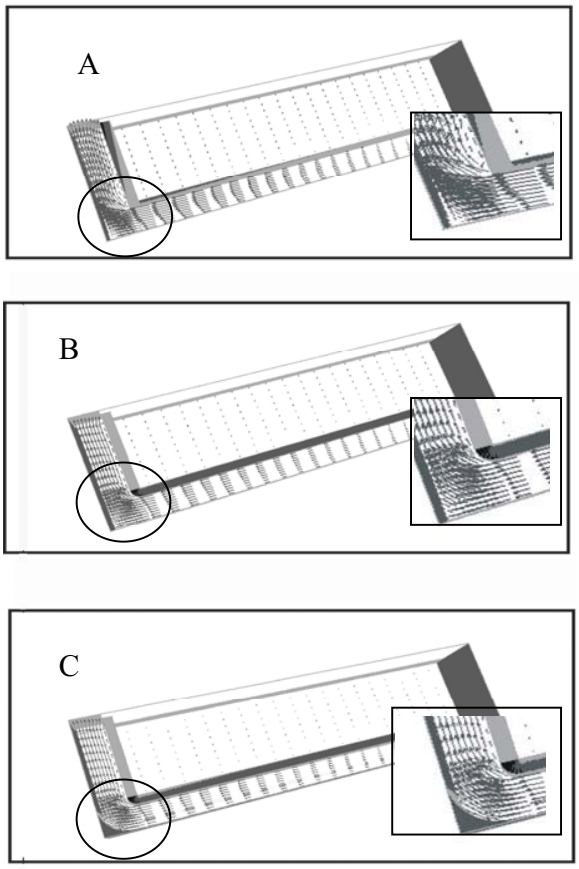

Fig. 3.7. Simulated velocity patterns of three different corner arrangements.

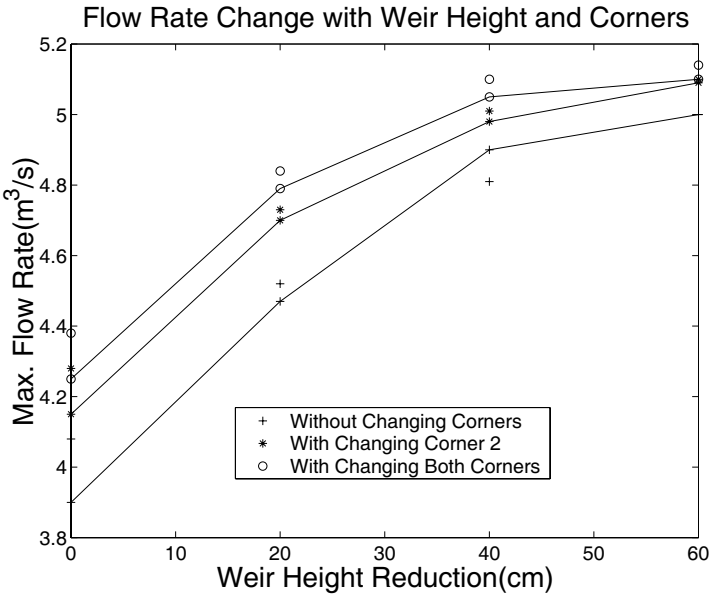

Fig. 3.8. Simulated water level profiles in the effluent channel with different corner arrangements and three final weir height reductions (20, 40 and 60 cm).

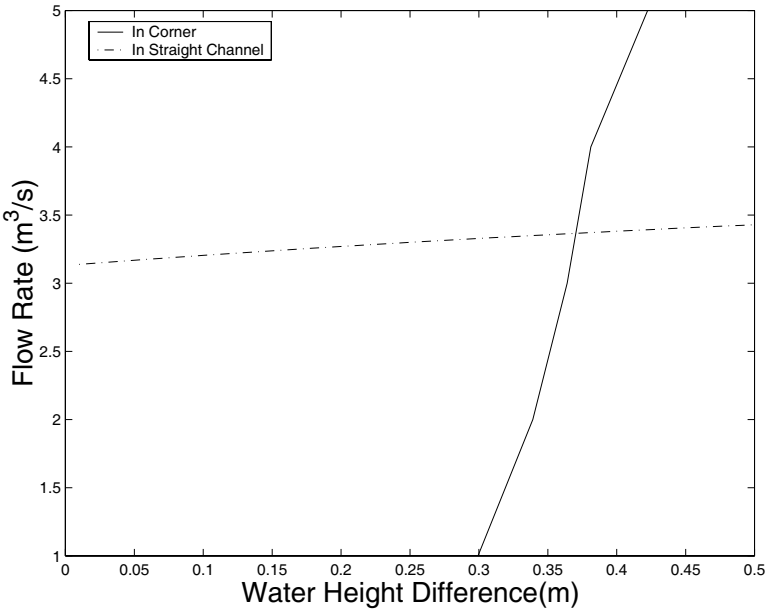

Fig. 3.9. Flow rates vs. the hydraulic headloss for: (a) a straight effluent channel, and (b) a 90^{o} bend.

Part 4: Hydraulic Optimization of the North Toronto CSO Storage Facility Using Numerical and Physical Modelling

4.1 Abstract:

Many older CSO (combined sewer overflow) storage facilities have insufficient capacities to meet the current performance standards for control and treatment of CSOs occurring in older parts of Canadian cities. The resulting CSOs represent a major cause of deterioration of water quality in receiving waters and impairment of their beneficial uses. One way of remediation of this problem is to increase the facility capacity by hydraulic optimization, as described in this study for the North Toronto CSO storage facility. Towards this end, a commercially available 3D hydrodynamic CFD (computational fluid dynamics) model (Star CD) was used to investigate hydraulic upgrading options for this facility and numerical modelling was verified against the data collected in a physical model (scale 1:116). The need for using both models was given by the complexity of the CSO facility, which comprises several interconnected tanks. One of the main functions of the physical model employed in this study was to verify the numerical model results. The verified numerical model was then applied to analyze hydraulic conditions in the whole facility for major structural modifications aimed to reduce or eliminate untreated overflows from the facility. Two scenarios were proposed and tested in the study. The results showed that both scenarios can possibly meet the design requirement for handling the 60 m^3/s flow rate. Even though the study focused on a particular CSO facility, hydraulic conditions in the studied facility represent general

flow conditions in typical wastewater settling tanks. Hence, the numerical modelling methods used are applicable to solving a wide range of hydraulic problems encountered at similar facilities. It is apparent that traditional design methods based on many simplifying assumptions could not adequately predict the operational performance of the modified facility. The results obtained also demonstrate that calibrated and verified numerical models represent very useful and flexible tools for investigating and optimizing older CSO storage and treatment facilities.

4.2 Introduction

Combined sewer overflows (CSOs) represent a major cause of deterioration of water quality in receiving waters and impairment of beneficial water uses (Weatherbe and Sherbin 1994). Although during the past 50 years all new sewers in Canada were built as separate sewers, CSOs can be found in older areas serviced by combined sewers and the abatement of CSO pollution remains to be one of the priorities of all large Canadian cities with combined sewers (XCG 2004). The means of CSO abatement are varied but can be classified into four broad categories: (a) control of inflow of stormwater into combined sewers, (b) sewer separation (requiring many other measures as well), (c) CSO storage and/or treatment (serving to increase the system collection efficiency and treat stored flows at central or peripheral wastewater treatment plants), and (d) increased collection efficiency by improved system operation (e.g., real time control).

In Canadian practice, CSO treatment options have received increased attention of municipal engineers in recent years, particularly retention treatment basins (RTBs)

serving to store and treat CSOs by settling (XCG 2004). In RTBs, the efficiency of treatment depends on CSO settleability and the hydraulic conditions in the basin (Li et al. 2003). The hydraulics of RTBs has been traditionally considered in a simplified manner, by addressing the "lumped" properties of the basin, typically described in general terms by the surface loading rate (SLR) defined as the inflow divided by the surface area of the sedimentation basin (Metcalf and Eddy 2003). During the past 10-15 years, research has shown that the efficiency of CSO settling can be affected by the settling basin hydraulics, and consequently, research into basin hydraulics was conducted using computational fluid dynamics (CFD) modelling (Saul and Ellis 1992). Saul and Ellis (1992) reported that the internal geometry of an on-line CSO storage tank influenced the efficiency of settling of a particular wastewater. The length to width ratio, the longitudinal and benching gradients, and the dry weather flow channel were the most significant geometrical properties affecting sedimentation. Other CFD applications to CSO hydraulics problems followed. Svejkovsky and Saul (1993) used the 3D CFD model to model the StormKing™ Hydrodynamic Separator, Pollert (1999, 2003) modeled a CSO overflow structure with free surface flow, and Hrabak et al. (1999) evaluated the general hydraulic performance of a CSO side weir structure. Harwood and Saul (1999) listed the advantages of CFD modelling, which include: (a) no need for laboratory test facilities, (b) the CSO structure geometry in CFD tests can be changed quickly, thus avoiding the time and costs associated with reconstructing a physical model, and (c) flow parameters, such as pressure and velocity, are calculated at all points within the facility, which may not be attainable in physical models.

But, most of the 3D numerical modeling studies on hydrodynamic behavior of CSO facilities were limited to simulating a simple part of the entire system due to complexity of the structure. However, in this study, the entire facility had to be simulated because the flow behavior was influenced by all parts of the entire facility. On the other hand, it is important to note that numerical modeling results always contain uncertainties arising from both approximations of actual processes and numerical schemes, and consequently, some verification of modeling results is desirable. For this purpose a hydraulic scale model of the facility was built which provided the opportunity to verify the prediction of the numerical model.

The numerical modeling studies on the same facility have been done before with different objectives and numerical models (He et al., 2004, He et al., 2006), they were mainly focused on possibly increasing particle settling by improving flow hydraulic conditions in CSO settling tank through reducing turbulent energy and on investigating a simple way to improve the facility treatment capacity with minor structure changes. However, all the previous studies did not address a solution to eliminate the untreated CSO overflow problem under the heavy storm events and showed that major structure modification should be considered in order to effectively control the unwanted CSO overflow problem. Based on information from previous study, the goal of this project is to explorer the various hydraulic upgrading options for the NT CSO Facility to greatly reduce or even totally eliminate CSO overflow. The study included a combination of numerical and physical models, and various structural modification scenarios were developed and evaluated. The results have been used by City of Toronto in decision making for upgrading of the NT CSO facility.

4.3 The NT CSO facility

The original NT CSO facility, consisting of the inlet channel and the stormwater storage tank, (see Fig. 4.1) was built in 1924. In 1991 three CSO storage and settling tanks were added to the facility connected by four pipes to improve the treatment capacity of the undersized CSO retention basin. In wet weather, CSOs escaping from an adjacent combined sewer enter the inlet channel of the facility and continue through four connecting pipes into a distribution channel, and over inlet weirs into three parallel storage tanks. The inlet weir elevations are such that the storage tanks are filled sequentially. Overflow from the CSO tanks is conveyed by the effluent channel into a stormwater tank where it mixes with the stormwater discharge from a separate storm sewer. When the stormwater tank is filled, the CSO and stormwater mixture overflows the final effluent weir and is blended with the secondary effluent from the North Toronto Water Pollution Control Plant (WPCP) before being discharged to the nearby Don River. After storms, the wastewater and sludge retained in the NT CSO Facility (approximately 6,000 m^3) is pumped to the trunk sewer and thereby to the Ashbridges Bay WPCP for treatment.

For larger volume events ($V > 6{,}000\ m^3$), or in the case of back to back events the facility overflows. Ideally, all CSO inflows should undergo settling in the CSO storage tanks. However, because of the limited transport capacity of the pipes connecting the inlet and the distribution channels, when the inflow rate exceeds about 4 m^3/s the excess flows are diverted from the inlet channel via a bypass weir directly into the stormwater tank without undergoing any settling (see Fig. 4.1).

Reducing or eliminating overflows has been a long time goal of the City of Toronto. Unfortunately, there is no easy solution to this problem due to the complexity of the hydrodynamic characteristics of the NT CSO treatment facility.

4.4 What we know from past studies

Numerical and physical modelling studies have been carried out during the past few years to investigate the most feasible options for improving the hydraulic performance of the facility (He et al. 2004, He et al. 2006). One of the main goals was to increase the treatment capacity without major structural changes. The proposal to increase the flow through the CSO tanks (to reduce inlet channel overflows) by reducing the elevation (overall height) of the final effluent weir was investigated, and several problems were identified. Modeling results showed that:

a) The treatment capacity of the three CSO tank components of the facility was controlled by the combination of the inlet connecting pipe size, effluent channel size, the two 90^{o} bends in the effluent channel and flow control weirs equipped with upstream scum baffles.
b) Reducing the height of the final effluent weir may only be a partial solution for this complex system. A more comprehensive plan was needed, which would address the whole structure configuration of the facility.
c) The increasing rates of flow going through CSO tanks also depend on the height of the final effluent weir itself. For lower weirs, increases in flow rate become smaller when reducing the final effluent weir by a constant step, because the water level in the stormwater tank is also affected by the hydraulic conditions

upstream. Thus, even if further reductions of the final effluent weir height may appear feasible, considering the decreasing efficiency of this measure and the environmental consequences of sacrificing the stormwater tank storage, a more balanced approach combining effluent channel improvements and lowering the final effluent weir should be taken.

The numerical simulations indicated that by lowering the final effluent weir by 60 cm and modifying both 90^{o} bends of the effluent channel, the maximum inflow rate could only be increased from 3.9 m^3/s to 5.12 m^3/s, which does not have a significant effect on the reduction of overflow. Therefore, in order to truly reduce or eliminate the CSO overflow, the consideration of modifying the whole structure is inevitable.

4.5 Facility Upgrading Considerations

It has been estimated by City of Toronto that the maximum inflow rate to the NT CSO facility can be as high as 60 m^3/s, and for this inflow, the existing structure is unlikely to achieve acceptable solids removal by gravity only. Therefore, the polymer flocculant addition was suggested in this CSO facility upgrading project to enhance particle settling for short hydraulic residence times.

Improvements in clarification efficiency with the use of polymeric flocculants (Averill et al, 2001, Wood et al. 2005, Wood et al. 2006) at this facility and in other CSO and stormwater facilities in Toronto have demonstrated acceptable treatment performance at high surface loads and with minimal residence times. The use of a polymer flocculant has increased the required hydraulic capacity of a clarification vessel by a factor of 10 or greater compared to clarification without flocculants. A recent study with stormwater

showed that surface loads of 46 m/h with a short 1-minute residence time provided TSS (total suspended solids) removal of 77%, using a polymer flocculant in pilot tests with a 3(L) x 1.4(W) x 2(D) m rectangular clarifier (Wood et al. 2005).

Therefore, the objectives for upgrading the NT CSO facility were set as follows:

1. On a seasonal basis, a maximum CSO inflow of 60 m^3/s, resulting from a thunderstorm event, would be anticipated for the duration of 30 minutes or less per year (or less than 1% of the time). Thus, the maximum facility capacity of 60 m^3/s should be targeted for the upgrading scenarios.
2. A CSO flow of 60 m^3/s would impart a surface load of 110 m/h considering the available total vessel surface area of 1,940 m^2. Based on the performance of full – scale experiments at the NTCSO facility with polymer flocculant addition and only one CSO tank on-line (Wood et al., 2006) TSS removals above 50% would be achieved at surface loads of 50 m/h with an 8-minute hydraulic residence time. Compared to the Etobicoke stormwater pilot testing (Wood et al., 2005) mentioned above, the two series of tests had roughly the same surface load, but very different residence times, and achieved similar TSS removal rates. This indicates that with polymer addition high TSS removal can be expected if some minimum residence time is satisfied. In this study, three-minute residence time will be set as the minimum residence time which should provide a good level of treatment at a surface load of 110 m/h, as long as the settling tanks are reasonably hydraulically efficient.

Sludge removal requirements after storm events is also a very import factor for the upgrading scenarios since removal of TSS with the polymeric flocculant is achieved by

both settling and flotation processes and the expected amount of sludge is much greater than for conventional gravity settling processes.

4.6 Study Methods

A 1:11.6 scaled physical model of the original facility structure built for a previous study was used in this study. A physical model could provide the accurate and reliable hydraulic information about the facility. However, since the ultimate goal of the study was to explore the best way to solve the overflow problem by increasing the capacity of an existing CSO facility, various scenarios were examined. Due to lack of flexibility, time requirements and costs to modify a physical model, it may not be the best choice to use a physical model only in this kind of experimental study. Also, under certain circumstances a physical model has difficulty to realistically simulate the true situations, which will be illustrated in a later section. Therefore, a numerical model was adopted in the study as a supplementary tool to first assess modification scenarios. The measurements from the physical model can also be used to calibrate the numerical model and a very well verified numerical model can be easily, quickly and accurately applied to search answers of various hydraulic problems. The study will provide a good example illustrating that the use of a physical and numerical model together can take advantage of both models and supplement the shortcomings of each in solving a complex hydraulic problem.

4.7 Physical Model

The physical model was built with epoxy-coated marine plywood for easy modifications and to reduce the construction cost. The physical model has been modified a few times to accommodate the previous studies. Fig. 4.2 shows the first version of the physical model which did not include the storm tank and part of effluent channel of the original structure. Inflows were provided from the circulation system of the NWRI hydraulics laboratory, the flow rate was measured with a V-notch weir on the downstream side of catch tank wall when the flow rate was less than 30 L/s. Otherwise, a magnetic flow meter mounted on a 6" inlet pipe was used to determine the flow during large flow capacity tests. In order to represent the real structure as close as possible, many details such as slopes on the bottom of tanks were incorporated in the physical model. One important thing worthy to be mentioned here is that because the whole physical model structure was made with the wood, it was inevitable to have some degree of structural distortion, the hydraulic conditions in NTCSO facility were mainly determined by the water head and weir heights, which was very sensitive to minor structure changes, especially so in scaled down physical model, the structure elevations had to be checked out and adjusted from time to time during the entire project.

4.8 Numerical Models

A general purpose computational fluid dynamics model (Star CD) capable of solving a variety of complex fluid flow problems using unstructured mesh was chosen for this study. The mathematical description of the flow consists of the continuity equation and three components of the Reynolds equations. The resulting equations of conservation of mass, momentum, and energy are solved using a finite difference method employing a

control volume. Full details of the CFD software and its use can be found elsewhere (Star CD user manual, 2004)

Since the flow in the NT CSO facility is open channel flow driven by hydraulic head at most locations, it is critical to chose a model that can resolve the water and air interface in order to accurately calculate the capacity of the facility. Unfortunately, there is no model available on the market that is able to predict the exact location of water free surface in a complex system such as the NT CSO facility, which includes both pressured and free surface flows. The available models in commercial CFD package can only predict the water and air interface in a narrow water-air transition region. There are several multiphase models which have been developed for this purpose. In this study, a so-called VOF (Volume of Fraction) model with unstructured mesh was chosen, which can resolve water-air interface sharper than the Algebraic-slip model did in the part 3.

The VOF model has been used widely in commercial CFD software for simulating multiphase flows. Its formulation is based on the concept of two or more mutually insoluble fluids (or phases) occupying a computational cell. For each additional phase, a new variable is introduced, describing the volume fraction of the phase in the computational cell. In each control volume, the sum of all volume fractions of all phases equals one. The fields for all variables and properties are shared by the phases and represent volume-averaged values, as long as the volume fraction of each phase is known at each location. The VOF model calculates the VOF variable, which ranges in value from 0 to 1, in every cell. For the two phase case such as air and water, if the value is 0, the cell is filled with only air, and a value of 1 indicates that water occupies the entire cell. Within the water and air interface transition region the VOF variable is in the range of 0

< VOF < 1. For the VOF model the time step size has to be very small in order to resolve the interface of the two phases with a large density difference. In this study 0.01 second was used as the time step in all flow field simulations with a segregated solver (explicit scheme), which would satisfy the criterion of Courant number less than 1 criterion. The details of VOF modeling are beyond the scope of this paper.

Considering the fact that turbulent fluid intensity varies greatly in the NT CSO facility under strong inflow event, the RNG two equation turbulent model was chosen in this study because, in general, it is more suitable and give better simulation results for wide range of turbulence phenomena than the widely used k-ε model does.

4.9 Model Verification

During previous numerical studies on the NT CSO facility, one of the main applications of the 1:11.6 scale physical model was to verify the numerical model. Even though most of the commercial CFD models have been verified in one way or others, the CFD model used in this study is a new model to us, and also numerical models do not behave always the same under different circumstances and some parameters have to be adjusted accordingly. Therefore, it is necessary to evaluate the model before it can be confidently applied in the study.

In a study 3, the flow velocities in the four connecting pipes were measured in a simplified version of the physical model as shown in Fig. 4.2, the corresponding structure arrangement built on computer for numerical simulation is shown in Fig. 4.3. The measurement location can be seen in Fig. 4.1 as indicated by the four small red dots on the connecting pipes. The interesting reason for simulating velocity in the four

connecting pipes is that because there are two manholes on the pipe 4, the velocity in it should be different compared with the three straight connecting pipes, which would test the models ability to simulate a pressurized flow. The comparison of measured and simulated velocities with 5 m^3/s inflow rate are list in table 1, very good agreements were achieved for velocities in the three straight connecting pipes, and in the pipe 4 connected with the manhole the agreement was also reasonably good.

As mentioned before, the hydraulic condition in the NTCSO facility is mainly controlled by hydraulic head difference, it is critical for the model to be able to predict the water level accurately. The comparison between simulated and measured water level under maximum inflow rate in the existing structure has been made. The 3D structure and mesh of the existing structure used for numerical modeling are displayed in Figs. 4.4 and 4.5. Modeling of the NT CSO facility with the existing structural configuration is not only able to utilize the information obtained in the previous study, but also able to set a basis for modified structure to compare with. The simulated water level in the whole facility with 3.9 m^3/s inflow rate is shown in Fig. 4.6. The red and blue colors represent the water and air, respectively. In the previous study, the measurements indicated that the maximum flow rate of the existing NT CSO facility before overflowing of the bypass weir was about 3.9 m^3/s (water level in the inlet tank has the same height as the bypass weir). The solid curve in Fig. 4.7 shows the simulated vertical profile of the VOF value in the inlet tank just beside of bypass weir under 3.9 m^3/s inflow rate, the straight line represents the height of the bypass weir. The region with $0 < VOF < 1$ represents water-air transition area which roughly covers from -2 m to -0.5 m, however, the solid curve in Fig. 4.7 does not exactly illustrate the water-air interface. How to explain the simulated

results from VOF model? First of all, since the VOF value only delineates the water-air transition region, the above simulation setting is not completely correct because the measurement was done when the water level in the inlet tank just reached the same height as the bypass weir. However, in the numerical simulation water would start overtopping the bypass weir before true water level reached the height of bypass weir because of the spread of the water-air interface. Therefore, the simulated water level may be lower than the measurement estimated from the scale model. In order to find out and to correct this problem the simulation was redone by extending the bypass weir height all the way to the top (effectively blocking the bypass weir), the simulated VOF curve is shown in Fig. 4.7 by solid curve with cross symbol. It can be seen that the water level in inlet tank is slightly increased indicated by higher VOF value at top part of the curve. The VOF value at cross point of the VOF curve and the straight solid line is around 0.42, which value would be used for representing the true water level in this numerical study. The accuracy of the simulated VOF curve can be checked with the following simple calculation,

$$WL = \sum_i (Z_{i+1} - Z_i)(VOF_{i+1} + VOF_i)/2 \qquad i = 1 \cdots N-1 \qquad (1)$$

Where WL and Z are, respectively, water level and vertical height of vertices of simulated cells, VOF_i is the computed VOF value at the vertices i and N is the total number of vertices in the vertical direction at calculated location. The water level calculated with above formula is shown in Fig. 4.7 with straight dash line which is just slightly lower than height of the bypass weir. Considering the factors that there were possible some small construction errors and structure changes due to building material distortion existing in physical model, and especially, that it was difficult to level the

whole physical model structure with water in it, the measured and computed water level shown in Fig. 4.7 agreed very well.

It has been observed that once or twice per year, the NT CSO inlet tank was completely overtopped or flooded due to excessive inflow. Reducing or even eliminating the flooding events by increasing the capacity of the NT CSO facility is one of the main goals of this hydraulic upgrade project. In order to provide necessary reference information in structure upgrading and to verify the numerical model, the physical model was used to determine the exact maximum capacity of the existing NT CSO facility before it was flooded. The measured results indicated that under around 25 m^3/s inflow rate the structure started to overflow. Numerical modeling result in Fig. 4.8 shows that under 25.0 m^3/s inflow rate water in the inlet tank may begin to splash out as indicated by the zone of other than dark blue surface colors. Fig. 4.9 is enlarged side view of the inlet tank, it can be clearly seen that large waves have been generated due to the strong inflow, which is consistent with those observed in operation. However, at this flow rate the water level in the inlet tank has not yet reached the top of the inlet tank. Further comparisons between scale model measurements and numerical simulations will be given in later sections.

4.10 NT CSO Facility Upgrading Options

The main focus of the current study was on exploring the best ways to eliminate overflow and to maximize the treatment capacity of the NT CSO facility, which requires a good understanding of the relatively complex hydraulics of the existing facility. It is infeasible to test many alternative structural modifications by direct field measurement due to

numerous uncontrolled factors, and also the scaled physical model is not very efficient to test many possible structures modification, therefore, the numerical model is a natural choice in these studies as a flexible and supplement tool to investigate the hydraulic conditions of the facility under different structural configurations once the numerical model has been verified

Two major scenarios were proposed and examined in the study, they were listed below. The simulations started with examining the scenario 1 which could achieve the largest hydraulic capacity, but might also be the most costly to be implemented in practice.

4.11 Scenario 1:

The configuration of this scenario is shown in Figs. 4.10 and 4.11, and differs substantially from the original structure, Thus it requires the most retrofit work compared with other possible modifications. A new inlet channel 40m (L) x 8m (W) x 5m (D) has to be built, the upstream ends of the CSO storage tanks need to be opened and connected together. Both sidewalls of the inlet tank have to be removed to let flow freely pass from the CSO tanks to the stormwater tank. The idea behind this design was to integrate various parts of the facility into one large settling tank, the flow enters the facility from one end and leaves from another end without any obstacles in between, which could disturb particle settling, therefore, the flow capacity is mainly controlled by the water head differential at two ends of the facility. Under such a configuration the highest treatment capacity could be achieved and flow could have the longest residence time. Because of this reason the physical model was modified correspondingly and used as the main tool to investigate this structure layout. Fig. 4.10 shows the modified physical model used for testing this scenario. To meet the target of 60 m^3/s maximum treatment

capacity for the retrofitted NTCSO facility, the available 1:11.6 scale physical model would have had to be able to handle 120 L^3/s inflow (flow scale = $11.6^{2.5}$) without overflowing the structure. Unfortunately, because of a limitation in the water supply system in the NWRI hydraulics laboratory, the maximum available flow for use in the physical model under present physical model setting was around 65 L^3/s which was about one half of required flow rate. In order to quickly examine the full ranges of flow capacity of the modified facility without doing more construction in the laboratory, a simple indirect method combining measurements and calculations was adopted. To do so, two manometer tubes were installed on the side wall of the two ends of the physical model to monitor the water level. After water levels at two locations were recorded under different inflow rates, the polynomial least squares fit was used to fit the measured low flow data and extrapolate them to a larger flow range. The test results in Fig. 4.12 showed that the flow capacity of the scenario 1 was about 43 m^3/s (95 L^3/s in the physical model). The symbol of crosses and circles in Fig. 4.12 represent the flow level measured at the upstream and downstream ends, respectively. Since the top elevation of the facility structure was the same everywhere, the overflow events in most of cases would occur in the upstream region, due to higher water levels, as shown in the Fig 4.12. The solid straight line at the top of Fig 4.12 indicates the height of the structure; therefore, the intersection between the straight line and dash fitted curve would indicate the maximum flow that the physical model can handle under the tested condition, before overflowing the structure.

The accuracy and reliability of the indirect method could be assessed with numerical model. Three different inflow rates, 38 m^3/s, 42 m^3/s and 47 m^3/s, were used in

simulations. For the 38.0m^3/s, simulations showed almost no sign of water splashing out as indicated in Fig. 4.13. At the 47.5 m^3/s flow rate, it could be seen clearly in Fig. 4.14 that flow started splashing out at locations in the inlet channel and just upstream of the scum baffle, even though the overflow probably was not very large. Fig. 4.15 displays simulation results with an inflow rate of 42 m^3/, it was just about indicating overflow in the inlet channel, which agreed with the indirect method result. The good agreement for the hydraulic capacity of the facility between measurements and numerical model indicated that the indirect calculating method should be reliable. Actually, it should not be surprising that the above combination method worked well, because the hydraulic condition in the facility under scenario 1 was very simple and similar to those in a channel flow, only the scum baffle makes hydraulic conditions slightly more complex. Obviously, the scum baffle would restrain the flow freely passing through the NTCSO facility because in the original structure the distance between scum baffle and the final weir was about 0.6m, which was too small to allow large amount of flow passing through smoothly. Additional experiments were conducted without the scum baffle and the result was showed in Fig. 4.16 using the same indirect method to obtain capacity of the facility. It apparently showed that there was still a lot of room before the flow surface reaches the structure top under inflow rate of 60 m^3/s (120 L^3/s in physical model). Without the scum baffle the water levels at two ends measured in the physical model were about the same, therefore, in Fig. 4.16 the flow level at only one location was plotted. For a channel flow its hydraulic condition can be described by a simple linear equation:

$$u\frac{du}{dx} = -g\frac{dh}{dx} \qquad (2)$$

Where h, u and x are the flow height, flow velocity and distance along the channel, respectively. g is the gravity acceleration. Solution of the linear equation (2) represents a linear line for relationship between flow rate (or velocity) and water height. In Fig. 4.16 the almost straight fitting line for measured data implied that without scum baffle the flow in NTCSO facility was indeed similar to an open channel flow.

If the scum baffle is moved about 1m upstream from the original position, it would reduce the flow restriction caused by distance between the scum baffle and the downstream weir, A graph of flow levels against the inflow rate, after modifying the scum baffle position, are shown in Fig. 4.17. which indicates that the facility can handle flow rate larger than the targeted 60 m^3/s.

In the above measurements the inflow weirs of the CSO tanks (see Fig. 4.1 for location) were removed with the objective to achieve the maximum flow capacity for the facility. If the original inflow weirs were left untouched, they could retain the sludge from small CSO events in the zone of the original CSO tanks, which would greatly reduce the cleaning efforts. The measurements showed that there was no real difference in the flow capacity of the facility, with or without the original inflow weirs of the CSO tank, because the weirs were deeply submerged under large flow rates.

In general practice, particle settling is enhanced by increasing the flow residence time and/or by reducing flow turbulence in the facility. Both observations in the physical model and numerical simulation (shown in Fig. 4.18) indicated that for the structure tested, most of the flow went through the CSO Tank 1, because of the momentum of the inflow deflected by end wall of the new inlet.

To improve the flow distribution and characteristics, in the physical model a few straight parallel baffles with different extension lengths were placed into the inlet channel at entrances to each CSO Tank to intercept the flow going into each CSO tank accordingly and arrangement of these baffles is illustrated in Fig. 4.19. However, experiments in the 1:11.6 physical model showed that the baffles did not work very well, as tested. This was caused by a short length of the inlet channel section in the physical model between the water supply pipe and the upstream wall of the CSO Tank 3; less than 1 meter. Because of very strong inflow, even with a horizontal tube array diffuser at the outlet of the water supply pipe, the highest flow velocities in the inlet channel were concentrated along the center part of the channel and, therefore, several of the upstream intercepting baffles situated near the inlet of each of the three parallel tank section did not intercept much of the inlet channel flow. In the prototype structure there is a 40 m long channel feeding inflow into the facility, therefore, the inlet flows at the end of this long channel should be much more evenly distributed across the channel width than in the physical model. To correct the inlet part of the physical model, the entire model structure would have to be reconstructed, which would not be a trivial task. An alternative way to evaluate the effect of the flow conditioning baffles is using a numerical model, which has provided accurate and realistic results in the previous study (He et. al, 2004) and indicated improved hydraulic conditions for various baffle designs. Simulated velocity distribution at the entrance of the CSO tanks with flow conditioning baffles in place is displayed in Fig. 4.20, and the baffle structural arrangement is similar to that tested in the physical model (illustrated in Fig. 4.19). There are a total of 9 straight flat baffles in this proposed design, the length of baffles gradually increase in the downstream direction (0.9 m), extending

into the inlet tank to form multiple narrow flow channels. The purpose of the baffles is to force inflow to enter the CSO tanks through small parallel flow channels with desired equal proportions. By comparing these flow patterns with the case without baffles Fig. 4.18, it is apparent that flow conditions are significantly improved, flow rates in the three CSO tanks are about the same and flow pattern in the three tanks become more uniform. All of these intercepting baffles would equalize the flow residence time and reduce turbulence, thus contributing to better particle settling.

One interesting hydraulic phenomenon after inserting the flow conditioning baffles is that there are small eddies at the entrances of the first a few baffles and the intensity of the eddies decreases with downstream distance and, eventually they are totally dissipated. The possible explanation is due to flow momentum. After flow mass was reduced because of escaped flows from the first a few intercepting baffles, there was not enough momentum to continue to generate eddy by left flows, even though the flow velocity is about the same indicated from similar length of velocity vectors.

As mentioned before because of the limitations of water supply in the NWRI Hydraulics Laboratory, it is difficult to directly measure the maximum hydraulic capacity of the proposed Scenario 1 in a 1:11.6 physical model as well as to test the flow conditioning baffles. In order to further verify the above conclusions, a 1:23.2 scale physical model, reproducing the same facility structure (Scenario 1) as the 1:11.6 physical model was built. Measurements show that the maximum hydraulic capacity of the 1:23.2 physical model is around 26.3 L/s which would equal to the maximum capacity of 149 L/s and 68 m^3/s in a 1:11.6 physical model and the prototype structure, respectively. To check the accuracy of the hydraulic capacity predicted from the 1:11.6 model with the above

mentioned indirect method, the water level was calculated for a 149 L/s inflow rate from the best-fit curve in Fig. 4.17. This result is marked by an asterisk in Fig. 4.17, which shows an almost perfect prediction from the 1:11.6 physical model. The flow conditioning baffles were also tested in the 1:23.2 physical model and observations showed that they worked well and confirmed what the numerical model indicated.

4.12 Scenario 2:

As mentioned above Scenario 1 could achieve the maximum hydraulic capacity of the facility, but with high cost, because it requires building a new long inlet channel (about 40 m (L) x 8 m (W) x 5 m (D)) connected to the facility. However, if there is another scenario, the capacity of which can satisfy the targeted flow rate of 60 m^3/s, but with much less construction cost, it could be also very attractive. The structural arrangement of Scenario 2 is shown in Fig. 4.21. Because the numerical model is much more flexible to be modified than the physical model, in studies of scenario 2 only the numerical model was used. By comparing Scenario 2 with the structural layout of Scenario 1 (as shown in Fig. 4.11), it can be seen that the main differences between the two cases are that in Scenario 2, one CSO settling tank is used as a part of the inflow channel and the two remaining CSO settling tanks were modified as the outflow channel, instead of using all three CSO settling tanks for conveying outflow in Scenario 1. The flow enters the facility through the existing inlet channel, then takes a 90 degree turn flowing through the original CSO tank 3, at the end of the CSO tank 3 it turns into CSO tank 1 and 2, and finally flows out through the stormwater tank. As mentioned before the existing exit weirs of the CSO storage tank, located between the CSO storage tank and the stormwater tank, have little effect on the hydraulic capacity of the facility because they are much

lower than the height of the stormwater tank weir, therefore, the original CSO tank inflow weirs were kept and a new scum baffle was added upsteam of the existing CSO tank inflow weirs to keep floating materials and sludge in the CSO tank for easier cleaning. The existing cleaning method can be applied on this new configuration and for small storm events the whole CSO volume will stay in the CSO tanks, without the need to clean other parts of the facility. With these changes, the numerically estimated maximum capacity of the facility is about 60.0 m^3/s as indicated in Fig. 4.22. Under this inflow rate, flow at the 90 degree bend connecting the original inlet channel and the CSO tank 3 begins to be overtopped lightly as indicated by the scattered red colour on the flow surface due to the strong incoming flow hitting the wall corner. Flow patterns of the whole facility are displayed by streamlines in Fig. 4.23 indicating that flow is not very evenly distributed when it passes through the facility, which can be seen more clearly from Fig. 4.24 with velocity vectors at the water level 0.5 m below the surface near the upstream end of the three CSO storage tanks. High CSO flows had difficulty passing through the 180 degree turn entering into Tank2 from Tank3, resulting in uneven flow velocity distribution, due to the flow momentum, inducing a permanent eddy at inner-side corner of the CSO tank 2 and due to strong shear. The eddy functions as a block reducing the effective width of the CSO tank. Therefore, more flows with a better spatial distribution were passing through the CSO Tank 1 than Tank2, which may reduce the flow residence time in the facility. To improve the flow conditions, a few minor structural modifications were proposed and examined by numerical model. In the first test an angled baffle was added as shown in Fig. 4.25. The installation of a baffle at this location was intended to restrict a certain amount of flow to enter the Tank 1 to make flow more

evenly distributed between Tank 2 and 1. The simulated result in Fig. 4.26 indicates (by the size of velocity vectors) that about the same amounts of flow are passing through the two CSO tanks. However, flow is very unevenly distributed in both tanks; a large eddy with similar pattern exists in both tanks, which reduces the effective tank width. Due to the added baffle, the hydraulic resistance at this location was increased, which caused more water splashing out as indicated by the simulated water level in Fig. 4.27. It is questionable whether this baffle design has achieved the desired hydraulic improvement. Two other baffle designs illustrated in Figs. 4.28 and 4.29 were also tested. The purpose of each of these baffle arrangements was the same as for the first tested baffle to increase the flow passing through the CSO Tank 2. The simulated velocity fields are shown in Figs. 30 and 31, and do not indicate any real improvements, compared to the earlier discussed baffle design 1. The flows are still very unevenly distributed in the both CSO tanks. The simulated water level also reveals a similar story as before with the baffle in place, the hydraulic capacity of the system was reduced slightly as shown in Figs. 4.32 and 4.33 with more water splashing out over the structure wall.

The difficulty of improving flow conditions in Scenario 2 is caused by the 180 degree turn when flow is passing from Tank3 and Tank2. Unless, more baffles are added at the 180 degree turn to force the flow to enter the CSO Tank 1 and 2 uniformly, which would greatly increase the flow resistance and reduce the facility hydraulic capacity, there is no simple solution for greatly improving flow conditions at the entrances of the CSO Tanks 1 and tank2.

However, since the purpose of upgrading the NTCSO facility is to treat all inflows and often the facility has to be operated under very high flow rates, it is very difficult to

achieve the desired total suspended solids removal rate, if relying only on physical settling. Therefore, chemical addition to enhance the solid settling during short flow residence time may be the only realistic choice serving to obtain the required total suspended solid removal. In order to make flocculant chemical addition work more effectively, a certain degree of mixing is required to increase the chance of chemical contact with suspended solids, which possibly also reduces the amount of chemical residuals remaining in the effluent. In practice, the common way to generate flow mixing is to utilize flow turbulent energy, which can be generated by static mixers. However, in Scenario 2, the turbulent flows at both 90 degree bends between the inlet channel and the CSO Tanks 3 and the downstream end of the CSO tank3 and the CSO Tanks 1 and 2 could provide the strong mixing energy to serve as natural flow mixer. The unevenly distributed flow in the CSO tank may impair only slightly particle settling because with chemical addition the suspended solid settling speed increases greatly due to larger particle size. After solids settle out from the strong surface flow layer (about 1 meter thick within a 40 m travel distance) into a less active region below the height of the CSO tank inflow weir, they will possibly continue settling until reaching the tank bed. Therefore, with chemical addition and the CSO tank inflow weir in place, the suspended solid settling process in the CSO tanks may not be very sensitive to the flow hydraulic conditions. In addition, it was pointed out before that if flow residence time in an upgraded structure was longer than 3 minutes, the suspended solid removal rate could be expected to be higher than 50% with the addition of chemical. Fig. 4.34 shows the picture of the simulated particle traces during a 3-minutes travel time in Scenario 2, for 60 m^3/s inflow rate, simulated with Lagurange particle tracking model and the released particles

having the same density as the carrying flow. It can be seen clearly that after 3 minutes no particles have escaped from the facility, which indicates that flow residence time, in general, should be longer than the 3-minutes targeted time. Therefore, the Scenario 2 could still be a valuable attractive alternative, especially, if construction costs are of large concern in the upgrade project.

4.13 Conclusions:

In this study, both the physical and numerical models were used to investigate two scenarios to improve hydraulic conditions in an older under-performing CSO facility located in North Toronto. The study showed that the physical and numerical models can well complement each other to solve complex hydraulic problems accurately. Two scenarios were proposed and tested. The results showed that both scenarios can possibly meet the design requirement for handling the 60 m^3/s flow rate. The scenario 1 has the following advantages:

1) Straight forward structural layout enables this design to possibly attain the maximum hydraulic capacity which is much larger than the targeted capacity of 60 m^3/s.
2) Flow conditions in the three CSO tanks can be easily controlled by adding some flow baffles.
3) Since the outgoing flows pass through the three CSO tanks instead of the two CSO tanks in Scenario 2, the flow residence time in the facility could be slightly longer.

However, considering all the simulation results and other factors, the facility modification utilizing the existing inlet channel (Scenario 2) can also be an attractive alternative based on the following reasons:

1) The capital costs would be much smaller compared to Scenario 1 which would require to build a new 40 metres long inflow channel from the interceptor sewer and other appurtenances
2) Even though the maximum capacities of Scenario 2 for various flow baffle arrangements are smaller than those of Scenario 1, it is conceivable from the numerical modelling results that the flow capacities of Scenario 2 would satisfy the design expectation of 60 m^3/s. Since chemical addition enhancing particle settling would be used in the upgraded facility to treat high flow loads, the non-uniform flow conditions in the surface layer of the two CSO tanks should not have large influence on particle settling, especially, after suspended solids fall down below the height of the CSO tank inflow weir.
3) Scenario 2 using the existing inflow channel offers the greatest flexibility, because all the modifications done for this scenario can be fully utilized in Scenario 1, should further needs for increased capacity be addressed in the future by installing Scenario 1. Thus, Scenario 2 provides a good opportunity for implementing the project in two phases.

4.14 Acknowledgements:

The contributions made by Government of Canada's Great Lakes 2020 Sustainability Fund, the City of Toronto staff Mingdi Yang, and NWRI Research Support Branch staff Bill Warrender, Doug Doede and John Cooper, are greatly appreciated.

4.15 Notation

The following symbols are used in this paper:

g = gravitational acceleration;

h = water depth;

x = distance in x direction;

v = velocity in x direction;

VOF = volume of flow fraction;

WL = water level in the facility;

Z = vertical height of vertices;

4.16 Reference:

Averill, D. et al, (2001). "Field Experience with Chemically-aided Settling of Combined Sewer Overflows" Proc. Novatech 2001 Innovative technologies in urban drainage. volume 1, 237-244.

Harwood, R. and Saul, A.J. (1999). "The Influence of CSO Chamber Size on Particle Retention Efficiency Performance." Proceedings of the 8th ICUSD. 30 Aug.-3 Sept., Sydney, Australia, 1-9.

He C., Marsalek J., and Rochfort Q. (2004). "Numerical Modelling of Enhancing Suspended Solids Removal in a CSO Facility." Water Qual. Res. J. Canada, Vol39 (4) 457-465.

He C., Marsalek J.,Rochfort Q., and Krishnappan B.G. (2006) "Case Study: Refinement of Hydraulic Operation of a Complex CSO Storage/Treatment Facility by Numerical and Physical Modeling" Journal of Hydraulic Engineering. Vol. 132(2), 131-139

Hrabak, D., Pryl, K., Richardson, J. and Zeman, E. (1999). "3-Dimensional Modeling –A New Tool for the Evaluation of CSO Hydraulic Performance." Proceeding of the 8th ICUSD, 30 Aug.-3 Sept.., Sydney, Australia, 928-933.

Li J, Dhanvantari S, Averill D, Biswas N. (2003). Windsor Combined Sewer Overflow Treatability Study with Chemical Coagulation. Water Qual. Res. J. Canada, 38, 317-334.

Metcalf and Eddy (2003). "Wastewater engineering:" treatment and reuse. 4th Ed., McGraw Hill, Toronto.

Pollert, J. (1999). "Free surface modeling in sewer system." Proceedings of the 5th Fluent User Conference,14-15 October 1999, Prague, Czech Republic, 61-69.

Pollert, J. and Stransky, D. (2003). "Combination of computational techniques – evaluation of CSO efficiency for suspended solids separation." Water Sci. Technol., 47(4): 157-166.

Saul, A.J. and Ellis, D.R. (1992). "Sediment deposition in storage tanks." Wat. Sci. Tech., 25(8): 189-198.

Svejkovsky, K. and Saul, A.J. (1993). "Computational Modeling of the StormKing™ Hydrodynamic Separator Using 3D Mathematical Model Fluent." Department of Civil and Structural Engineering, University of Sheffield, UK.

Weatherbe, D.G. and Sherbin, I.G. (1994). "Urban drainage control demonstration program of Canada's Great Lakes Cleanup Fund." Water Sci. Technol., 29(1-2): 455-462

Wood, J., He, C., Rochfort, Q., Marsalek, J., Seto P., Yang, M., Chessis P., and Kok, S., (2005) “High Rate Stormwater clarification with polymeric flocculant addition” Water Science & Technology 51(2) 79-88.

Wood, J, (2006) “North Toronto Combined Sewer Overflow Storage Tank Facility Flocculant Treatment Study Final Report.” A report submitted to the City of Toronto, the Great Lakes Sustainability Fund and Environment Canada.

XCG Consultants Ltd. (2004). “Combined sewer overflow treatment technologies manual.” A report submitted to the Great Lakes Sustainability Fund, Environment Canada, Burlington, Ontario.

4.17 Tables:

	Pipe 1	Pipe 2	Pipe 3	Pipe 4
Measured Velocity (m/s)	2.28	2.18	2.31	1.28
Modeled Velocity (m/s)	2.29	2.19	2.20	1.42
Difference (%)	0.4	0.5	4.9	10.4

Table 1: Measured and modeled velocities in the four connecting pipes

4.18 Figures:

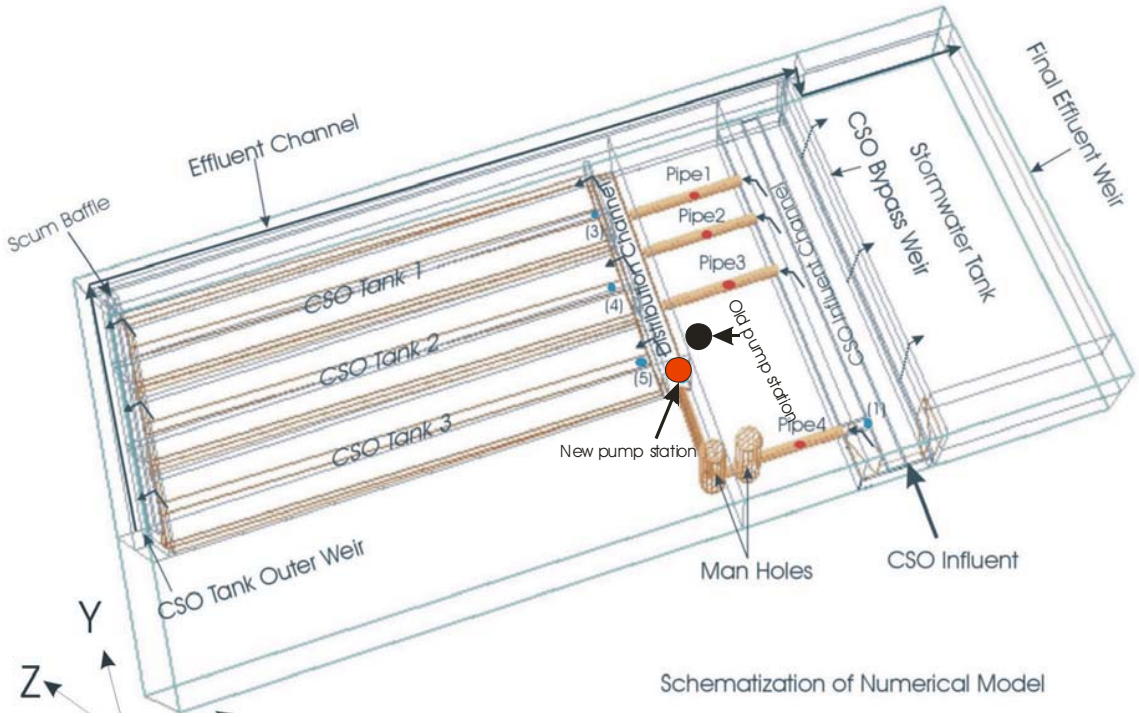

Fig. 4.1. 3-D Schematization of the North Toronto CSO Facility used in numerical modeling.

Fig. 4.2. The picture of the 1:11.6 scale physical model (first version) of the North Toronto CSO facility used in study to measure various hydraulic conditions and verify the numerical model.

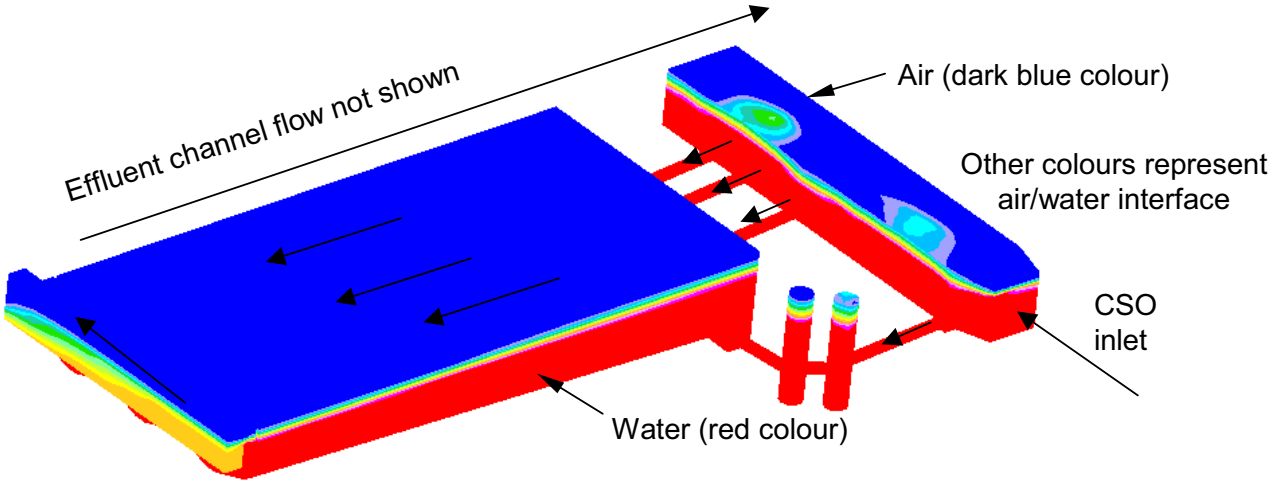

Fig. 4.3. The simplified structure used in velocity measurement in the four connecting pipes and obtaining other hydraulic information of the facility.

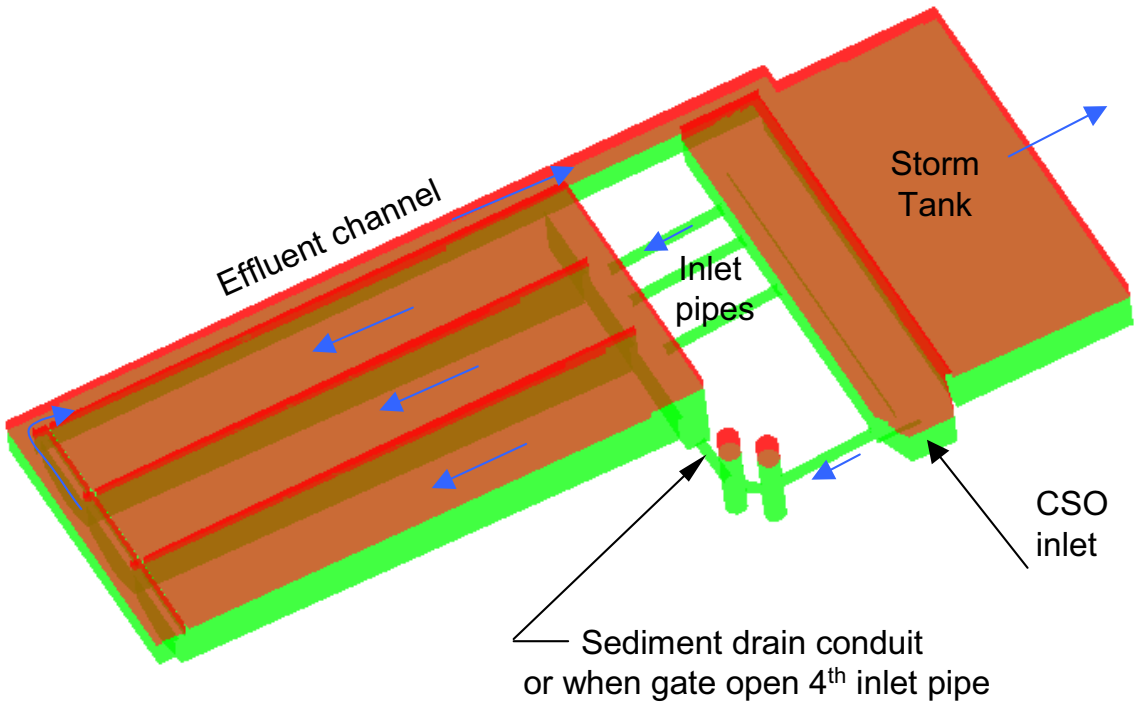

Fig. 4.4. The 3D structure of the existing NT CSO Facility used in the numerical modeling**.**

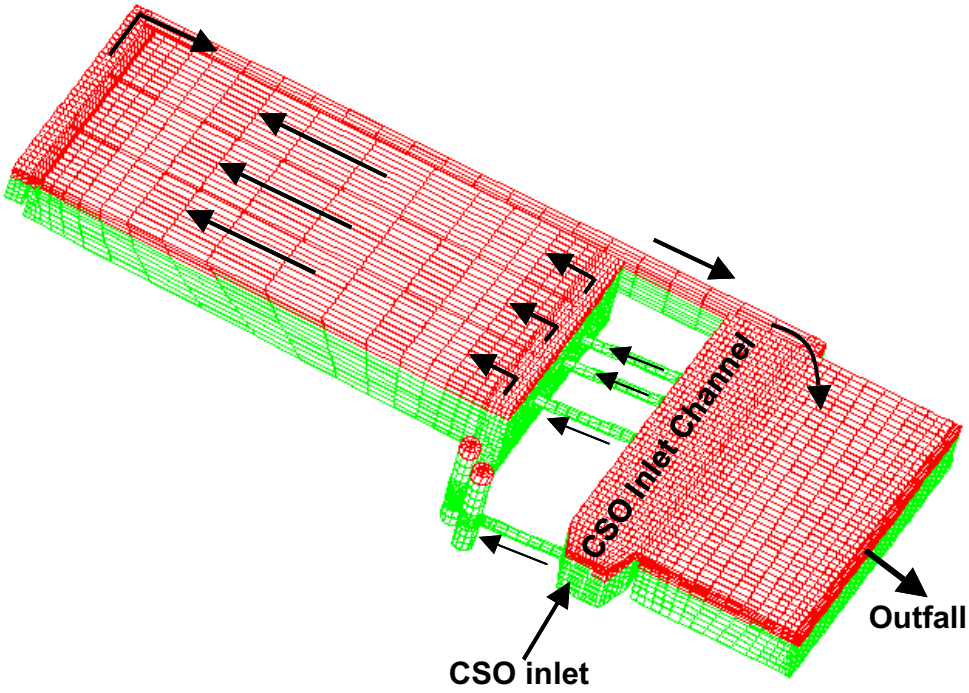

Fig. 4.5. One of the 3D unstructured meshes used for numerical modeling, the vertical mesh resolution in the top layer is much higher than below it in order to very well define water-air interface.

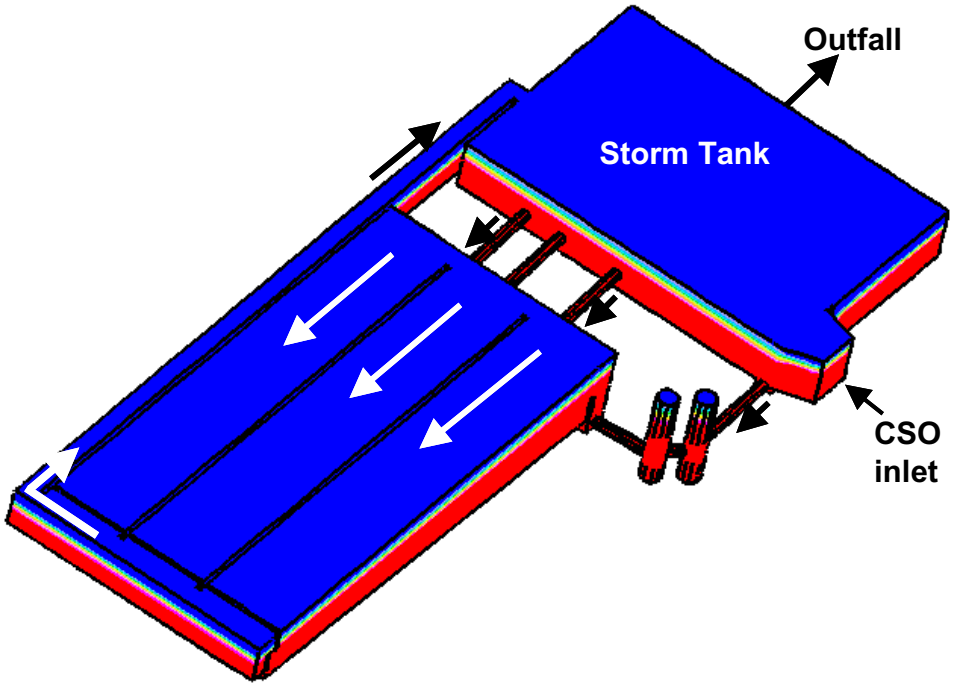

Fig. 4.6. Simulated water levels in the NT CSO facility, the red and blue colors represent water and air, respectively

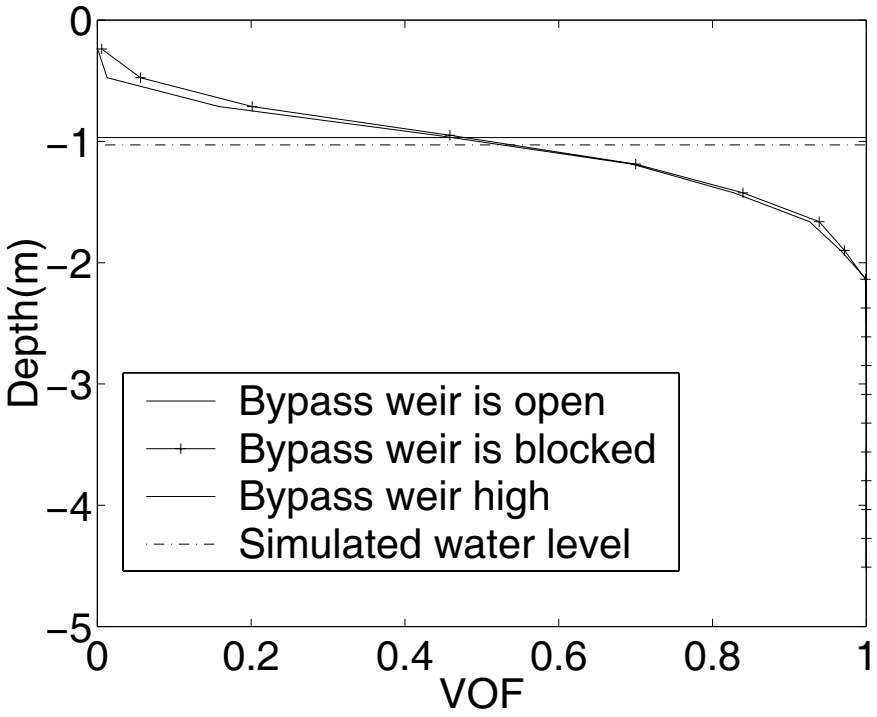

Fig. 4.7. Simulated water level represented by curve at a location beside the bypass weir. Straight line indicates the height of the bypass weir.

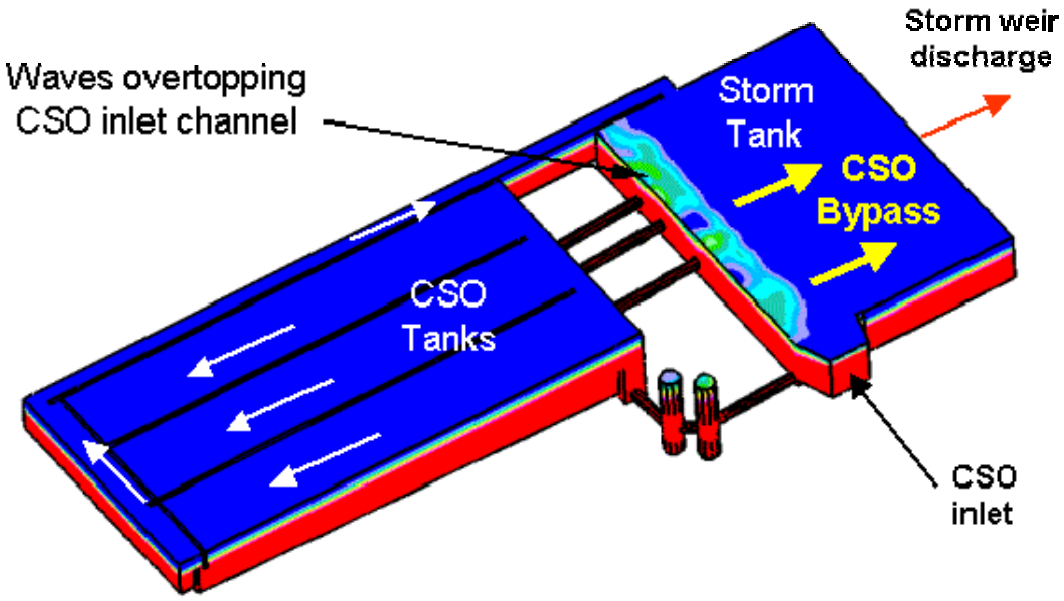

Fig. 4.8. Model simulation at 25.0 m^3/s CSO inlet flow rate, indicating waves overtopping inlet channel structure walls and CSO bypass. red colour = water, blue colour = air interface.

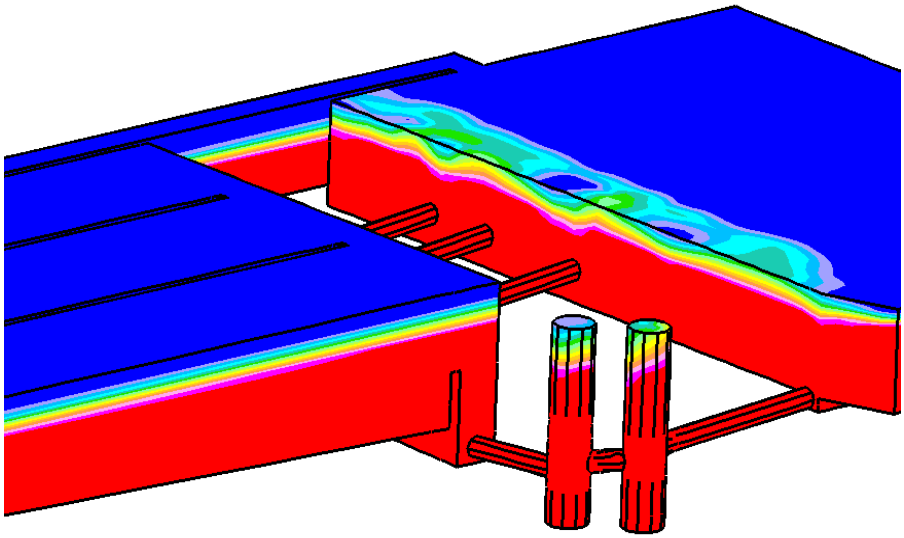

Fig. 4.9. Enlarged side view of inlet channel of the same simulation as shown in Figure 4.8. Strong waves (depicted in green and yellow), which have been observed in field operations, are generated in the original facility configuration at 25.0m^3/s CSO inlet flow.

Fig. 4.10. modified physical model. The inlet channel was opened up to connect the CSO settling tanks with the stormwater tank.

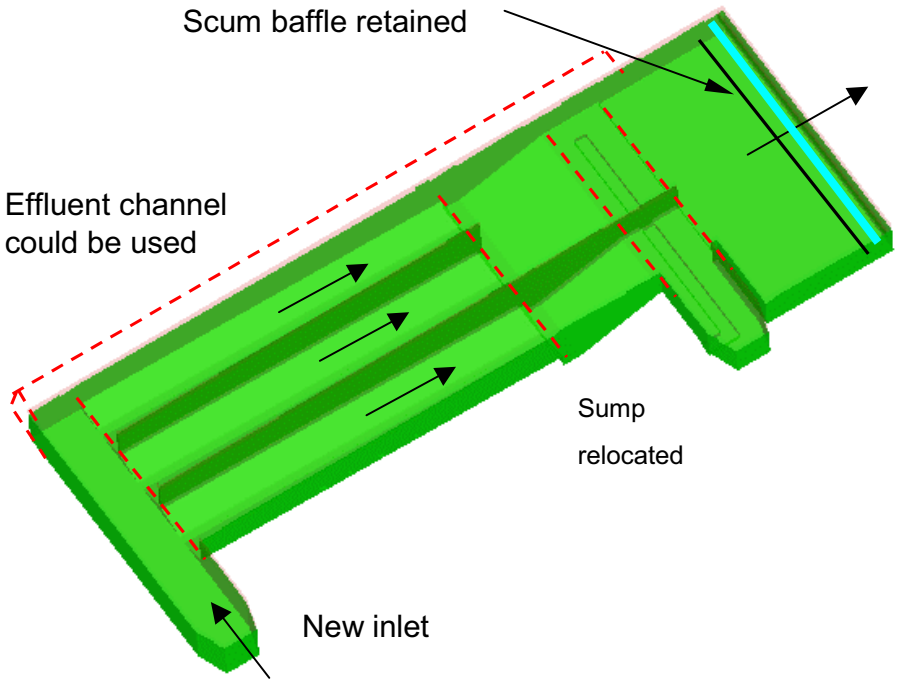

Fig. 4.11. Configuration for Scenario 1. A new inlet is connected to the original outlet ends of the CSO storage tanks. Red dashed lines represent the locations of walls removed from the original structure.

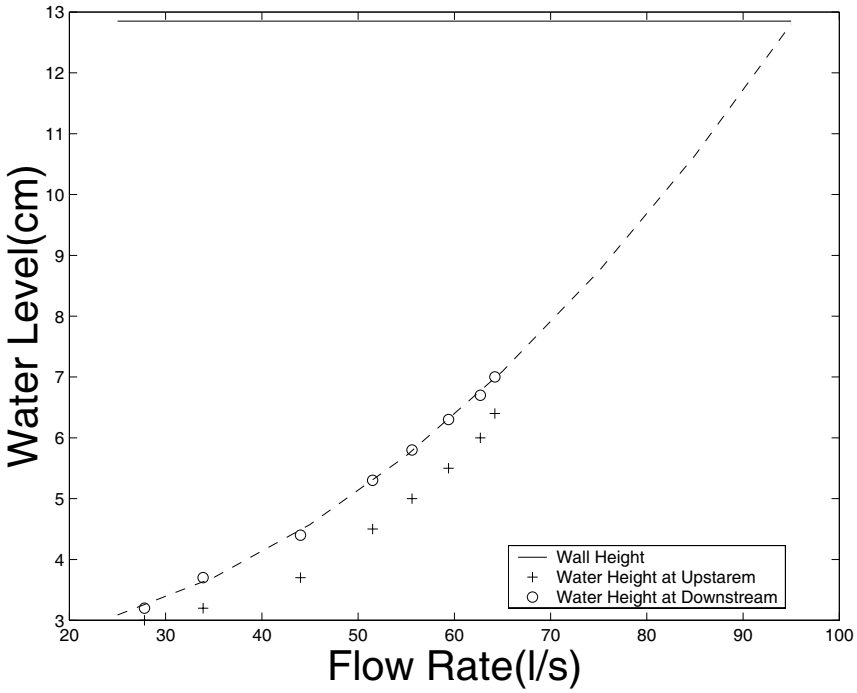

Fig. 4.12. least squares curve fitted to measured low flows, with the scum baffle in the original location. The maximum flow rate was calculated by extrapolating the curve.

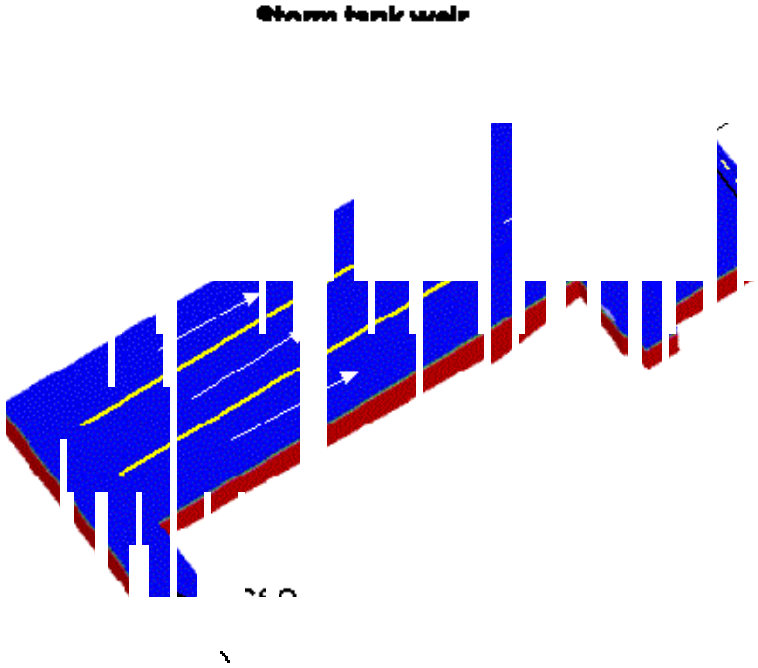

Fig. 4.13. Simulated water level for Scenario 1 with the inflow rate of 38.0 m^3/s and the original scum baffle; no signs of overflow.

.

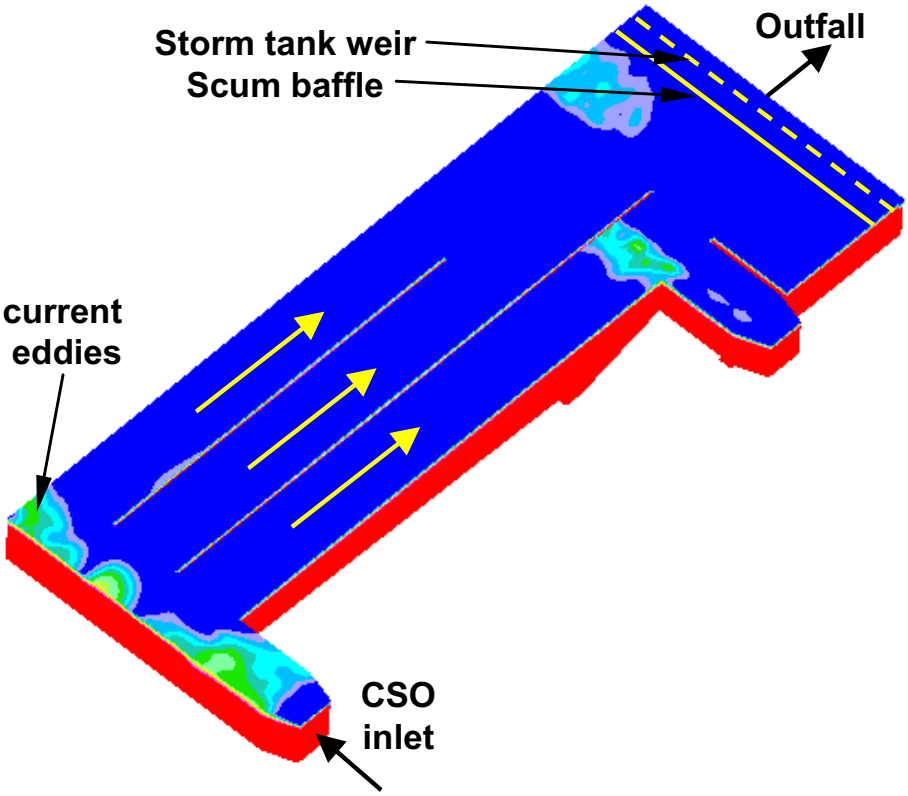

Fig. 4.14. Simulated water levels for Scenario 1, with the inflow rate of 47.5 m^3/s and the original scum baffle; no signs of overflow

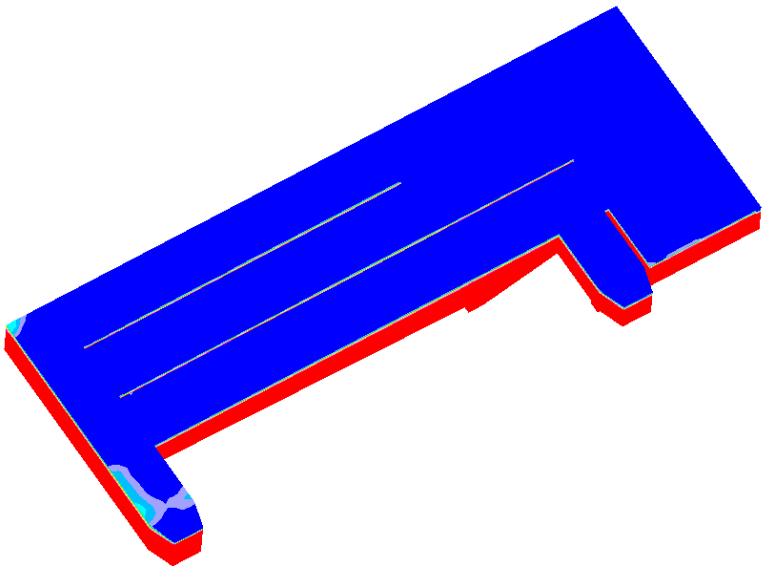

Fig. 4.15. Simulated water level for Scenario 1, inflow rate = 42.0 m^3/s and the original scum baffle in place, no signs of overflow from the settling tank, slight water splashing in the inlet channel due to a very fast inflow.

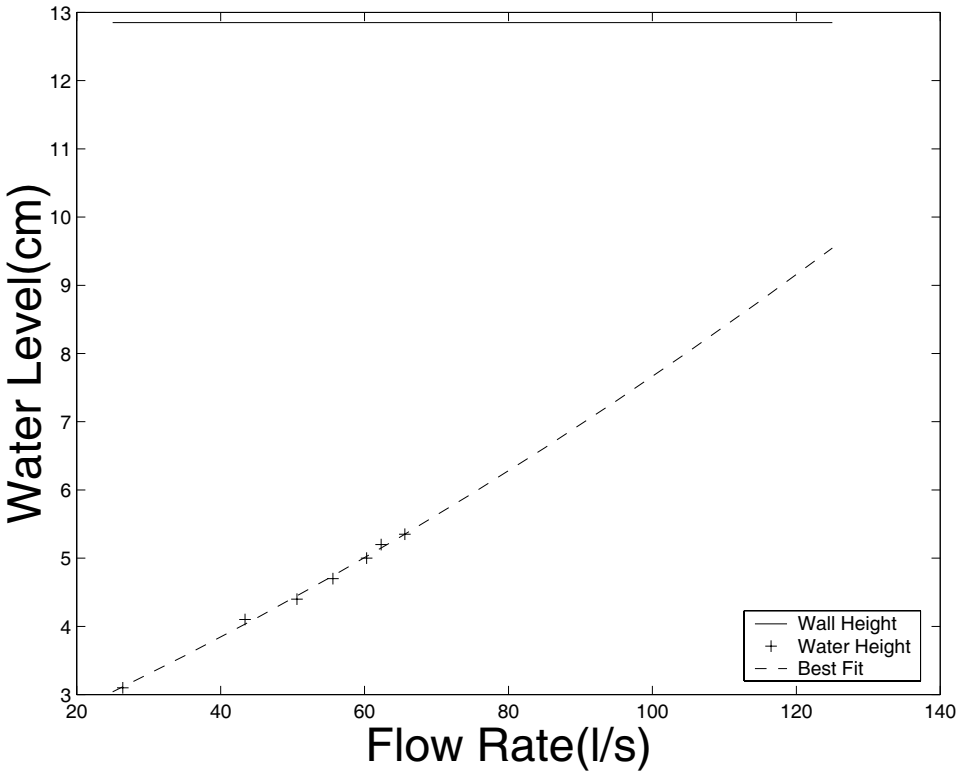

Fig. 4.16. The least-squares curve fitted to measured low flows, the scum baffle was moved. The maximum flow rate was calculated by extrapolating the curve.

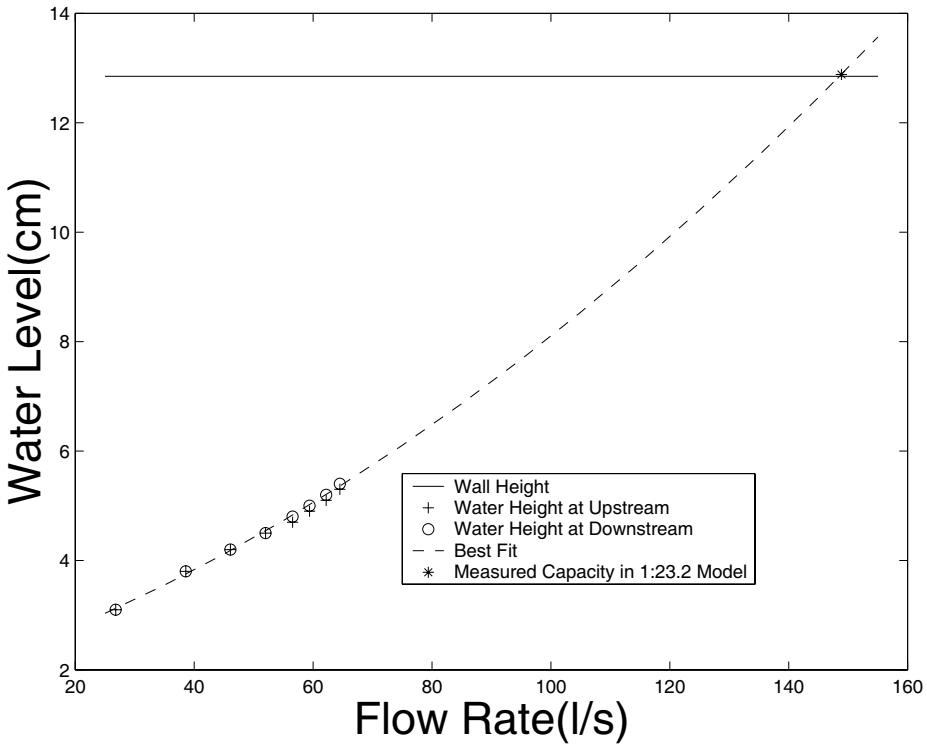

Fig. 4.17. The least-squares curve fitted to measured low flows, the scum baffle was moved back by 1 metre. The maximum flow rate was calculated by extrapolating the curve.

.

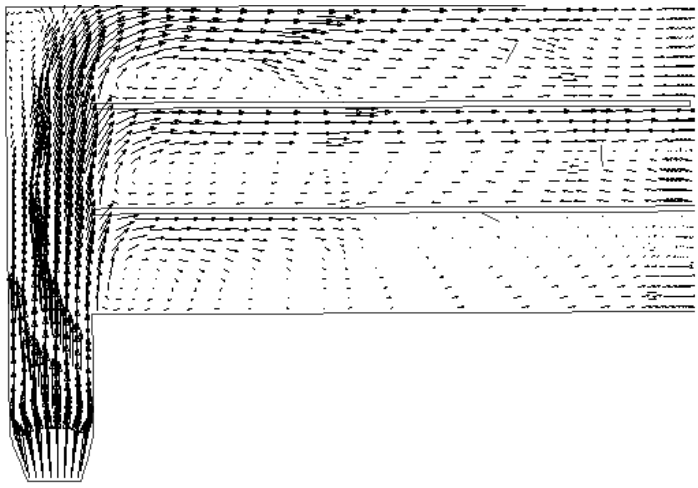

Fig. 4.18. Flow distribution in the inlet section of the facility at the depth of 0.5 m below the water surface.

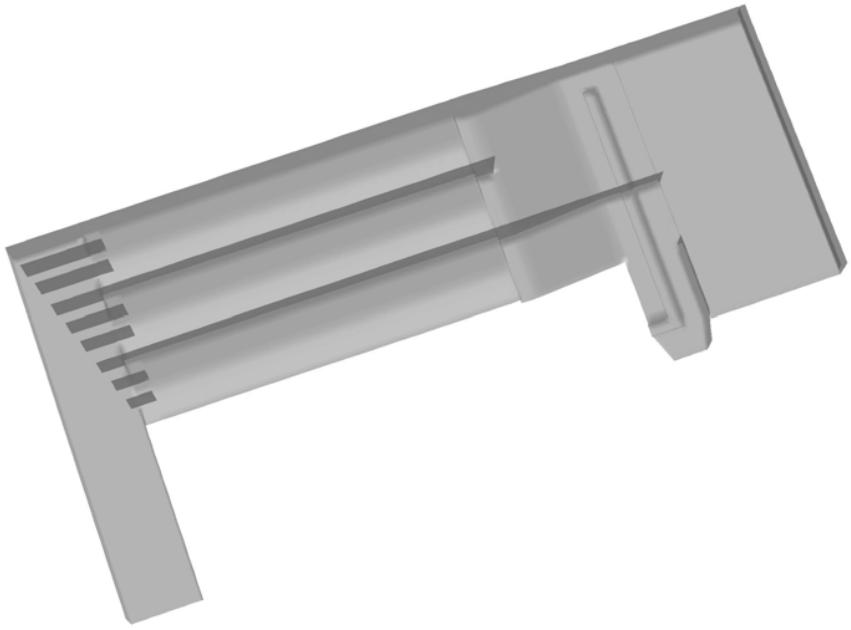

Fig. 4.19. The arrangement of the flow conditioning baffles in the modified structure (Scenario 1). Flows were forced into multiple parallel narrow channels.

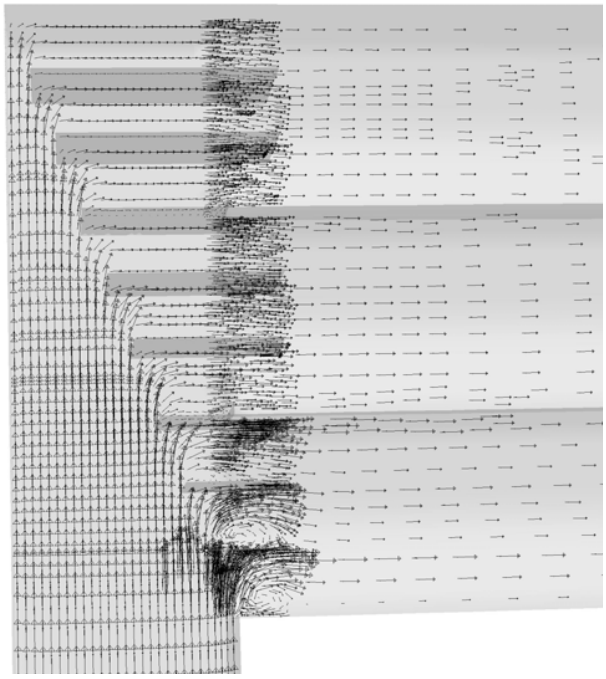

Fig. 4.20. Simulated flow patterns at the entrance to the three CSO tanks, with flow conditioning baffles.

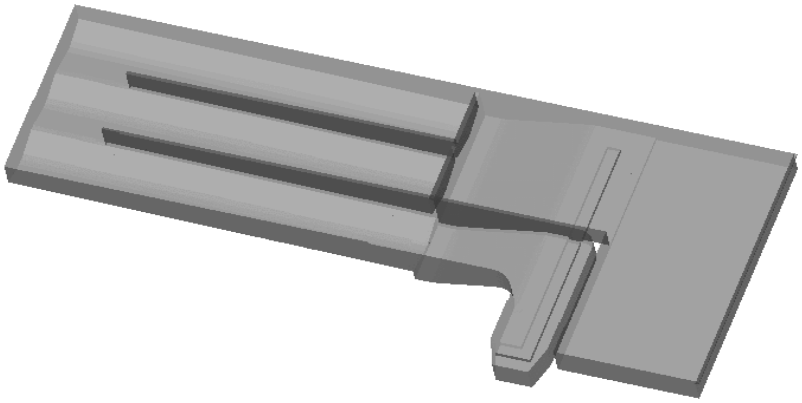

Fig. 4.21. Structure layout of Scenario 2: one CSO settling tank is used as the inlet channel and the other two tanks provide space for outflow.

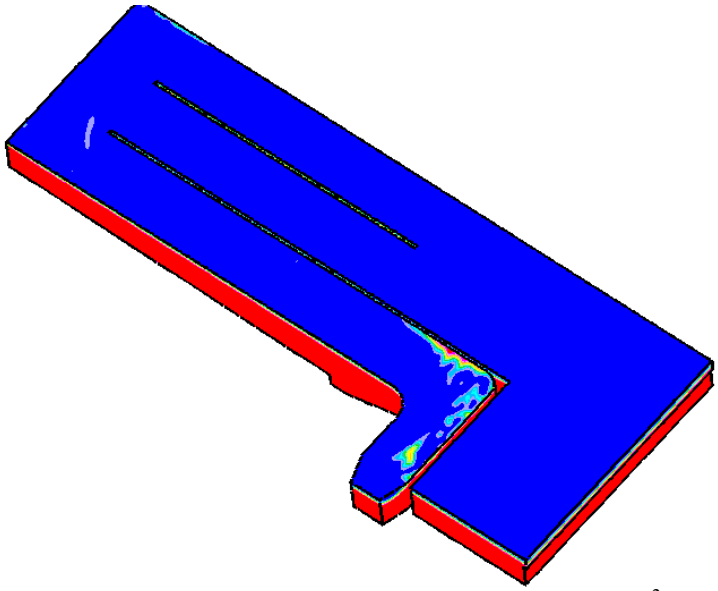

Fig. 4.22. Simulated water levels for Scenario 2, inflow rate = 60.0 m^3/s, no scum baffle. There are no signs of overflow from the settling tanks, except for some water splashing in the upstream corner of the inlet channel and the CSO tank wall, due to fast inflow hitting the front wall.

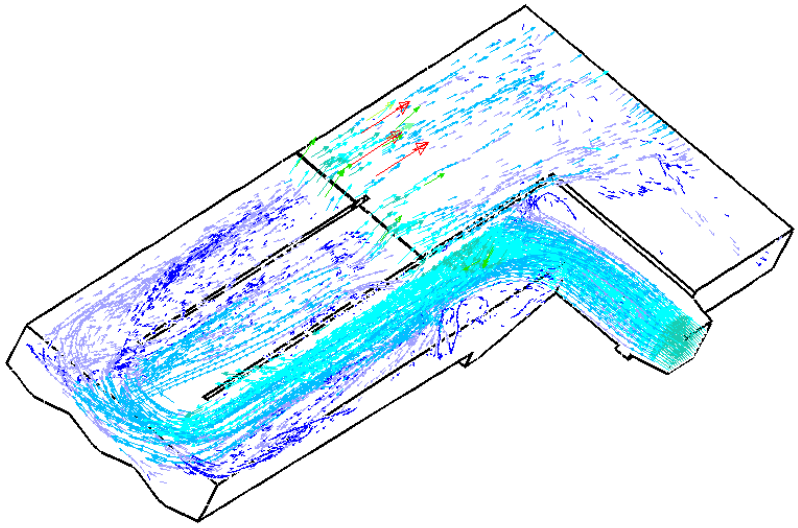

Fig. 4.23. Flow patterns in the whole facility described by streamlines. Flows at the near end of the CSO tanks are not evenly distributed due to a sharp turn.

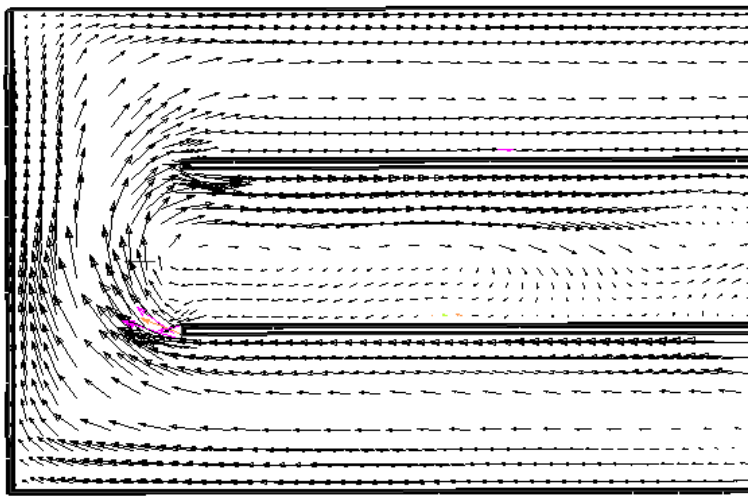

Fig. 4.24. The same flow field as in Fig. 13, characterized by velocity vectors at the depth of 0.5 m below the water surface.

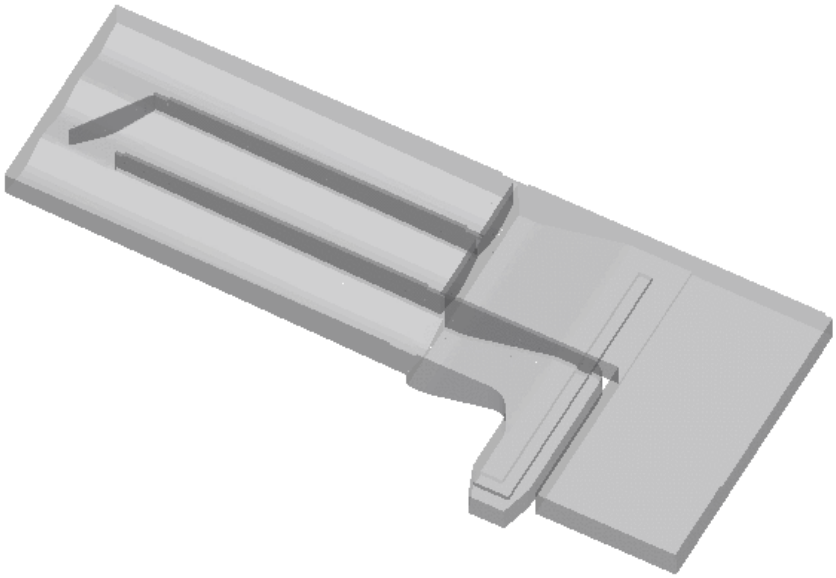

Fig. 4.25: One of the simulated baffle arrangements for flow conditioning.

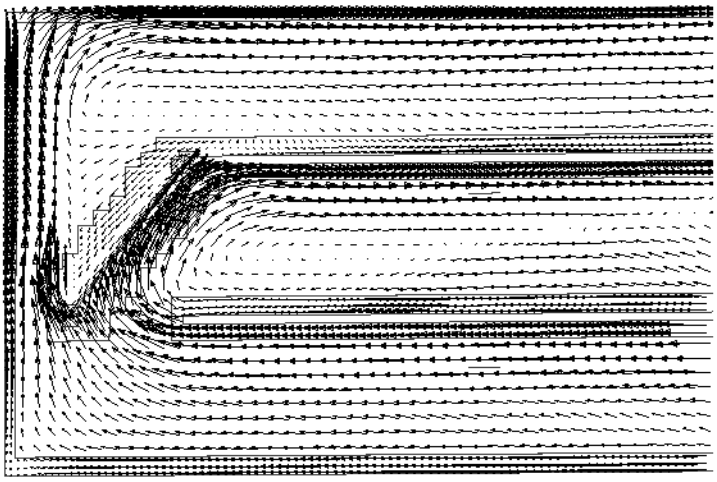

Fig. 4.26: Simulated flow distribution for baffles shown in Fig. 4.25.

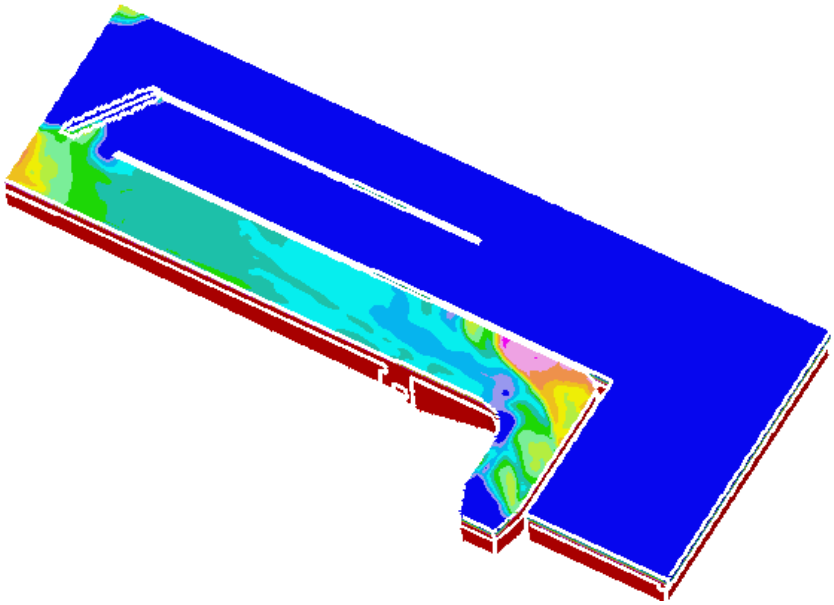

Fig. 4.27. Simulated water levels for Scenario 2; inflow rate = 60.0 m^3/s, with flow conditioning baffles in place. Possible overflow is shown in Tank 3 and may be caused by the increased hydraulic resistance resulting from putting the baffle in.

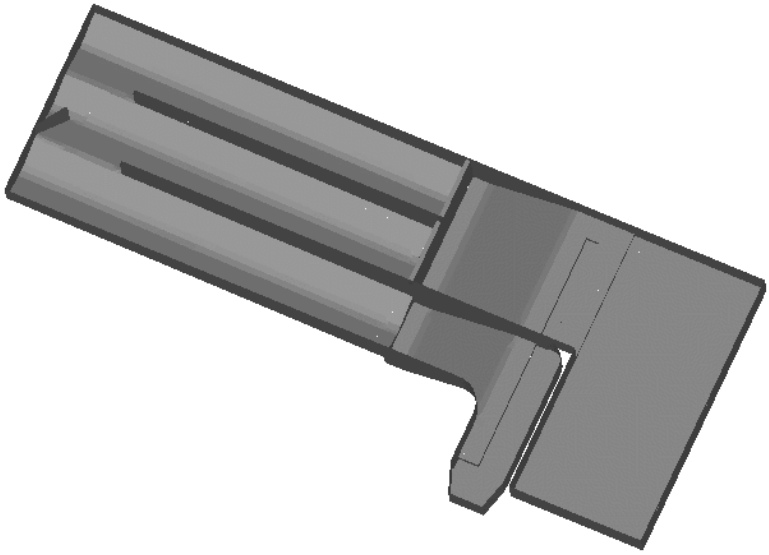

Fig. 4.28. The second numerically tested structural arrangement of the flow conditioning baffle.

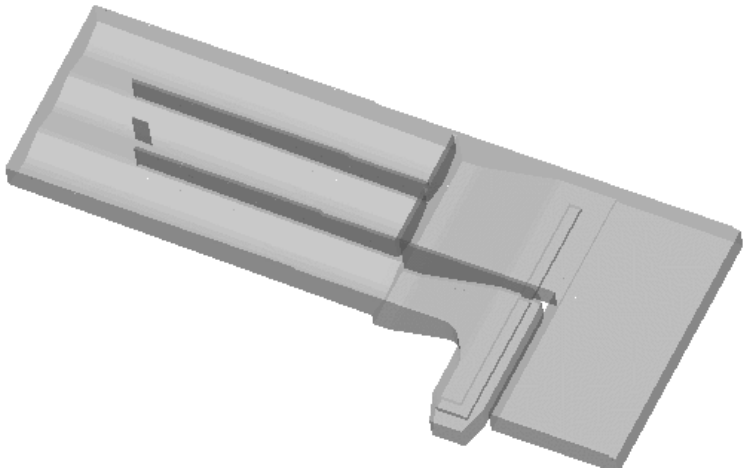

Fig. 4.29: The third numerically tested structural arrangement of the flow conditioning baffle.

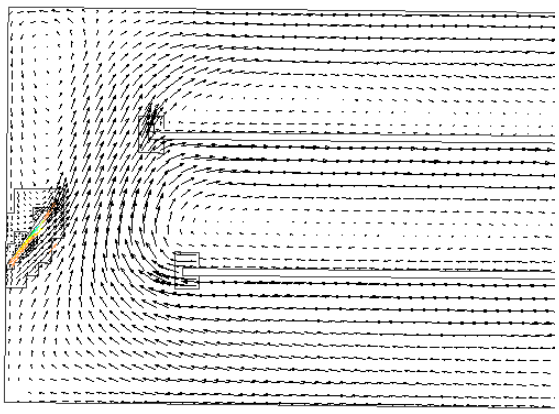

Fig. 4.30: Simulated flow distribution for the second baffle arrangement, at the depth of 0.5 m below the water surface. .

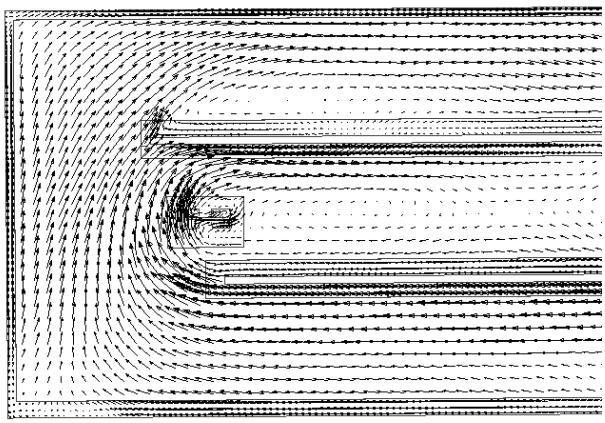

Fig. 4.31: Simulated flow distribution for the third baffle arrangement at the depth of 0.5 m below the flow surface.

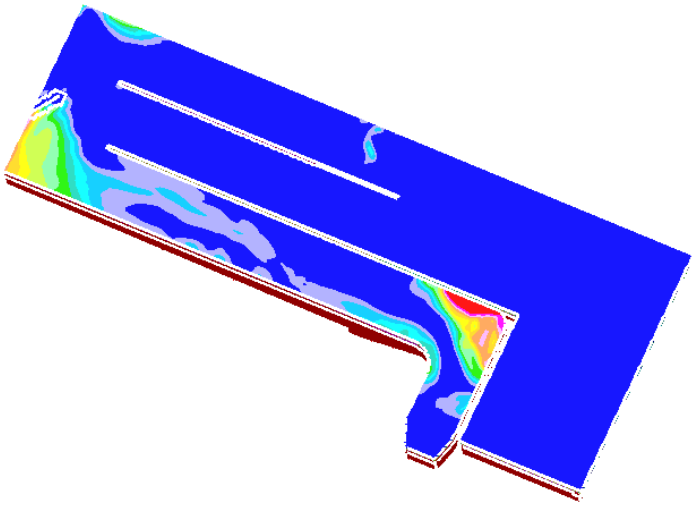

Fig. 4.32 Simulated water levels for the second baffle arrangement, with an inflow rate = 60.0 m^3/s.

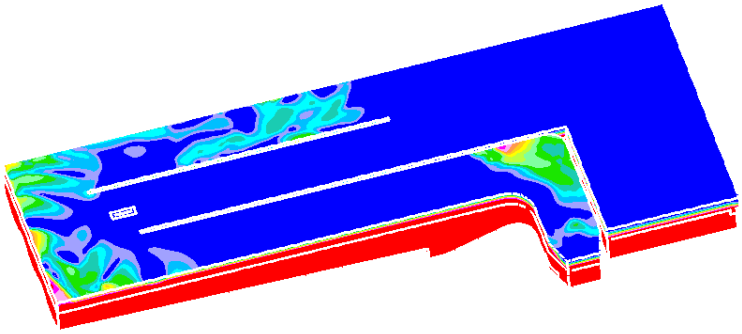

Fig. 4.33: Simulated water levels for the third baffle arrangement, with an inflow rate = 60.0 m^3/s.

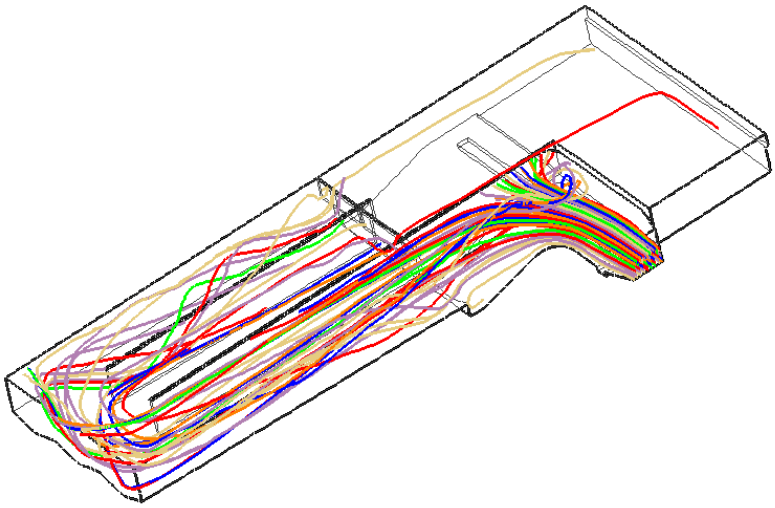

Fig. 4.34: Particle traces for 3 minute travel in the upgraded structure of Scenario 2, simulated with a particle tracking model.

Summary

This thesis presents four relatively independent studies on the hydraulic conditions of various particle removal facilities for possible ways to increase their treatment capacity and performance by utilizing and improving hydraulic conditions. The studies cover the following topics: a newly proposed particle settling enhancement plate, the redesign of the inlet zone of a high-flow rate clarifier, identify the hydraulic problems of an old partially functioned CSO facility and investigate possible ways to entirely eliminate untreated CSO by improving its hydraulic capacity and performance, and all studies were carried out with a combination of numerical model and measurements.

In the first part of the thesis a new concept of using a vortex to increase particle removal from liquid was proposed and the new particle settling enhancement plates, Vortex Plate, were tested under various flows and settling conditions. Structure of the Vortex Plate consists of multiple long narrow parallel slots which are built on a flat plate. Vortices are generated by cross-flow passing the long narrow parallel slots. The Vortex Plate can be used in the same way as the widely used lamellar plates with cross flow configuration. However, the Vortex Plate takes advantage of high flows, which generate stronger vortices and entrainment of solids in the downward direction inside the slots, the sliding particles are protected from the strong incoming main flow field. The study results show that under the tested flow conditions and particles the new Vortex Plate outperforms the conventional lamellar plate, especially for higher inflow rates and smaller particle size.

Part 2 presents a detailed numerical approach to redesign of the inlet structure of a high-rate stormwater clarifier. The inlet zone of an existing rectangular stormwater clarifier

was redesigned to improve the fluid flow conditions and reduce the hydraulic head loss in order to remove the lamellar plates and adapt the clarifier to the needs of high-rate clarification of stormwater with flocculant addition. The redesign procedure was directed according to 3-dimensional flow and particle behavior as simulated with hydrodynamic and particle transport models under various configurations of the hydraulic structure. The new inlet design has two advantages: (a) improved flow conditions in the settling zone inducing more effective settling, and (b) greatly reduced energy head losses. The field data also indicated that the TSS removal efficiencies of the original clarifier with lamellar plates and the clarifier without lamellas but with the new inlet design were comparable. Thus, the main goal of this study, reducing maintenance costs by removing lamellas, but without sacrificing settling efficiency, has been achieved.

In part 3, the performance of an old combined sewer overflow (CSO) storage/treatment facility was investigated by conjunctive numerical and physical (hydraulic) modeling. The main objectives of the study were to assess the feasibility of increasing the hydraulic loading of the CSO facility without bypassing and major structural modification. Numerical simulations identified excessive local head losses and helped to select structural changes to reduce such losses. The analysis of the facility showed that with respect to hydraulic operation, the facility is a complex, highly non-linear hydraulic system. Within the existing constraints, even though a few structural changes examined by numerical simulation could increase the maximum treatment flow rate in the CSO storage/treatment facility by up to 31%, but its treatment capacity is still too small to effectively reduce amount of by passing flows.

In the last part, the same CSO facility as studied in part 3 was re-investigated because only the limited treatment capacity could be increased if only doing few simple structure changes as indicated by the results of study 3. The main goal of this study was to investigate major structure upgrading options to totally eliminate the untreated CSO overflow. Two possible scenarios of structural changes were proposed and examined in detail by both physical and numerical models. The results showed that both scenarios can possibly meet the design requirement for handling the 60 m^3/s flow rate with its own advantages. Even though the study was focused on a particular CSO facility, the hydraulic conditions in the facility should represent general flow conditions in a typical water treatment facility. The numerical modeling method used in the study could be applied to solve a wide range of hydraulic problems faced in environmental and hydraulic engineering.

Recent publications in the DCE Thesis Series

Frandsen, Henrik Lund. / Selected Constitutive Models for Simulating the Hygromechanical Response of Wood. Aalborg : Aalborg University : Department of Civil Engineering, 2007. 134 s. (DCE Thesis; 10).

Tedd, James. / Testing, Analysis and Control of Wave Dragon, Wave Energy Converter : PhD Thesis defended in public at Aalborg University (101207). Aalborg : Aalborg University : Department of Civil Engineering, 2007. 116 s. (DCE Thesis; 9).

Li, Zhigang. / Characteristics of Buoyancy Driven Natural Ventilation through Horizontal Openings : PhD Thesis definded public at Aalborg University (101106). Aalborg : Aalborg University : Department of Civil Engineering, 2007. 123 s. (DCE Thesis; 8).

Larsen, Kim André. / Static Behaviour of Bucket Foundations, vol. 1 : Thesis submitted for the degree of Doctor of Philosophy. Aalborg : Aalborg University : Department of Civil Engineering, 2007. 216 s. (DCE Thesis; 7).

Laursen, Jesper. / WWTP Process Tank Modelling : The Integration of Advanced Hydrodynamicand Microbiological Models. Aalborg : Aalborg University : Department of Civil Engineering, 2007. 245 s. (DCE Thesis; 6).

Lai, Yoke-Chin. / IT-CODE : IT in COllaborative DEsign. Aalborg : Department of Civil Engineering : Aalborg University, 2006. 183 s. (DCE Thesis; 5).

Augustesen, Anders. / The Effects of Time on Soil Behaviour and Pile Capacity : PhD Thesis defended public at Aalborg University (17 November 2006). Aalborg : Aalborg University : Department of Civil Engineering, 2006. 301 s. (DCE Thesis; 4).

Liingaard, Morten. / Dynamic Behaviour of Suction Caissons. Aalborg : Aalborg University : Department of Civil Engineering, 2006. 183 s. (DCE Thesis; 3).

Larsen, Tine Steen. / Natural Ventilation Driven by Wind and Temperature Difference. Aalborg : Department of Civil Engineering : Aalborg University, 2006. 140 s. (DCE Thesis; 2).

Kramer, Morten. / Structural Stability of Low-crested Breakwaters. Aalborg : Hydraulics, 2006. 174 s. (DCE Thesis; 1).

ISSN 1901-7294
DCE Thesis No.